THE ROLE OF AORTIC STIFFNESS AND VASCULAR DYSREGULATION IN BRAIN AGING

By

Francis Elena Cambronero

Dissertation

Submitted to the Faculty of the

Graduate School of Vanderbilt University

in partial fulfillment of the requirements

for the degree of

DOCTOR OF PHILOSOPHY

in

Neuroscience

May 12th, 2023

Nashville, Tennessee

Approved:

Timothy J. Hohman, Ph.D.

Angela L. Jefferson, Ph.D.

Joshua A. Beckman, M.D.

Manus J. Donahue, Ph.D.

To my family, who have always provided unwavering love and support.

ACKNOWLEDGMENTS

This work would not have been possible without the financial and social support of the Howard Hughes Medical Institute's Gilliam Fellowship Program, the National Institutes of Health (F31-AG059345, T32-MH064913, R25- GM062459), and Vanderbilt University's Initiative for Maximizing Student Development (IMSD) Program. I am especially grateful for Dr. Angela L. Jefferson, my primary mentor, who has been supportive of my career goals since the start, provided me with countless opportunities for professional development, and helped me develop my career interests and intersectional scientific identity in long-lasting ways.

I am grateful to all of those with whom I have had the pleasure to work during this and other related projects. Each of the members of my Dissertation Committee has provided me extensive personal and professional guidance and taught me a great deal about both scientific research and how to effectively navigate scientific environments. I would especially like to thank Dr. Timothy J. Hohman, the chair of my committee, who is one of the most selfless people I know when it comes to sharing his time and expertise. I would also like to thank the Vanderbilt Memory and Aging Project research participants, without whom this work would not have been possible.

Nobody has been more important to me in the pursuit of this project than the members of my family. I would like to thank my parents, whose love and guidance are with me in whatever I pursue and who will always be my biggest role models. Equally importantly, I wish to thank my supportive friends, who provide unending inspiration and truly special moments of joy.

TABLE OF CONTENTS

LIST OF TABLES

Table Page

LIST OF FIGURES

Figure Page

LIST OF ABBREVIATIONS

1. Alzheimer's disease (AD)
2. Alzheimer's disease and related dementias (ADRD)
3. Cerebrovascular disease (CVD)
4. Vascular contributions to cognitive impairment & dementia (VCID)
5. Cerebral small vessel disease (SVD)
6. Amyloid-beta (Aβ)
7. Cerebral blood flow (CBF)
8. Pulse wave velocity (PWV)
9. Arterial spin labeling (ASL)
10. Magnetic resonance imaging (MRI)
11. Cerebral perfusion pressure (CPP)
12. Mean arterial pressure (MAP)
13. Apolipoprotein gene (*APOE*)
14. Apolipoprotein E protein (ApoE)
15. Cardiac magnetic resonance imaging (CMR)
16. Normal cognition (NC)
17. Mild cognitive impairment (MCI)
18. Pseudocontinuous arterial spin labeling (pCASL)
19. Regional CBF (rCBF)
20. Single-nucleotide polymorphism (SNP)
21. Framingham Stroke Risk Profile (FSRP)
22. Body mass index (BMI)
23. Circle of Willis (CoW)
24. Posterior communicating artery (PcoA)
25. Fetal-type posterior cerebral artery (FTP)
26. Internal carotid arteries (ICA)
27. Basilar artery (BA)
28. Posterior cerebral arteries (PCA)
29. Anterior communicating artery (AcoA)
30. Magnetic resonance angiography (MRA)
31. Delis-Kaplan Executive Function System (DKEFS)
32. California Verbal Learning Test, 2nd edition (CVLT-II)
33. Biber Figure Learning Test (BFLT-II)

CHAPTER 1[a]

Introduction

As the population continues to age, the public health impact of age-related cognitive decline, Alzheimer's disease (AD), and related dementias (ADRD) is rapidly expanding.[1] Cognitive dysfunction associated with normal aging and disease is common among older adults (**Table 1.1**), and AD burden is expected to double nationwide[2] and triple internationally[3] by 2060 due increasing numbers and proportions of older adults. In lieu of treatments to effectively manage this public health crisis, there is a substantial need to better understand modifiable risk factors that accelerate normal and pathological aging at the earliest stages (i.e., when intervention efforts may be most effective). Unfortunately, clinical diagnosis, symptom management, and intervention efforts are significantly complicated by the multifactorial nature of both age-related cognitive decline and ADRD, particularly the exceedingly high prevalence of cerebrovascular disease (CVD) in aging.

In recognition of 1) the strong links between cardiovascular disease, CVD, and cognitive impairment and 2) the fact that it is often difficult to disentangle the cognitive contributions of vascular factors, the concept "vascular contributions to cognitive impairment and dementia" (VCID) has been proposed to encompass all vascular-related cognitive disorders regardless of pathogenesis (e.g., cardiovascular, cerebrovascular, genetic).[4,5] Recently, the National Institutes of Health designated VCID as a critical research priority given the proven ability to prevent and treat cardiovascular disease and hypertension.[6] The first large-scale clinical trial investigating modifiable risk factors for dementia, SPRINT-MIND, revealed that intensive blood pressure

[a] This chapter is adapted from "Hemodynamics in Alzheimer's Disease and Vascular Cognitive Impairment and Dementia" published in *Vascular Disease, Alzheimer's Disease, and Mild Cognitive Impairment: Advancing an Integrated Approach* (edited by Drs. David J. Libon, Melissa Lamar, Rodney A. Swenson, and Kenneth M. Heilman) and has been reproduced with the permission of the publisher and my co-author, Dr. Angela L. Jefferson.

control was effective at reducing the risk of prodromal dementia but not dementia itself.[7] Subsequent analyses of SPRINT-MIND data have revealed that blood pressure variability was associated with the development of probable dementia despite excellent blood pressure control, indicating that blood pressure variability has an independent effect on cognition that warrants further investigation.[8] Age-related stiffening of the arteries, particularly the aorta, is a primary driver of blood pressure variability, the development of hypertension, and many other markers of blood pressure dysregulation during aging.[9] The following research will thus investigate the role of aortic stiffness in cerebrovascular and cognitive dysfunction during aging. Findings will elucidate the roles of aortic stiffness as a biomarker for identifying individuals at hemodynamic and cognitive risk and as a potential mechanism leading to worse brain aging outcomes.

Table 1.1: Prevalence of Age-Related Cognitive Dysfunction & Neuropathology

Specific Condition or Disorder	Prevalence (adults aged 65+)	General Category
Age-associated Memory Impairment[10,11]	up to 38%[12]	Mild-to-modest cognitive impairment (up to 50% prevalence[13])
Age-associated Cognitive Decline	up to 27%[14,15]	
Mild Cognitive Impairment[16,17]	22%[2,18]	
Late Onset Alzheimer's Disease (i.e., 60-80% of dementia cases[1])	[A]11%[2,19]	Dementia (10-18% prevalence[18,20])
Vascular Dementia (i.e., 15-20% of dementia cases[21])	[B]2-3%	
Neuropathology	**Prevalence (general population without dementia)**	**General Category**
Amyloid positivity	20-40%	—
Cortical Infarcts	11-35%[21]	Small Vessel Disease Biomarker
Lacunar Infarcts	5-20%[21,22]	
Microbleeds	15-40%[21]	
Mixed Pathology (Alzheimer's + Small Vessel Disease)	>50%	—

Note. Cognitive dysfunction associated with normal aging is very common (27-38%), and can be clinically applied in healthy persons as young as age 50.[10] Age-associated memory impairment represents the mildest form of age-related cognitive dysfunction and is characterized by self-perception of memory loss and a standardized memory test score showing a decline in objective memory performance compared with younger adults.[23] As many as 50% of older adults experience mild-to-modest cognitive impairment that does not interfere with normal daily living but may reduce the

ability to learn new information, slow mental processing and performance speeds, and increase susceptibility to distractions.[13] Dementia is a general term reflecting more severe cognitive impairment that interferes with daily life. Specific types of clinical dementia include Alzheimer's disease, vascular, mixed, Lewy body, frontotemporal, and less common forms (e.g., Huntington's disease).

[A] Alzheimer's disease dementia estimates reflect the presence of amyloid-beta, tau, and other neuropathology associated with dementia. Mixed dementia is more common than previously recognized, with more than 50% of people diagnosed with Alzheimer's dementia showing co-occurring neuropathology.[24,25]

[B] Vascular dementia estimates reflect the presence of cerebrovascular disease neuropathology alone.

1.1 Early Cerebrovascular Dysfunction Accelerates Cognitive Aging

Vascular risk factors are a significant contributor to both age-associated cognitive decline and dementia.[26-28] Cerebrovascular pathologies are commonly reported in 50-84% of older adults and independently relate to cognitive decline, particularly features of cerebral small vessel disease (SVD).[29] In fact, CVD may help partially explain patterns of age-related cognitive decline given that CVD predominantly affects the same neural systems, particularly the prefrontal cortex and medial temporal lobe, and patterns of SVD in neurodegenerative diseases are remarkably similar.[30] In the last half-century, a growing body of evidence has shown that the majority of AD pathology co-occurs with cerebrovascular disease.[31] Specifically, up to 80% of clinical dementia cases are thought to have a cerebrovascular pathological etiology[31] and over 56% of autopsy-confirmed AD cases include cerebrovascular pathology.[32] However, it has been incredibly difficult to disentangle the effects of SVD from AD and other related disease processes.

SVD likely increases the risk for both pathological and clinical AD in its earliest stages (**Figure 1.1**, top), interacting with neuropathological proteins to lower the threshold for the clinical expression of dementia and promote more rapid cognitive decline. Co-occurring cerebrovascular pathologies contribute to earlier clinical onset and more rapid decline in cognition,[33] lowering the threshold of AD pathology needed to develop clinical dementia,[34-36] and magnifying the effect of early AD changes. However, whether co-occurring neuropathology interact or independently affect clinical disease progression remains an open question. Strong evidence suggests each neuropathology likely contributes to clinical progression along shared pathways. Furthermore, the

clinical impact of co-occurring neuropathology may depend on the severity of AD neuropathology, with greater effects of co-occurring neuropathology when detectable AD neuropathology is lowest.

SVD pathologies and radiological features likely result from hemodynamic dysregulation promoted by aortic stiffness, including increasing blood pressure variability and systolic blood pressure. Specifically, blood pressure dysregulation induces arteriolar wall disintegration (e.g., arteriolosclerosis, cerebral amyloid angiopathy) and hemodynamic events (e.g., capillary dysfunction in the absence of physical flow-limiting vascular pathology[37]), both of which weaken the vulnerable endothelium of cerebral vessels and capillaries and promote blood-brain barrier (BBB) permeability.[38-40] Confirming this tight relationship between SVD and hemodynamic dysregulation, the first integrative data-driven model of AD progression demonstrated that cerebral hypoperfusion is the earliest alteration in the clinical progression of AD (**Figure 1.1**, bottom).[41] Findings suggest vascular dysregulation may have a role in the early cascade of events associated with the AD.

Figure 1.1: Cerebrovascular Disease & Cerebral Hypoperfusion Occur Early in AD (from Kalaria et al., 2021[30] and Iturria-Medina et al., 2016[41])

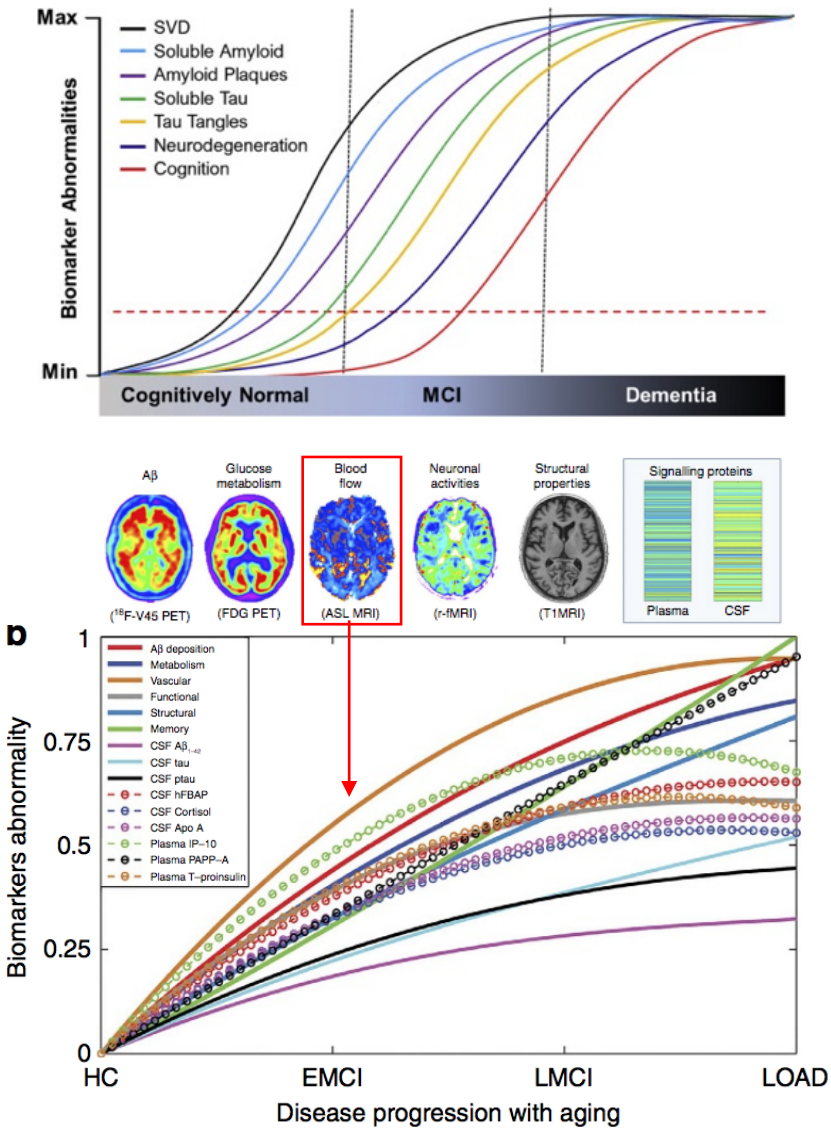

Note. Top Panel: Newer theoretical models of AD progression (Kalaria et al., 2021[30]) propose that SVD features, especially clinically silent lesions or covert changes, precede classically recognized AD biomarkers and may be a part of and modify clinical progression by shifting the threshold for cognitive impairment. The proposed spectrum of early SVD features includes changes in vascular function, such as CBF, blood pressure variability, perfusion pressure, PWV, and BBB damage, but whether cerebrovascular and hemodynamic markers precede the classically recognized biomarkers of disease is debatable. **Bottom Panel:** Iturria-Medina et al., 2016[41] published the first integrative data-driven model of AD progression using Alzheimer's Disease Neuroimaging Initiative biomarkers (e.g., spatiotemporal alterations in brain Aβ deposition, metabolism, vascular, functional activity at rest, structural properties, cognitive integrity, and peripheral protein levels), which suggested cerebral hypoperfusion is the earliest alteration; their proteomics findings also indicate peripheral vascular and inflammatory CSF proteins are the strongest protein alterations (i.e., higher sensitivity to disease progression than CSF $A\beta_{42}$ and tau), including peripheral inflammation (i.e., plasma IP-10), peripheral insulin resistance (i.e., plasma proinsulin), and lipid/fatty acid metabolism (CSF hFABP,[42] CSF ApoA[43]) proteins. While interactions between vascular and neurodegenerative processes may not be understood, findings suggest vascular dysregulation may have a role in the early cascade of events associated with the AD progression.

1.1.1 Cerebral Hemodynamic Regulation is Normally Protective but Susceptible to Aging

The brain is one of the most metabolically demanding organs in the human body, consuming 20% of total oxygen[44,45] and glucose[46] metabolism and 10-15% of cardiac output[47,48] despite only accounting for 2-3% body mass. Since the brain has minimal local energy reserves available, its metabolism is highly dependent on a continuous supply of blood for access to oxygen and glucose. Given its high energy demands, the brain is thus one of the highest perfused organs and is incredibly sensitive to metabolic deficits, with ischemia-hypoxia causing irreversible neuronal damage within five minutes. To maintain appropriate blood flow levels, the brain has sophisticated mechanisms of cerebrovascular regulation that 1) ensure consistent cerebral blood flow (CBF) levels regardless of external, ongoing fluctuations in systemic blood pressure and 2) meet internal, activity-based fluctuations in metabolic demand for additional blood.

CBF is tightly controlled by different mechanisms depending on the stimulus, including variations in steady-state perfusion pressure (i.e., cerebral autoregulation), neural metabolism (i.e., neurovascular coupling), and rapid changes in perfusion pressure (i.e., neurogenic control). Cerebral autoregulation is the primary process that maintains stable CBF in the face of changes in cerebral perfusion pressure driven by successive cardiac cycles (**Figure 1.2A**). Autoregulation mechanisms regulate cerebrovascular resistance to flow by changing cerebral vessel diameters (i.e., the myogenic response defined by vasoconstriction or vasodilation in response to intravascular blood pressure).[49] Vasoconstrictions increase resistance to counteract high cerebral perfusion pressures, while vasodilations reduce flow resistance to supplement low perfusion conditions. Autoregulation thus protects the brain against central blood pressure fluctuations by counterbalancing changes in the cerebral perfusion pressure gradient. Cerebral autoregulation is maintained across the healthy mean arterial pressure (MAP) range of 60-150 mmHg, but pathological elevations in pressure outside of this range (e.g., hypertension) as well as alterations in vascular resistance (e.g., head trauma) can lead to a loss of these homeostatic mechanisms (**Figure 1.2B**). When cerebral autoregulation is compromised, cerebral perfusion becomes more

affected by central blood pressure and susceptible to pathological changes. In addition to dynamic changes in diameter determined by the myogenic response, basal cerebrovascular tone is also influenced by inherent structural properties that alter fluid dynamics, including compliant wall structures,[50] variable blood viscosities,[51] and non-laminar flow profiles near vessel branches[52] that promote countercurrent, disorganized, or higher velocity patterns (e.g., vortex and turbulent flow). Ultimately, age-related compromises in the structural and functional properties of cerebral arteries compromises the brain's hemodynamic regulation mechanisms and make it more vulnerable to systemic hemodynamics (e.g., age-related cardiovascular changes).

Figure 1.2: Hemodynamic Determinants of Cerebral Autoregulation

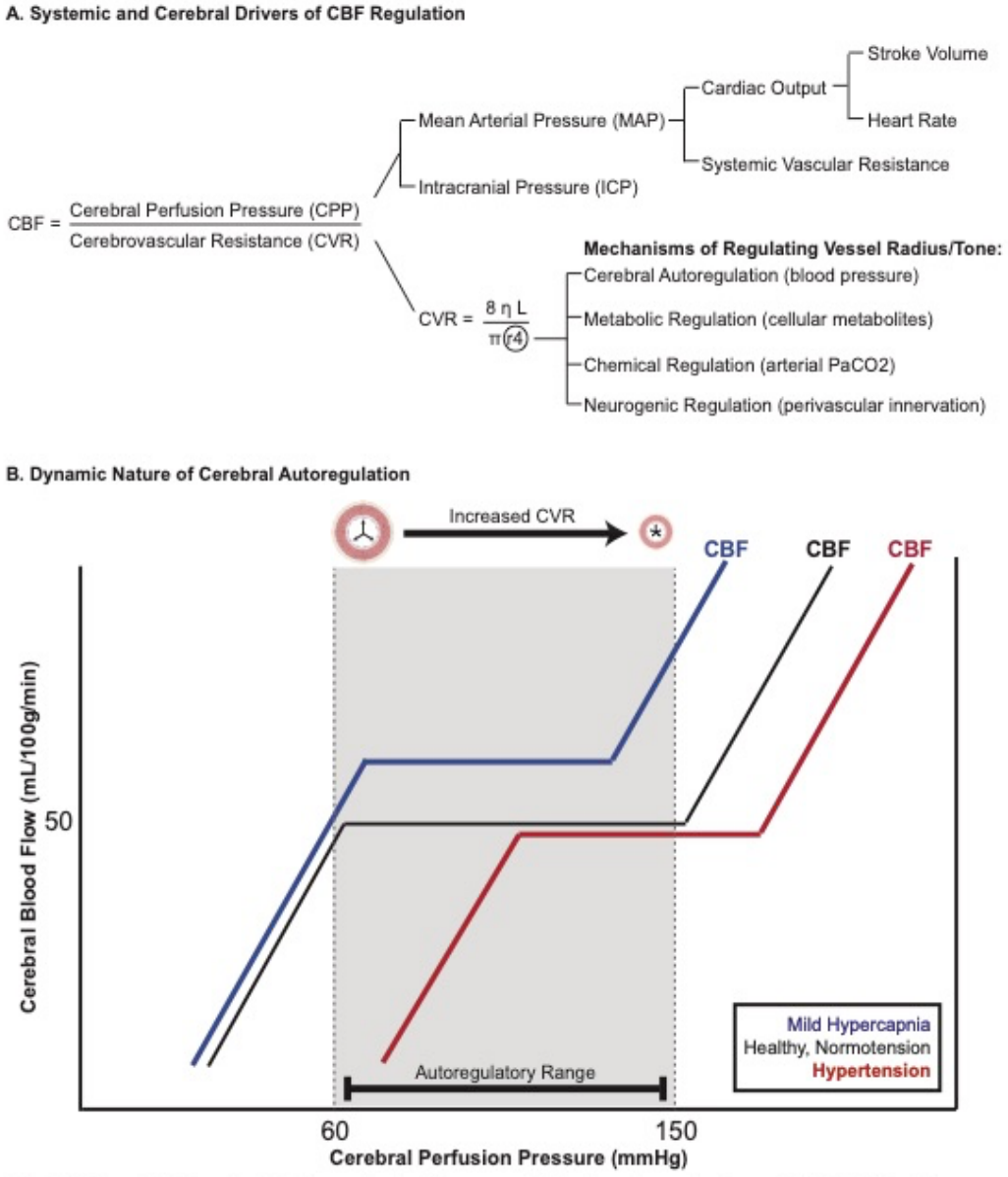

Note. Panel A: Cerebral blood flow (CBF) regulation is based on the balance of cerebral perfusion pressure (CPP) and cerebrovascular resistance. CPP is driven by mean arterial pressure (MAP), a measure of inflowing blood pressure determined by systemic cardiovascular function. Cerebrovascular resistance is driven by arterial radius (i.e., myogenic tone), which is regulated by a combination of cerebral autoregulation, metabolic regulation, chemical regulation, and neurogenic regulation mechanisms. **Panel B:** Cerebral autoregulation is the primary mechanism that maintains stable CBF in the presence of fluctuating central blood pressure. Although CBF is thought to remain constant over CPP of 60-150 mmHg, conditions such as hypercapnia (end-tidal CO_2 >45mmHg) and hypertension (blood pressure >130/90 mmHg) may cause shifts in the autoregulatory curve and promote increased vulnerability to hemodynamic dysregulation.
L = vessel length
η = blood viscosity
r= vessel radius

1.2 Cardiovascular Dysfunction Increasingly Impacts Brain Health over the Lifespan

As the central blood pump of the human body, the heart plays an essential role in hemodynamic regulation and determines critical characteristics of initial blood flow, including volume, pressure, and pulsatility. Like dementia, cardiovascular dysfunction becomes increasingly common with advancing age, with 28% of older adults experiencing some form of prevalent cardiovascular disease (e.g., coronary heart disease, angina, heart attack, heart failure, or peripheral artery disease).[53] Furthermore, as many as 97% of older adults also have at least one key cardiovascular risk factor, including high blood pressure, diabetes, high cholesterol, or smoking, all of which are associated with a higher burden of subclinical cardiovascular dysfunction.[54] Strongest evidence suggests both mid-life hypertension and obesity are associated with future risk of dementia.[55] It is clear that alterations in cardiovascular structure and function has implications for brain health, particularly among older adults with more vulnerable cerebrovascular systems.

Outside of dementia outcomes, severe cardiac dysfunction in the form of clinical heart failure is a known risk factor for cognitive impairment,[56-58] likely through microvascular dysfunction and reduced CBF.[59,60] However, evidence from our group[61-63] and others[64,65] suggests even subclinical reductions in cardiac output are associated with worse cognitive outcomes. Lower cardiac output is associated with worse executive function in aging cardiac patients,[61] worse information processing speed and executive function in middle-age and older community dwelling adults,[62,65] and a higher risk of incident clinical dementia and AD in community-dwelling aging adults.[63] Nearly all of these findings persist when excluding participants with heart failure, prevalent cardiovascular disease, or arrhythmias,[62,63,66] suggesting subclinical changes in cardiovascular function with advancing age correspond to worse cognition and cannot be explained by shared vascular risk factors or disease.

Theoretical models linking more severe cardiac dysfunction to AD support reduced systemic perfusion as a primary driver of reduced CBF (as we have recently observed in a subclinical

setting[67]) but further implicate maladaptive neurohormonal changes, inflammation, and microvascular dysfunction as secondary contributors to impaired CBF.[59] These more mild, prolonged damage pathways are likely larger drivers of cerebrovascular and neuronal dysfunction in subclinical cardiac dysfunction rather than outright ischemia and neuronal failure. It is important to note that although cerebral autoregulation mechanisms generally serve to maintain a constant CBF level (see **Section 1.1.2** above**)**, the accumulation of vascular risk factors and vascular damage with older age may compromise the integrity of these mechanisms.[68] Thus, in the setting of advanced aging with a lifetime of vascular burden exposure, subtle cardiovascular dysregulation may exert a larger adverse impact on brain health, including the development or progression of SVD, AD pathology, and neurodegeneration.

1.3 Age-Related Aortic Stiffness Relates to Compromised Brain Aging

Most recently in human studies, age-related aortic stiffness (as assessed by aortic pulse wave velocity (PWV)) has been associated with compromised white matter microstructure (e.g., demyelination and axonal degeneration biomarkers on diffusion tensor imaging), SVD[69] (e.g., silent subcortical infarcts,[70] white matter lesions[70,71]), and neurodegeneration (e.g., lower grey matter volume [71,72]). While age-related aortic stiffness is purported to drive microvascular tissue damage via earlier-stage cerebral hemodynamic dysfunction (e.g., increased pulsatility, cerebral hypoperfusion), this hypothetical link has yet to be well characterized among older adults (**Figure 1.3**). However, studies at the research forefront suggest broader central arterial stiffness may relate to numerous determinants of the CBF response (e.g., cerebrovascular resistance among older adults, blood pressure dysregulation among older adults, cerebrovascular hemodynamic pulsatility among younger adults, impaired ability to augment blood flow in response to stimuli among older adults), all of which are likely functional consequences of stiffness-induced target organ damage (e.g., arterial remodeling, endothelial dysfunction) in theoretical models. Yet, no studies to-date have examined associations between age-related aortic stiffness and CBF among older adults,

although smaller studies using middle-aged adults or indirect (and severely limited) ultrasound indices of CBF suggest this may be the case among older adults. Furthermore, most PWV-cognition studies have relied on cross-sectional approaches and measures of global cognition,[69] highlighting the need for longitudinal cognitive studies capable of examining numerous cognitive domains reflective of distinct region- or network-related brain function.

Figure 1.3: Purported Effects of Aortic Stiffness on Brain Health (adapted from Jefferson, Cambronero et al., 2018[73] and Iulita et al., 2018[74])

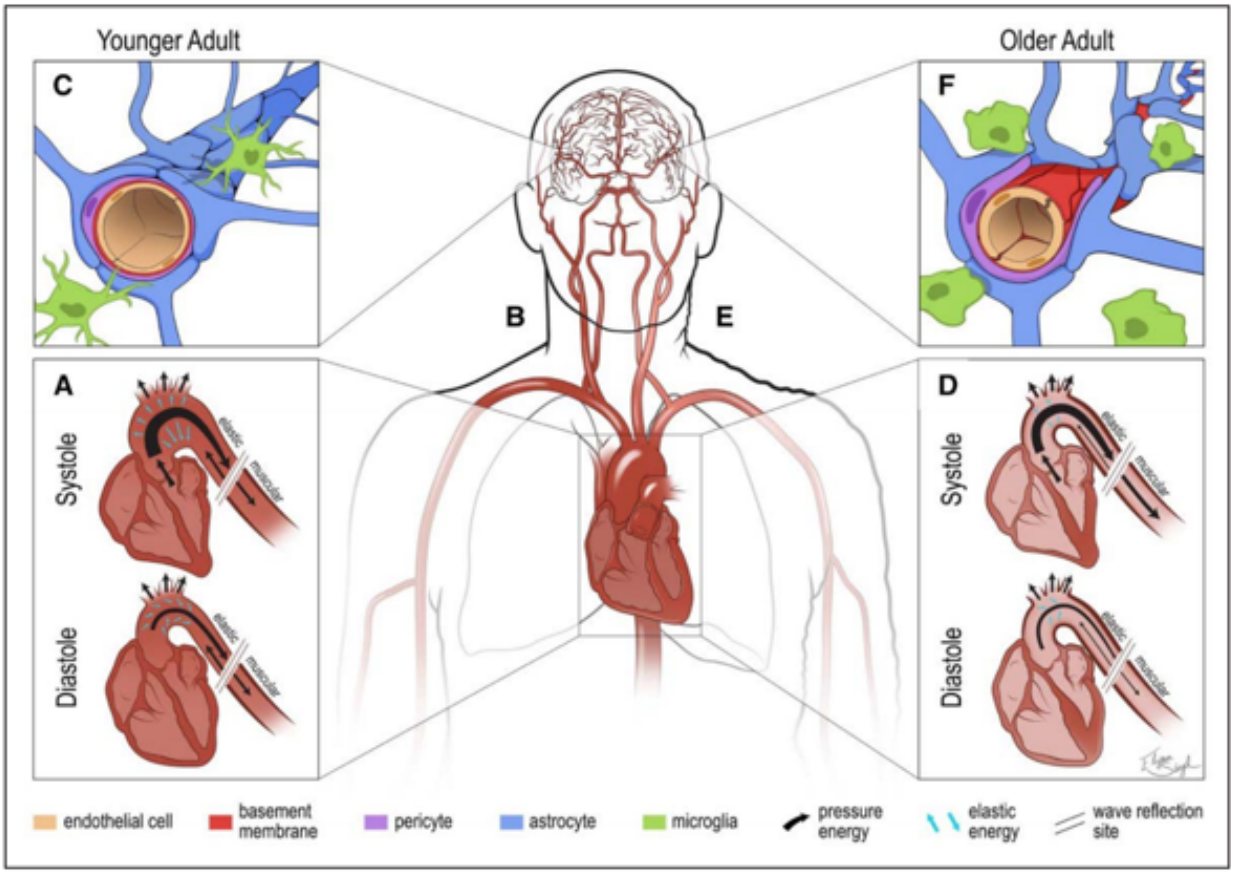

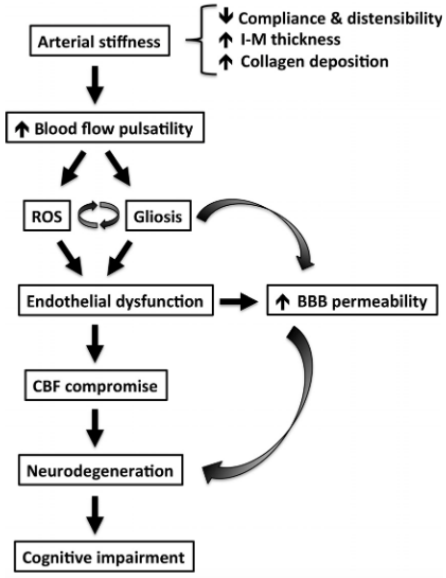

Note. Top Panel: (A) A healthy aortic wall is compliant, and vascular segments gradually stiffen toward the periphery. Mismatch in vascular wall properties and gradual arterial branching creates beneficial wave reflection sites that reduce forward pulsatile transmission and reflect backward waves for cardiac reperfusion. (B) A compliant aorta mediates continuous blood flow throughout the cardiac cycle and dampens pulsatility. (C) Blood flow from the heart into the brain is further regulated by microvascular vasodilation and vasoconstriction. These mechanisms can ensure adequate delivery of energy substrate to tissue and serve to dampen pulsatile energy. (D) With advancing age, the aorta thickens and stiffens, reducing impedance mismatch, increasing transmission of damaging pulsatility into end organs, and contributing to early retrograde waves that augment systolic pressure and reduce diastolic flow over time. (E) These changes may contribute to reduced perfusion in high-flow vulnerable organs and possibly more turbulent flow throughout the system. (F) The effect of aortic stiffness on cerebrovascular structure and function in humans is less well studied. Existing evidence suggests that aortic stiffness contributes to altered vascular resistance, corresponding cerebral perfusion pressure, and compromises in blood-brain barrier integrity, potentially contributing to reduced brain perfusion. **Bottom Left Panel:** Based on animal studies, proposed mechanisms by which arterial stiffness leads to cognitive impairment include higher pulsatility of large and medium-sized blood vessels, increased state of oxidative and inflammatory damage, and disruption of endothelial cell function, leading to blood-brain barrier permeability, neurovascular uncoupling, and CBF compromises.

1.4 Patterns of Cerebral Hemodynamic Dysregulation in Aging & AD

1.4.1 Aging-Related Perfusion Changes

Brain structure, activity, blood flow patterns, and cognitive abilities all undergo patterned changes with normal aging. While AD and other dementias impair daily function, age-associated cognitive impairments are subtle, including occasional forgetfulness and slower information processing speeds.[75] These cognitive impairments reflect similarly subtle structural and functional brain changes, including tissue perfusion. The earliest CBF studies using gold-standard PET measurements demonstrated CBF reductions in the aging brain, particularly in limbic or association cortices.[76] More recent studies using arterial spin labeling (ASL) magnetic resonance imaging (MRI) have reliably confirmed global hypoperfusion with age but also revealed regional hyperperfusion patterns. Older adults experience decreased perfusion predominantly in precuneus, superior temporal region, and orbitofrontal region, but they also experience increased perfusion in caudate, posterior cingulate, anterior cingulate and amygdala.[77] Furthermore, flow asymmetry is inversely related to memory performance in cognitively normal adults,[78] suggesting increasingly asymmetrical perfusion patterns may be a marker of worse cognitive aging.

Unlike neurodegeneration, the mechanisms underlying age-related changes in CBF remain harder to isolate and largely unclear. Decreased regional CBF (rCBF) in older adults may result from a reduction in neuronal and synaptic number or activity, which can manifest as brain atrophy and reduced CBF demand. However, age-related declines in CBF also occur independent of atrophy,[79,80] and in these cases, decreased rCBF may be due to microvascular damage which can also act as a primary driver of neurodegenerative processes in aging and AD. Theories in the AD literature further suggest that hypoperfusion patterns may serve as a remote indicator of medial temporal cortex damage or a general indicator of functional disconnection.[81,82] On the other hand, increased rCBF can indicate pathological neural overactivation[83] or compensation for failing neighboring regions.

It is very likely that a lifetime burden of systemic vascular risk factors may contribute to dysregulation of blood supply, particularly when cerebral autoregulation mechanisms begin to fail. For example, autoregulation may become compromised in hypertension,[84] leading to a rightward shift in the pressure-perfusion curve (**Figure 1.2B)** for which higher perfusion pressures are needed to maintain the same level of CBF. Failing autoregulatory mechanisms may make the brain more susceptible to central hemodynamic changes. Recent research suggests among older adults with no history of clinical dementia or stroke, subclinical and modest alterations in systemic hemodynamics, including arterial stiffness[73] and reductions in cardiac output,[67] are related to reductions in CBF independent of co-occurring vascular risk factors (e.g. hypertension, diabetes) and prevalent cardiovascular disease. These associations are particularly evident in the temporal lobes. Growing evidence supports widespread relationships between common cardiovascular risk factors and alterations in CBF. Theoretical models, such as Zlokovic's "two-hit hypothesis," suggest these initial, mid-to-late life vascular alterations may increase the brain's susceptibility to oligemic or ischemic injury, cognitive impairment, and AD later in life.[85]

1.4.2. AD-Related Perfusion Changes

Deviations from normal aging CBF profiles occur early in AD progression, before detectable tissue atrophy,[41,86] and most noticeably as global hypoperfusion that correlates with cognitive impairment.[87] However, many studies have reported a mismatch in regions affected by cerebral hypoperfusion and neurodegeneration in AD, indicating that early hypoperfusion may relate to neurodegeneration through general functional disconnection (e.g., across the default mode network) or serve as a biomarker of damage in the distal but connected medial temporal cortex.[81] For example, while early hypoperfusion of the medial parietal cortex (i.e., precuneus, posterior cingulate cortex) and posterior temporoparietal cortex appear to be most consistently implicated in AD,[81,88,89] atrophy of the distant medial temporal cortex (in particular the entorhinal cortex and

hippocampus[90]) is the earliest structural change in AD.[91] Associations between hypoperfusion in watershed regions (i.e., precuneus, angular gyrus) and medial temporal cortical atrophy support their interconnectedness.[81] Interestingly, unlike normal older adults, flow territory asymmetry is positively correlated to memory performance in adults with prodromal AD,[78] suggesting flow asymmetry may further develop as a protective mechanism in early, prodromal AD to recruit additional resources for tissue operating at maximal cerebrovascular capacity. However, the question of whether vascular insufficiencies reflect emerging neurodegeneration or pathology, rather than serving as primary drivers of neurodegeneration in aging and AD, remains highly debated. Hypoperfusion in AD likely reflects the combined disease burden of neurodegeneration and SVD,[92] and longitudinal evidence in community-dwelling adults suggests lower CBF may drive brain atrophy over time in adults over age 65.[93] Furthermore, watershed cortical infarcts have been associated with AD, indicating that cerebral hypoperfusion may aggravate the degenerative process and worsen dementia by inducing cortical watershed microinfarcts in addition to well-established white matter changes.[94] The most prominently featured vascular dysfunction pathways linked to AD in the literature to-date include BBB breakdown, hypoperfusion-hypoxia, and endothelial metabolic dysfunction.

1.4.2.1 AD Pathology Promotes Vascular Dysfunction

Cerebrovascular pathology has overlapping and even possibly synergistic effects with amyloid and tau pathologies, the pathological hallmarks of AD.[85] In autopsy series, cerebrovascular pathology reflects the second most common pathology after AD[31] and the most common pathology to co-occur with AD.[95,96] Furthermore, vascular dysfunction is common in AD. Both patients with prodromal AD[97] and transgenic AD mouse models [98,99] have accelerated BBB breakdown, along with focal microcirculatory changes, such as string vessels, alterations in capillary density, rises in endothelial pinocytosis, decreases in mitochondrial content, accumulation of basement

membrane proteins,[100] and loss of tight junctions.[85] These prominent AD-related vascular changes have intimate interactions with Aβ and tau pathology, as described below.

Amassing evidence suggest cerebrovascular compromise may contribute to impairments in amyloid transport across various clearance pathways. Aβ is eliminated from extracellular spaces primarily via exchange across the BBB.[101] However, a smaller percentage of Aβ clearance is also supported by interstitial fluid (ISF) bulk flow pathways, including traditional perivascular clearance[102] (i.e., CSF drainage through the periarterial space and along smooth muscle cell walls of capillaries and arteries)[103-106] and glymphatic perivascular clearance (i.e., CSF drainage through the perivenous space).[107-109] Small vessel injury likely affects Aβ accumulation across varied perivascular[110,111] and BBB[112] clearance pathways. Molecular evidence in AD further indicates impairments in Aβ receptor expression along the BBB, including increased receptors for advanced glycation end products involved in Aβ influx into the brain and decreased lipoprotein receptor-related proteins involved in Aβ efflux into the circulation.[113] In addition to clearance impairments, hypoperfusion in AD creates a metabolically deregulated environment (e.g., glucose hypometabolism) and stimulates both entry and aggregation of peripheral Aβ into the vasculature as well as production and deposition of Aβ in the parenchyma.[114,115] Furthermore, although Aβ is known to be produced from neuronal membranes, local Aβ release from degenerating smooth muscle cells highlights potentially overlapping roles of cerebrovascular cells in Aβ production.[116] Chronic hypoperfusion may promote Aβ pathology across tissues through aberrant amyloid precursor protein processing (e.g., increases in β-secretase/γ-secretase amyloidogenic activity[117]), but stronger evidence suggests cerebrovascular dysfunction may promote Aβ accumulation more so through abnormal clearance pathways rather than upregulated production pathways.

Evidence supporting Aβ-vascular interactions suggests pathological changes in CBF may occur along shared pathways with Aβ pathology (**Figure 1.4**). For example, higher global Aβ loads are associated with reduced CBF.[118] Notably, various forms of Aβ can impair vessel function,

including parenchymal plaques, toxic soluble oligomers,[119] and widespread vascular deposits (i.e., cerebral amyloid angiopathy), the latter of which occurs in 82-98% of AD cases.[120] On a cellular level, Aβ pathology promotes oxidative stress and inflammation, which cause endothelial and pericyte damage, basement membrane thickening, and degeneration of smooth muscle cells, a common feature of AD. This Aβ-induced cerebrovascular disruption is thought to promote BBB permeability, inducing angiogenesis as a regenerative (but likely maladaptive) response. However, alternative hypotheses suggest Aβ may directly stimulate pathological angiogenesis in AD independent of vascular damage, thereby implicating hypervascularization as the cause (rather than the effect) of BBB disruption and a potential therapeutic target.[121] Regardless of the underlying causality, Aβ-associated loss of vascular integrity compromises the structural and functional integrity of cell types involved in hemodynamic regulation, driving BBB transport impairments, endothelial dysfunction, and CBF dysregulation throughout the arterial tree.

Figure 1.4: Spatial Progression of AD Neuropathology (from Jucker et al., 2013[122])

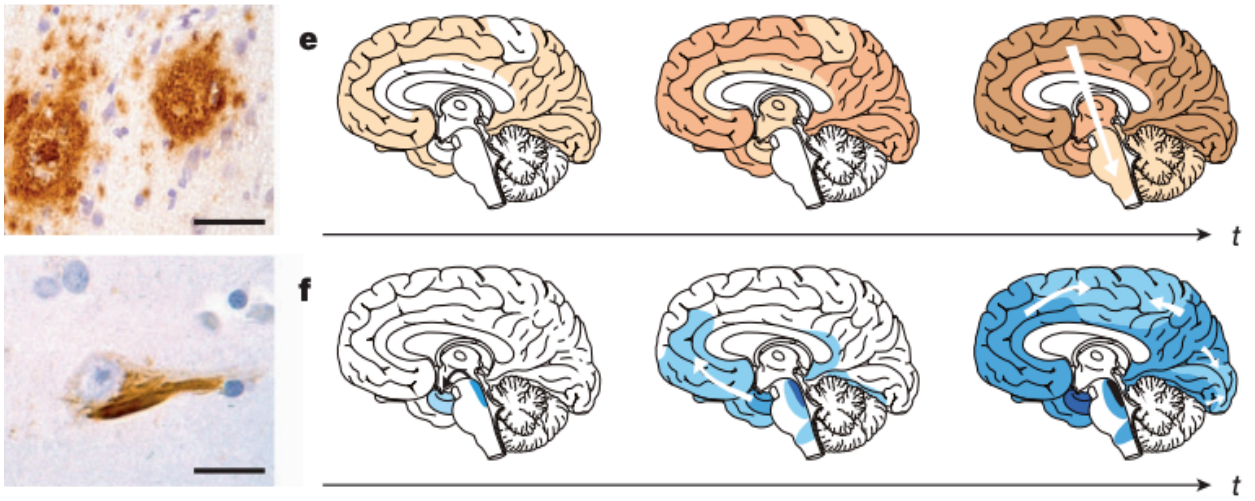

Note. AD is characterized by diffuse extracellular, neuritic Aβ plaques (top left) along with intracellular neurofibrillary tangles and neuropil threads composed of hyperphosphorylated tau (bottom left). As the level of Aβ reaches a tipping point, there is a rapid spread of tau throughout the brain, and the currently most accepted model indicates Aβ pathophysiology may be an upstream pathophysiological event that triggers/facilitates downstream tau pathways (e.g., tau misfolding, tau-mediated toxicity, accumulation in tangles, tau spreading that leads to cortical neurodegeneration).[123] **Panel E:** The Thal et al., 2002 Aβ phase (TAP) scoring system describes Aβ spread from neocortex, to allocortex, and finally subcortical regions; darker regions indicate continued Aβ deposition in the same areas.[124] Preclinical stages (Phases 1-3) include neocortical temporobasal and frontomedial areas (e.g., anterior and posterior cortical midline structures, lateral temporo-parietal association areas, and the inferior temporal lobe) (Phase 1); allocortex (e.g., entorhinal region, hippocampus CA1) (Phase 2); subcortical regions (e.g., diencephalic nuclei, striatum, the cholinergic nuclei of the basal forebrain, thalamus) and primary sensory-motor areas (Phase 3). Clinical stages (Phases 4-5) include brainstem nuclei (e.g., substantia nigra) (Phase 4); and cerebellum and lower brainstem nuclei (e.g., pontine nuclei, locus coeruleus) (Phase 5).[124] Competing theories propose that Aβ accumulates i) due to transmission from a small number of seed regions through neuroanatomically connected regions [124] (e.g., retrograde transport from axon terminals near Aβ plaques by means such transynaptic spread[125-127]) or ii) due to different inherent regional carrying capacities,[128] wherein Aβ starts in all brain regions simultaneously but regions with higher carrying capacities will accumulate more amyloid over time (e.g., anterior cingulate gyrus, precuneus, frontal operculum cortex).[124] **Panel F:** The six Braak et al.,1991[90] tau stages describes tau tangles first in the transentorhinal cortex, subsequent spread throughout the medial and basal temporal lobes, then into neocortical associative regions, and finally into the unimodal sensory and motor cortex; darker regions indicate continued hyperphosphorylated tau deposition in the same areas. Unlike long-term transmission of Aβ aggregates, tau aggregates are likely successively re-generated; various tau species spread along neuroanatomically connected regions via prion-like self-propagation, wherein pathogenic misfolded tau is internalized and acts as "seeds" that recruits soluble endogenous tau into larger aberrant conformations that continue to propagate across interconnected brain regions.[129] While strong evidence suggests neurofibrillary tangles and neuropil threads occur first in the locus coeruleus (i.e., transentorhinal cortex), evidence of the earliest regions accumulating amyloid is mixed, including reports of temporal lobe regions[130] (consistent with early neuropathological estimates) and default mode network core regions[131-133] (i.e., precuneus, medial orbitofrontal cortex, anterior and posterior cingulate cortex).

In addition to Aβ pathology, hyperphosphorylated tau oligomers have been shown to accumulate in the microvasculature of AD patients[134] and induce blood vessel abnormalities (e.g., spiraling morphologies, lower vessel density) as well as CBF obstructions.[135] Although cerebrovascular effects of hyperphosphorylated tau may be a consequence of increased soluble Aβ around cortical arteries,[136] hyperphosphorylated tau may also have Aβ-independent associations with CVD. Recent evidence indicates that neurofibrillary tau pathology mediates cognitive decline independent of Aβ pathology.[137] Furthermore, chronic cerebral hypoperfusion enhances tau hyperphosphorylation,[138] including through hypertension-induced vascular dysfunction,[139] suggesting that hyperphosphorylated tau production may also be implicated in early CBF dysregulation events. Tau pathology is suggested to induce cerebral arterial remodeling prior to AD-related microvascular cerebral amyloid angiopathy,[140] and tau alone is known to initiate breakdown of the BBB.[141] Although it is not well-established whether tau pathology predominantly contributes to or is driven by the development of Aβ pathology, it undoubtedly serves a pivotal role as the final common pathway for cognitive impairment due to both vascular and AD pathologies.[137]

The vascular structural abnormalities in AD brains described above likely increase vascular resistance and contribute to hypercontractility and hypoperfusion. Indeed, recent studies show increased pulsatility and resistance indices in AD.[142] Moreover, functional deficits in neurovascular unit signaling may contribute to neurovascular uncoupling, which is well-documented in AD.[143-146] Age- and AD-related alterations in cerebrovascular structure and functional reactivity may reduce the efficacy of cerebral autoregulation,[147,148] especially when vascular risk factors are present.[68,147,149-151] In this manner, the brain may be more vulnerable to damage over time, particularly from exposure to subtle age-related alterations in cardiovascular hemodynamics.

1.4.2.2 AD Genetic Risk Promotes Cerebrovascular Dysfunction

Classic AD pathology does not fully account for cognitive impairment in clinical AD however, so other factors, such as cerebrovascular pathologies, likely contribute to a portion of clinical symptoms (in addition to potential overlapping synergistic effects with existing AD pathology discussed above). Cerebrovascular risk factors may worsen pathological AD progression or may be an initial contributor in dysfunction. In particular, the apolipoprotein E (*APOE*) ε4 allele, the strongest genetic risk factor for AD,[152] is also a well-supported molecular moderator of vascular damage. Furthermore, *APOE* ε4 is also among the most common AD risk alleles with a 25% heterozygote prevalence and 2-3% homozygote prevalence.

ApoE is a secreted lipoprotein whose major function is to transport cholesterol and other lipids in the bloodstream, and the e4 variant of this protein impairs intracellular lipid metabolism, thereby driving lipid imbalances that impair normal cellular function (e.g., molecular transport, generating energy).[153] In the brain specifically, ApoE4 (i.e., protein) is primarily expressed by astrocytes and microglia (i.e., cell types playing key roles in AD pathogenesis) and thus disrupts unique functions (i.e., lipid buildup in *APOE* ε4 astrocytes[153]).[154] While ApoE4 is known to drive Aβ pathology through both disruptions in metabolism and aggregation, it also drives disruptions in numerous Aβ-independent pathways that include synaptic plasticity, neuroinflammation, and cerebrovascular integrity and function.[155]

APOE ε4 genotype relates to decreased Aβ clearance and increased deposition,[156] which may drive vascular damage. However, *APOE* ε4 carrier status has also been shown to exert stronger effects than Aβ positive status on CBF changes in clinical AD and MCI,[157] suggesting this genetic risk factor may impact CBF through Aβ-independent pathways (i.e., outside the context of classical AD). Furthermore, *APOE* ε4 carrier status strengthens vascular associations with brain health outcomes, including atrophy and white matter integrity.[158] Individuals with AD have increased

blood brain barrier permeability, a pathology which is even more pronounced for *APOE* ε4 carriers[99] and associated with reduced cortical and hippocampal pericytes.[159] Experimental models in transgenic AD mice suggest cyclophilin A (CypA), a proinflammatory cytokine, is a key target for treating *APOE* ε4-mediated vascular damage, as astrocyte-derived *APOE* ε4 leads to activation of the proinflammatory CypA-matrix-metalloproteinase-9 pathway in pericytes, enzymatic degradation of tight junction proteins, blood brain barrier breakdown, and CBF reductions.[160] This damage to cerebrovascular integrity appears to occur prior to neuronal dysfunction.[160,161] Recent studies also suggest *APOE* ε4 presence drives pericyte degeneration and accumulation of CypA in pericytes and endothelial cells.[162] If individuals at genetic risk for AD experience impaired angiogenic or vasculogenic potential, they may be more susceptible to hypoperfusion and compromised vessel reactivity mechanisms.

1.5 Hypoperfusion-Hypoxia Drives Neuronal Dysfunction & Damage

To continuously process neural activity underlying cognition, the brain is highly dependent on neurovascular coupling to cellular demands, subsequent vascular blood supply, and efficient nutrient extraction/transport from blood to cells. Hypoperfusion-hypoxia (i.e., insufficient supply of oxygen relative to the tissue's metabolic demand due to low blood flow) rapidly increases vulnerability to cognitive impairment. Longer periods of hypoperfusion-hypoxia induce cell dysfunction and death that is exacerbated by reperfusion (see Kalogeris et al., 2012[163] for review of ischemia cell biology). In short, hypoperfusion-related tissue damage results from metabolic failure, including impairment of ionic pumps; ionic imbalance and accumulation of cytosolic sodium and calcium ions and extracellular potassium; resultant water influx into cells and tissue swelling; and permanent depolarization of cell membranes.[164] Ischemia-related cell injury ultimately promotes microvascular dysfunction (e.g., BBB breakdown), cerebrovascular pathology (e.g., white matter lesions, infarcts), and secondary neurodegeneration along with network-wide dysfunction.[165] Interestingly, animal models suggest the dominant mechanisms

underlying vulnerability to both oligemia and ischemia may very across the lifespan, including both BBB permeability and cellular vulnerability.[166] Across cell types, target cells for damage include vascular smooth muscle cells, endothelial cells (including BBB junctional complexes), oligedendrocytes, and neurons with high metabolic demands or within regions predisposed to low CBF supply (i.e., watershed regions). Among humans, regional differences in vulnerability to ischemia and tissue infarction also exist.

1.5.1 Regional Patterns of Vulnerability to Cerebral Hypoperfusion-Ischemia

The brain regions most vulnerable to hypoperfusion-hypoxia in normal aging are those with anatomical susceptibility to global hypoperfusion (e.g., watershed regions where the tissue is furthest from arterial supply), tissue with high metabolic demands (i.e., lower thresholds for hypoxic brain injury), and susceptibility for neurovascular unit dysfunction (e.g., neurovascular uncoupling; BBB permeability; impaired dilation reactivity and capillary tone). Thus, we can expect patterned susceptibility to hypoperfusion in regions such as lateral frontal and occipital cortex as well as white matter in the centrum semiovale or corona radiata (i.e., watershed regions); highly active grey matter; and hippocampus (i.e., sites of early-stage BBB breakdown in aging[167,168]). Additional characteristics that may affect vulnerability to hypoperfusion-hypoxia and underlie the heterogeneity of the blood oxygen-level dependent signal[169] include regional differences in the determinants of flow (e.g., pressure, resistance, vessel reactivity) as well as network-wide factors (e.g., reduced collateral support from neighboring regions), but these factors are less well investigated. Overall, vulnerability to hypoperfusion-hypoxia in aging is likely to occur due to a combination of intrinsic tissue factors and network-wide characteristics.

Evidence from animal models indicates that neuronal populations selectively vulnerable to ischemic damage include cortical pyramidal neurons; cerebellar Purkinje cells; subpopulations in the amygdala, striatum, thalamus and brainstem nuclei; and particularly consistent evidence in

support of CA1 hippocampal neurons.[170,171] In addition, oligodendrocytes (i.e., the dominant cell type of white matter tracts and producers of lipid-rich myelin) are particularly sensitive to brief global ischemia[171-173] and targeted by *APOE* ε4 effects.[174] Within white matter, the degradation of the frontal lobes is one of the earliest detectable changes in aging and AD, suggesting susceptibility to shared pathways such as vascular dysfunction.[174] Immediately outside of the infarct core, salvaged penumbra may also be affected by selective neuronal loss which hampers functional recovery.[175] Rodent occlusion models generate selective neuronal loss predominantly in the striatum and cortex,[175] specifically neocortex (layers 3, 5, and 6), the dorsolateral striatum (small to medium-sized neurons), and the hippocampal CA1 region.[176,177]

Among humans, patterns of regional ischemic vulnerability in the brain can be also be observed (**Figure 1.5**). The caudate body, putamen, insular ribbon, paracentral lobule, and precentral, middle, and inferior frontal gyri are among the top 20% of locations most highly sensitive to reductions in CBF.[178] In these highly vulnerable locations, approximately 60% reduction in rCBF distinguishes infarct core compared to approximately 85% in the remainder of the brain, providing further evidence for regional variations in the hypoperfusion-hypoxia threshold to neuronal damage among humans.[178] Findings also suggest selective neurophysiologic vulnerability of these brain regions (e.g., different neurochemical response to ischemia). Taken together, overlapping evidence from animal and human studies suggest dorsal striatum, frontal cortex, and CA1 hippocampal regions may be most vulnerable to hypoperfusion and ischemia.

Figure 1.5: Regional Ischemic Vulnerability to Hypoperfusion in the Brain (from Payabvash et al., 2011[178])

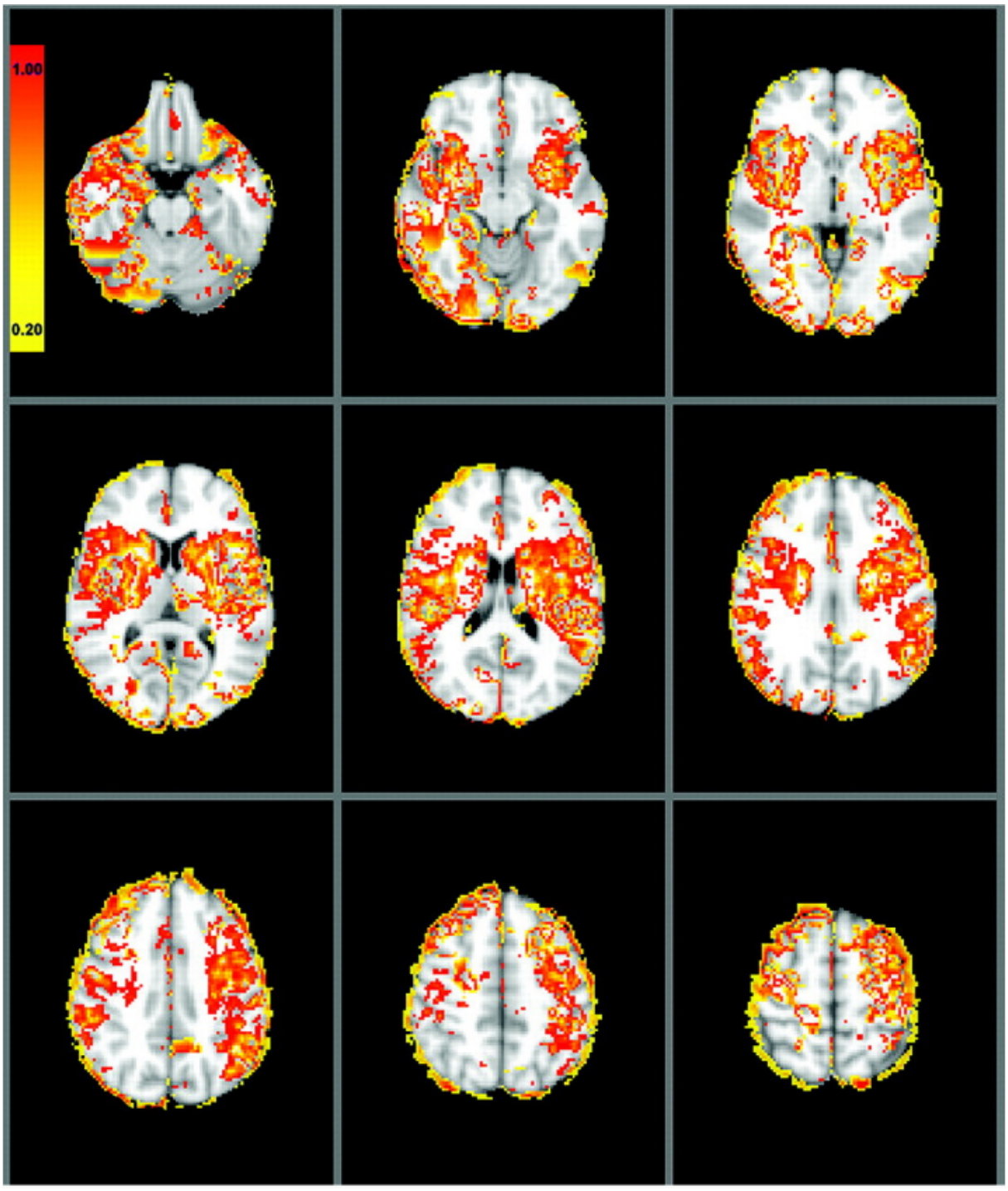

Note. The spatial patterns of cerebral ischemic vulnerability to hypoperfusion among 90 stroke patients demonstrated different brain regions had different percent infarction increase per unit rCBF reduction, including highest ischemic vulnerability to hypoperfusion among caudate body and putamen (i.e., dorsal striatum); insular ribbon (i.e., grey-white matter differentiation in the insular cortex); paracentral lobule (i.e., spanning frontal and parietal lobes); and precentral, middle, and inferior frontal gyri regions (i.e., widespread frontal involvement).

1.5.2 Significance of Oligemia & Early-Stage Neuronal Dysfunction

Prior to irreversible neuronal cell death and overt tissue damage (i.e., infarction), a spectrum of neuronal changes is induced by hypoperfusion-hypoxia, from mild reductions (i.e., oligemia) to partial or total restriction (i.e., ischemia) of blood. Stroke literature has revealed that tissue ischemia results in graded tissue damage, characterized by an infarct core and surrounding penumbra. The infarct core consists of dead, non-functioning tissue, which can further grow over time[179] due to peri-infarct depolarizations that create spreading waves of neuronal inactivation, vasoconstriction, and ischemia.[180] Interestingly, spreading depressions are exaggerated in AD models wherein they promote prolonged hypoxia.[181] However, outside of the infarct core, the penumbra is composed of reversibly injured brain tissue that is nonfunctioning but still living (provided blood flow is restored). The outermost region of the penumbra is referred to as oligemic, and hypoperfused tissue here will either function normally or suboptimally (but will survive irrespective of improvement in blood supply).[182] Beyond its traditional definition in stroke literature, oligemia also refers to an episode of low blood flow that causes molecular changes and subclinical neuronal dysfunction without cell death.

Among aging populations, oligemia sustained for years is often characterized as chronic cerebral hypoperfusion, a condition which is reflective of normal vascular aging and largely thought to be asymptomatic at its earliest stages.[183] While these common reductions of CBF are moderate, the fact that this mild hypoperfusion lasts for several years promotes progressive tissue damage. Thus, depending on the duration and severity of hypoperfusion (**Figure 1.6**, top) as well as the age of the subjects, chronic cerebral hypoperfusion likely promotes progressive cognitive impairment (e.g., executive dysfunction).[184] On a cellular level, chronic cerebral hypoperfusion induces a number of changes affecting the small cerebral vessels (e.g., BBB dysfunction, endothelial dysfunction), primarily through the promotion of worse tight junction integrity, excitotoxicity, inflammation, oxidative stress, and expression of matrix metalloproteinases (**Figure 1.6**, bottom).[184] Transient oligemia (i.e., short and mild hypoxia–ischemia) has been shown to induce

subtle changes in highly vulnerable neurons of the hippocampus and parietal cortex despite no gross tissue damage (e.g., long-term changes in receptor binding densities).[185] Furthermore, transient oligemia can also promote tau and amyloid-beta (Aβ) neuropathology, including long-lasting effects for several weeks post-oligemia.[186] Both the high prevalence of mild hypoperfusion among older populations and its well-documented contributions to neuronal dysfunction suggest it may be a potential mechanism underlying early-stage cerebrovascular dysfunction and subtle, subclinical cognitive impairment.

The onset of mild (but chronic) cerebral hypoperfusion from vascular risk factors is complicated as risk factors lead to multiple layers of damage before inducing cognitive dysfunction. However, as discussed in this chapter's opening paragraph, there is strong evidence to suggest that blood pressure dysregulation promoted by aortic stiffness may be a strong candidate precursor. Ultimately, the degree of association between vascular risk factors and cerebrovascular dysregulation (including early-stage hemodynamic dysregulation) is dependent on age, lifestyle, genetic susceptibility, comorbidity of other diseases, and differential brain reserves.

Figure 1.6: Chronic Hypoperfusion Promotes Cognitive Dysfunction via a Spectrum of Molecular & Cellular Injury (adapted from Rajeev et al., 2022[184])

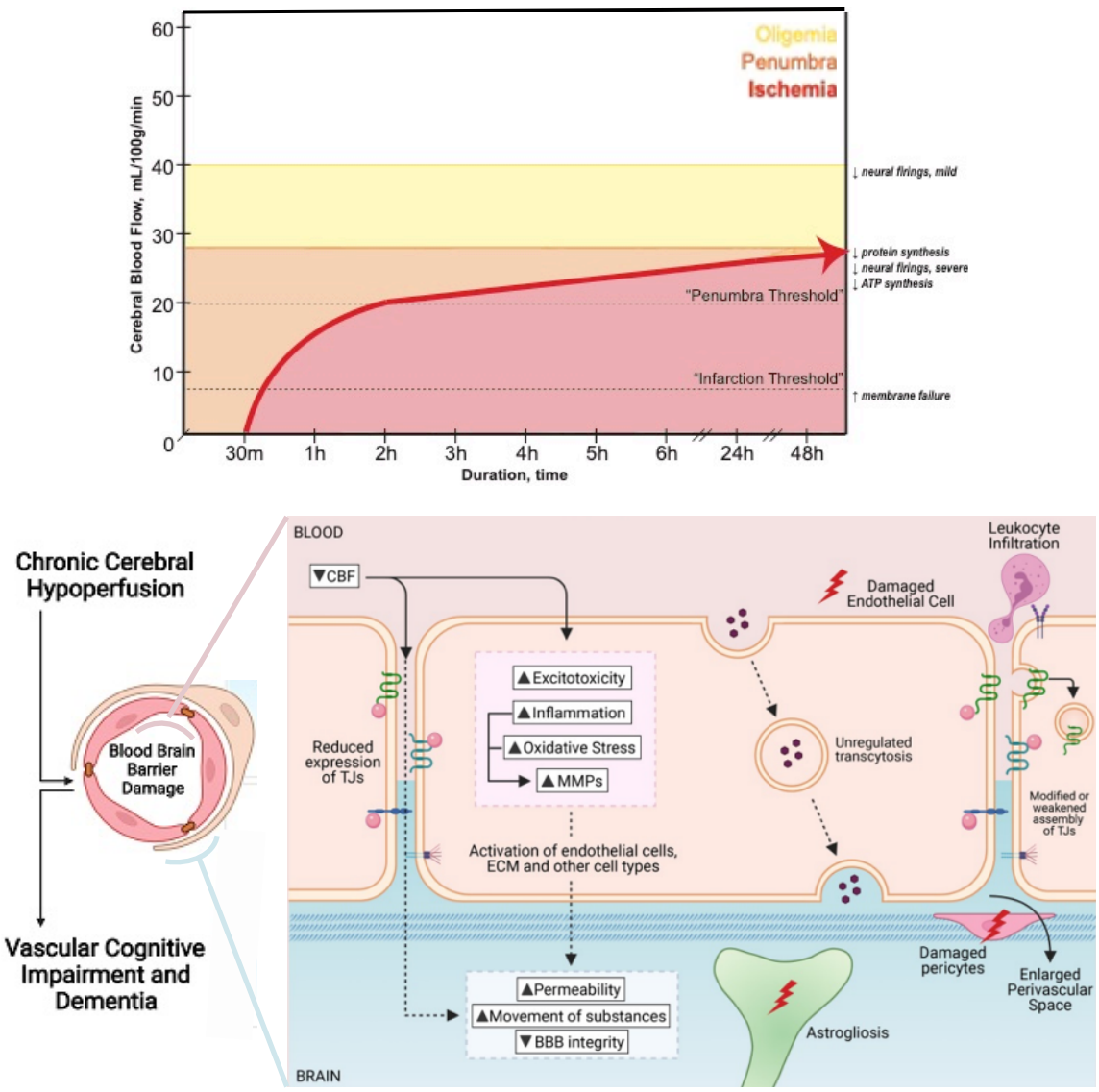

Note. Top Panel: The response of neurons to oligemia and ischemia is governed by the severity and duration of hypoperfusion and by the pathological events that are initiated upon reperfusion.[163] Whereas traditional models suggest oligemia occurs at CBF <40 mL/100g/min, penumbra occurs at CBF <20 mL/100g/min, and irreversible ischemic damage occurs at CBF <8 mL/100g/min, duration of exposure may lower these thresholds even more. Changes in neuronal function occur in oligemic stages (e.g., decreased electroencephalography-based neural firings), but the clinical consequences of these functional alternations remain unknown. Reversible dysfunction and damage occur in the penumbric range, while irreversible cell death occurs in the ischemic range. Ultimately, neuronal dysfunction depends on the level and duration of hypoperfusion-induced hypoxia, a marker of cellular metabolism that is dependent on baseline energy demands. **Bottom Panel**: Chronic cerebral hypoperfusion associated with vascular aging promotes blood-barrier dysfunction through numerous pathways, including directly compromising tight junctions (e.g., reduced protein expression, weakened assembly) and indirectly promoting microvascular cell dysfunction (e.g., increased excitotoxicity, inflammation, oxidative stress, expression of matrix metalloproteinases). Collectively, these effects increase endothelial cell activation, blood-brain barrier permeability, and related downstream effects of leukocyte infiltration, unregulated transcytosis, damaged pericytes, increased perivascular space, and astrogliosis.

1.6 Overarching Rationale

Cerebral hypoperfusion changes with aging are complex and likely interact with vascular risk, hemodynamic dysregulation, and pathological factors to reach a critical hypoxia threshold for tissue dysfunction and cognitive impairment. The complex vascular architecture of the brain and variable mechanisms of blood flow regulation promote region-specific vulnerabilities to hypoperfusion-hypoxia, particularly among high-demand vulnerable neuronal populations, regions susceptible to neurovascular unit dysfunction, and low-supply watershed regions. Ultimately, the effectiveness of tissue perfusion depends on blood supply into the parenchyma via the macrocirculation as well as the ability of the microcirculation to transport vital substrates across the blood brain barrier. Strong evidence suggests coexisting vascular abnormalities, including cardiovascular contributions, may exacerbate the clinical manifestation of AD. Particularly impactful cardiovascular changes, such as aortic stiffness, should be further examined as potentially modifiable targets to reduce risk of both normal aging- and AD-related cognitive decline. As the lifespan expands and chronic vascular risk factors accumulate, the prevalence of cerebrovascular dysfunction will likely rise as will the incidence of cerebrovascular abnormalities underlying dementia. More research is needed to examine not just the many vascular pathways to neuronal death but also the degree to which subtle changes in neuronal dysfunction are related to blood flow across the spectrum of perfusion. Further research into cerebrovascular pathways to cognitive impairment are critical for prevention efforts, which is an especially pressing need given the lack of effective AD treatments.

CHAPTER 2[b]

Microvasculature

2.1 Introduction

Arterial stiffness intensifies with age,[187] and its estimates such as PWV, are associated with increased incidence of cardiovascular disease[188] and accelerated brain aging, including cognitive impairment and SVD.[69] An elastic aorta is critical for distributing blood and buffering pulsatile flow.[189] Age-related reductions in aortic wall compliance can contribute to increased transmission of harmful pulsatile energy into the microcirculation, increased microvascular remodeling, and impaired oxygen delivery to tissue.[189] Highly perfused organs like the brain may be particularly susceptible. In response to excessive pulsatility, larger cerebral arteries and smaller arterioles coordinate to limit penetration of pulsatile flow into the capillaries.[189] The consequence of increased aortic stiffening would thus be reduced cerebral perfusion.

Prior research relating arterial stiffness to cerebral hemodynamics has relied mostly on systemic measures of arterial stiffness rather than regionally specific aortic measures, low-sensitivity or global measures of cerebral hemodynamics (e.g., cerebral middle cerebral artery velocity[190]), young or middle-aged adult cohorts,[191] and cross-sectional analytical approaches that limit evaluations of aortic stiffness' predictive value. Limited research has attempted to understand aortic stiffness in the context of its influence on regional CBF patterns in older adults, including how AD-related genetic risk and cognitive staging alter relative risk of vascular dysfunction in aging adults. Using the gold standard measurement of central arterial stiffness by directly

[b] This chapter is adapted from "Higher Aortic Stiffness Is Related to Lower Cerebral Blood Flow and Preserved Cerebrovascular Reactivity in Older Adults" published in *Circulation* and has been reproduced with the permission of the publisher and my co-authors: Dr. Angela L. Jefferson, Dr. Dandan Liu, Dr. Elizabeth E. Moore, Dr. Jacquelyn E. Neal, James G Terry, Sangeeta Nair, Dr. Kimberly R. Pechman, Dr. Swati Rane, Dr. L. Taylor Davis, Dr. Katherine A. Gifford, Dr. Timothy J. Hohman, Dr. Susan P. Bell, Dr. Thomas J. Wang, Dr. Joshua A Beckman, and Dr. John Jeffrey Carr.

measuring thoracic aortic PWV on cardiac magnetic resonance imaging (CMR),[192] we related aortic stiffness to resting CBF in older adults free of clinical dementia or stroke, both at baseline and longitudinally.

APOE ε4 is the strongest genetic risk factor for late-onset, sporadic AD with diverse neuropathological effects, including toxic effects on both neurons and the cerebrovasculature. *APOE* ε4 lipid metabolism pathways promote cerebrovascular dysfunction (e.g., molecular cerebrovascular damage[160-162] and BBB dysfunction[193]) and *APOE* ε4 carriership enhances the adverse effects of clinical cardiovascular disease on brain health[194]. Given that *APOE* ε4 mediates risk for cross-sectional[195] and longitudinal CBF changes during aging,[196] aortic stiffness may exert stronger effects and promote compromised cerebral hemodynamics in *APOE* ε4 carriers. Therefore, we also examined the interaction of aortic PWV and *APOE* ε4 on CBF outcomes.

2.2 Methods

2.2.1 Study Cohort

The Vanderbilt Memory & Aging Project (VMAP)[197] is a longitudinal study investigating vascular health and brain aging. Inclusion required participants to be ≥60 years of age, to speak English, to have adequate auditory and visual acuity, and to have a reliable study partner. At eligibility, participants underwent a medical history and record review, a clinical interview (including functional questionnaire and Clinical Dementia Rating[198] with the informant), and a neuropsychological assessment for cognitive diagnosis by consensus, including normal cognition (NC) or mild cognitive impairment (MCI) based on the National Institute on Aging/Alzheimer's Association Workgroup clinical criteria.[16] Specifically, MCI was defined as (1) a Clinical Dementia Rating of 0 or 0.5 (reflecting mild severity of impairment); (2) relatively spared activities of daily living; (3) objective neuropsychological impairment; (4) concern of a cognitive change by the participant, informant, or clinician based on information obtained during the clinical interview;

and (5) absence of a dementing syndrome. Participants were excluded for MRI contraindication, history of neurological disease (e.g., stroke), heart failure, major psychiatric illness, head injury with loss of consciousness for >5 minutes, and systemic or terminal illness that could affect follow-up participation. At enrollment, participants completed a comprehensive evaluation, including (but not limited to) morning fasting blood draw, physical examination, clinical interview with medication review, neuropsychological assessment, echocardiogram, CMR imaging, and brain MRI. Identical procedures were repeated at each time point, including 18 months, 3 years, 5 years, and 7 years for longitudinal follow-up of the cohort. Participants were excluded from the current study for missing baseline PWV, baseline covariate data, or brain MRI data across all timepoints (**Figure 2.1**).

The Vanderbilt University Medical Center Institutional Review Board approved the protocol. Written informed consent was obtained from all participants before data collection. Because of participant consent restrictions in data sharing, a subset of data is available to others for purposes of reproducing the results or replicating procedures. These data, analytical methods, and study materials can be obtained by contacting the corresponding author.

Figure 2.1: Participant Inclusion & Exclusion Criteria

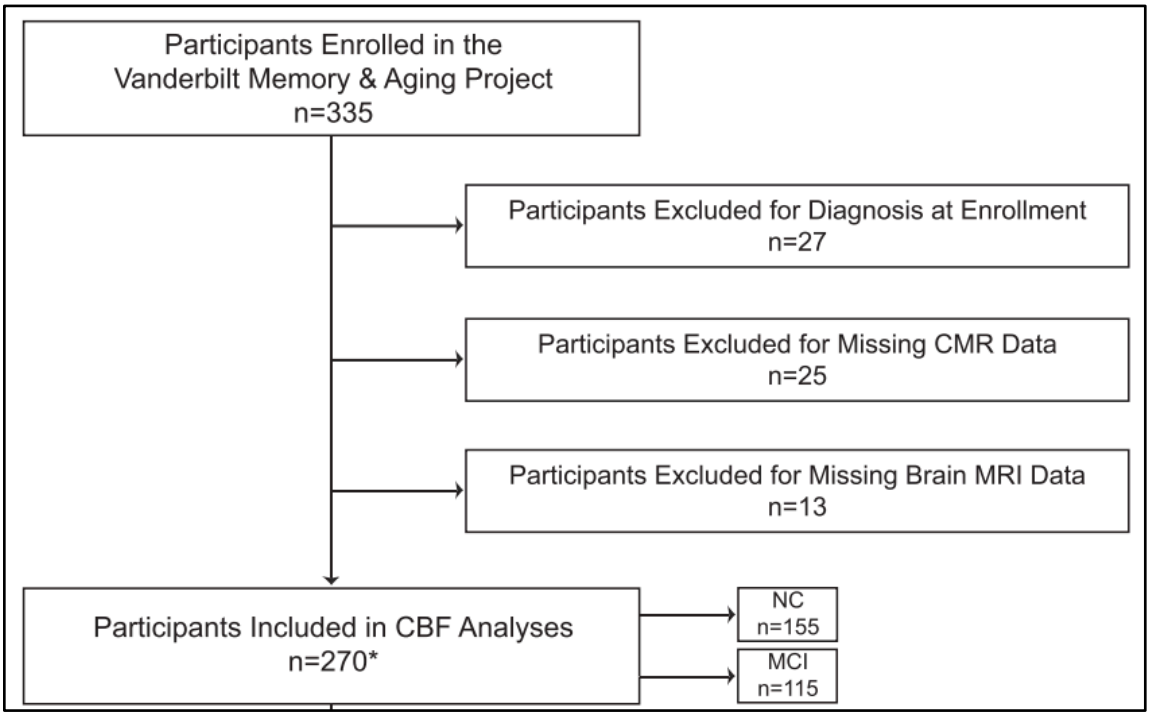

Note. Missing data categories are mutually exclusive. CMR indicates cardiac magnetic resonance imaging; MRI, magnetic resonance imaging; CBF, cerebral blood flow; NC, normal cognition, MCI, mild cognitive impairment. *Sensitivity analyses excluding cardiovascular disease or atrial fibrillation removed 12 participants with NC and 9 participants with MCI.

2.2.2 CMR Imaging

CMR imaging was acquired at Vanderbilt University Medical Center with a 1.5-T Siemens Avanto system (Siemens Medical Solutions USA, Inc, Malvern, PA) with a phased array torso receiver coil. Velocity-encoded flow data were acquired from the ascending and descending thoracic aorta (**Figure 2.2**, Left Panel). Under the supervision of a board-certified radiologist (Dr. J. Jeffrey Carr), trained raters blinded to clinical information (James G. Terry, Sangeeta Nair) used the 2-dimensional flow sequence to draw contours on the ascending and descending aorta using the QFLOW 5.6 Enterprise Solution (Medis, Leiden, the Netherlands). The thoracic aorta centerline length (centimeters) from the ascending aorta to the descending aorta was measured with the OsiriX (PIXMEO SARL, Bernex, Switzerland). Transit time was calculated with a custom MATLAB script to calculate the difference in time (milliseconds) at half maximum between the

leading edges of the ascending and descending aortic flow curves (**Figure 2.2**, Right Panel). PWV (meters per second) was calculated as distance traveled across the aorta (meters) divided by time delay in onset of velocity waves (seconds). Interreader reliability (coefficient of variation, 6.6%) was determined by independent review of 34 scans by 2 readers (James G. Terry, Sangeeta Nair). Pulsatile wave transmission increases with decreasing arterial wall elasticity, such that a higher PWV indicates higher arterial stiffness.

Figure 2.2: Representative PWV Measurement Across the Aortic Arch (adapted from Cambronero et al., 2018199)

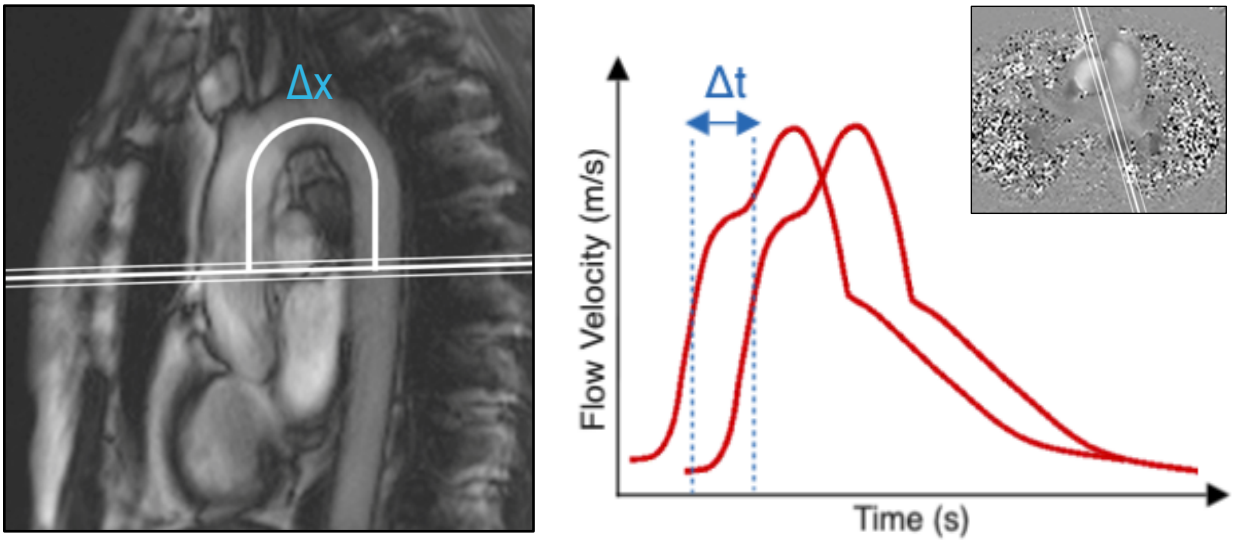

Note. PWV indicates pulse wave velocity. **Left Panel:** CMR was used to acquire PWV-encoded flow data across the ascending and descending thoracic aorta with slice angulation adjusted to maximize perpendicular flow; distance traveled across the aorta was calculated from the thoracic aorta sagittal view. **Right Panel:** Aortic flow waveforms were generated from PWV-encoded flow image data (top right) and transit time was calculated as the time delay between the ascending and descending aortic flow curves using the difference between their half-maximum points. PWV (meters/second) was calculated as distance traveled across the aortic arch (meters) divided by the transit time (seconds).

2.2.3 Brain MRI

Participants were scanned at the Vanderbilt University Institute of Imaging Science on a 3-T Philips Achieva system (Best, the Netherlands) using 8-channel phased-array SENSE (sensitivity encoding) reception. T_1-weighted magnetization-prepared rapid gradient echo (isotropic spatial

resolution, 1 mm^3) images were postprocessed with an established Multi-Atlas Segmentation pipeline[200,201] with parcellation of 5 regions of interest, including whole brain, frontal, temporal, parietal, and occipital lobes.

Pseudocontinuous arterial spin labeling (pCASL) MRI (label duration, 1.65 seconds; postlabeling delay, 1.525 seconds; spatial resolution, 3×3×7 mm^3; repetition time/echo time, 3900/13 milliseconds) assessed CBF (milliliters of blood per 100 g tissue per minute) using a reproducible protocol.[78,202] Data were corrected for motion and baseline drift with the Functional MRI of the Brain (FMRIB) Software Library FMRIB's Linear Image Registration Tool.[203] Additional postprocessing was completed with MATLAB. Images were slice-time–corrected, normalized by the equilibrium magnetization (M0), which was calculated from a separately acquired image with identical geometry but repetition time of 20 seconds, and converted to absolute CBF units following recommended guidelines.[204] This image was coregistered to the anatomic T_1-weighted map and standard Montreal Neurological Institute template.[205] Transformation matrices were applied to CBF maps. Region-specific mean resting CBF was calculated in gray matter regions of interest described above.

2.2.4 Echocardiography

Evaluation of relevant cardiac structure and function variables (i.e., left ventricular hypertrophy, atrial fibrillation) was performed using standard 2-dimensional, M-mode, and Doppler transthoracic echocardiography by a single research sonographer (JoAnn Gottlieb) at the Vanderbilt University Medical Center Clinical Research Center on a Philips IE33 cardiac ultrasound machine (Philips Medical, Andover, MD). Digital images with measurements were confirmed by board-certified cardiologists (Dr. Deepak K Gupta, Dr. Lisa A Mendes) using commercially available software (HeartLab; AGFA Healthcare, Greenville, SC). All raters were blinded to clinical information.

Image acquisition and quantification was performed according to American Society of Echocardiography (ASE) guidelines.[206] Briefly, LV volumes were calculated by the biplane Simpson's method. LV mass was calculated from LV linear dimensions using the ASE recommended formula (0.8 × [1.04[(LV internal diameter during diastole + posterior wall thickness during diastole + septum wall thickness during diastole)3 - (LV internal diameter during diastole)3]] + 0.6 g) and indexed to body surface area. LV hypertrophy (LVH) was defined as LV mass index >115 g/m2 in men or >95 g/m2 in women.

In addition, Early (E) and late (A) transmitral velocities and the E deceleration time were measured from pulsed wave spectral Doppler images acquired in the apical 4-chamber view with the sample volume positioned at the tip of the mitral leaflets. Peak lateral and septal mitral annular early relaxation and atrial contraction velocities were assessed using tissue Doppler imaging. Final values were taken from measurements of a single cardiac cycle for participants in normal sinus rhythm or the average of three cardiac cycles for those participants in atrial fibrillation. Atrial fibrillation at the time of echocardiography was determined by the absence of A waves on transmitral spectral Doppler flow and tissue Doppler mitral annular velocity profiles, as well as the lack of organized electrocardiographic P waves.

2.2.5 Genetic Testing

As previously published,[197] a TaqMan® single-nucleotide polymorphism (SNP) genotyping assay from Applied Biosystems (Foster City, California, USA) was used on whole blood samples to determine the two SNPs that define the *APOE* ε2, ε3, and ε4 alleles. Briefly, *APOE* alleles are distinguished by non-synonymous mutations at codon 112 (Cys112Arg) and codon 158 (Arg158Cys) within exon 4 of the *APOE* gene on chromosome 19.[207] The most common ε3 allele encodes a Cys112-Arg158 protein isoform (defined by SNPs rs429358-T and rs7412-C), while the

e4 allele encodes Arg112-Arg158 (defined by SNPs rs429358-C and rs7412-C) and the e2 allele encodes Cys112-Cys158 (defined by SNPs rs429358-C and rs7412-C).[208] See **Figure 2.3** for further details. Polymerase chain reaction (PCR) in 5 µl reactions was performed on a Life Technologies 7900HT real-time PCR machine, and results were analyzed using Life Technologies SDS 2.4.1 software.

Figure 2.3: Structure of *APOE* Gene & Protein Isoforms (from Abondio et al., 2019[208])

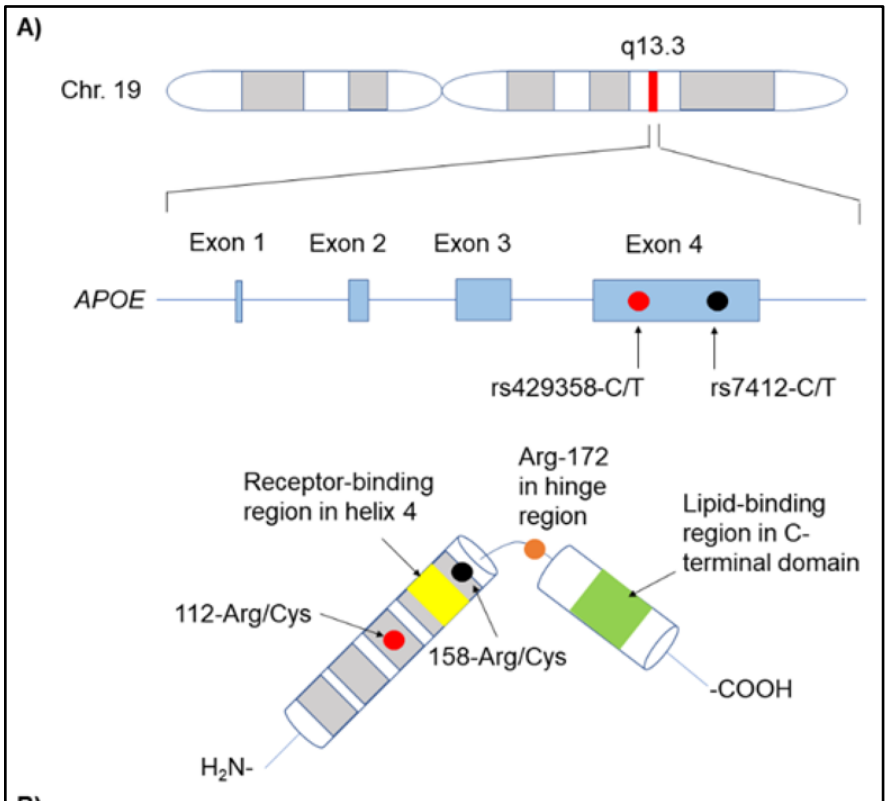

Allele	ε2	ε3	ε4
Haplotype	rs429358-T rs7412-T	rs429358-T rs7412-C	rs429358-C rs7412-C
Residue combination	112-Cys 158-Cys	112-Cys 158-Arg	112-Arg 158-Arg

Note. *APOE* indicates apolipoprotein E. **Panel A:** The *APOE* gene is located at position 19q13.2 (red) of chromosome 19 and contains 4 exon regions (blue). Exon 4 encodes over 80% of the protein and contains the two most well-known disease-associated SNPs (indicated by arrows), which result in distinct protein isoform structures. **Panel B:** Compared to the wild-type sequence of *APOE* ε3 (Cys112, Arg158), *APOE* ε4 is produced by a T→C point mutation (Cys112Arg) and *APOE* ε2 is produced by a C→T mutation (Arg158Cys).

2.2.6 Covariate Definitions

Based on known associations with cardiovascular function and brain health, a series of covariates were identified *a priori* for their potential to confound the analytical models, including age,[209] sex,[210,211] education,[212] race/ethnicity,[213] Framingham Stroke Risk Profile (FSRP) (excluding points for age),[214,215] and *APOE* ε4 carrier status.[216] Body mass index (BMI) was calculated as weight in kilograms divided by height in meters squared (i.e., kg/m^2). FSRP assigned points by sex for age, systolic blood pressure (accounting for antihypertensive medication use), diabetes mellitus, cigarette smoking, left ventricular hypertrophy, cardiovascular disease, and atrial fibrillation.[215] Systolic blood pressure was the mean of 2 measurements. Diastolic blood pressure was the mean of 2 measurements. Hypertension was defined as antihypertensive medication use, systolic blood pressure ≥140 mm Hg, or diastolic blood pressure ≥90 mm Hg. Diabetes mellitus was defined as fasting blood glucose ≥126 mg/dL, hemoglobin A1c ≥6.5%, or oral hypoglycemic or insulin medication use. Medication review determined antihypertensive medication use. Left ventricular hypertrophy was defined on echocardiogram as left ventricular mass index >115 g/m2 in men or >95 g/m2 in women. Self-report or history of atrial fibrillation was corroborated by any one of the following sources: echocardiogram, CMR, documented prior procedure/ablation for atrial fibrillation, or medication use for atrial fibrillation. Current cigarette smoking (yes/no within the year before baseline) was ascertained by self-report. Self-report prevalent cardiovascular disease with medical record documentation included coronary heart disease, angina, or myocardial infarction (heart failure was a parent study exclusion). *APOE* genotyping was performed on whole blood as described above, and *APOE* ε4 status was defined as positive (ε2/ε4, ε3/ε4, ε4/ε4) or negative (ε2/ε2, ε2/ε3, ε3/ε3).

2.2.7 Analytical Plan

Before analyses, scatterplots with linear fit and locally weighted smoothing fit were visually inspected for linearity. Linear regression models with ordinary least square estimates stratified by

cognitive diagnosis related aortic PWV to resting CBF for whole brain and frontal, temporal, parietal, and occipital lobes (one region per model). Models were adjusted for age, race/ethnicity, education, hypertension, modified FSRP score (excluding points assigned for age and systolic blood pressure accounting for antihypertensive medication use), BMI, *APOE* ε4 status, and corresponding gray matter region of interest to account for CBF reductions resulting from tissue volume loss[82] (e.g., gray matter in the temporal lobe was a covariate for temporal lobe CBF). To test hypotheses related to cognitive diagnosis, models were diagnostically stratified and then repeated in sensitivity analyses excluding participants with cardiovascular disease or atrial fibrillation to assess whether these conditions accounted for any significant results. To test hypotheses related to *APOE* ε4 status, models were repeated with a PWV × *APOE* ε4 interaction term, with follow-up models stratified by *APOE* ε4 status (carrier, noncarrier). In post-hoc analyses, significant cross-sectional models were re-analyzed to assess allele dosage effects where *APOE* ε4 status was defined as zero, one, or two ε4 alleles. Finally, the effect of hypertension in cross-sectional models was examined post-hoc by relating a PWV × hypertension interaction term to CBF outcomes and stratifying primary models by hypertension status (yes, no). Lower order terms were retained in the interaction models. Significance was set *a priori* at p-value<0.05.

Linear mixed-effects regression models related baseline PWV to resting CBF over time for whole brain and frontal, temporal, parietal, and occipital lobes (one region per model), including an interaction with time to follow-up between baseline and last follow-up visit (in years) as the term of interest. We model the trajectory of cognition using these linear mixed-effect regression models, where terms involving follow-up time capture cognitive decline. Models were adjusted for age, race/ethnicity, education, diagnosis, hypertension, modified FSRP score (excluding points assigned for age and systolic blood pressure accounting for antihypertensive medication use), BMI, *APOE* ε4 status, corresponding gray matter region of interest, and follow-up time. To test hypotheses related to cognitive diagnosis, models were repeated with a PWV × follow-up time × diagnosis interaction term, with follow-up models stratified by diagnosis (NC, MCI). To test

hypotheses related to *APOE* ε4 status, models were repeated with a PWV × follow-up time × *APOE* ε4 carrier status interaction term, with follow-up models stratified by *APOE* ε4 carrier status (carrier, non-carrier). Lower order terms were retained in the interaction models. Significance was set *a priori* at p-value<0.05.

To determine if outliers were driving the cross-sectional or longitudinal results, additional models were calculated excluding predictor or outcome values >4 standard deviations from the group mean. For all models, follow-up sensitivity analyses were performed excluding participants with prevalent cardiovascular disease or atrial fibrillation to test if these conditions accounted for significant results. All analyses were conducted using R version 3.2.3 (www.r-project.org).

2.3 Results

2.3.1 Participant Characteristics

The sample included 155 participants with NC and 115 with MCI. Participants did not differ on covariates or global cognitive status (as assessed by the Montreal Cognitive Assessment) compared with those individuals missing data who were excluded from analyses (n=65). The mean sample age was 73±7 years (range, 60–92 years); 58% were men; and 86% self-identified as non-Hispanic white. Baseline aortic PWV ranged from 3.5 to 25.5 m/s. Total sample and diagnostic group characteristics are presented in **Table 2.1.**

Table 2.1: Baseline Participant Characteristics

	Combined (n=270)	NC (n=155)	MCI (n=115)	*p*-value
Demographics				
Age, years	73±7	72±7	73±7	0.36
Sex, % male	58	59	57	0.83
Race, % White non-Hispanic	86	86	86	0.93
Education, years	16±3	16±2	15±3	**<0.001**
MOCA, total score	25±3	27±2	23±4	**<0.001**
APOE ε4, % carrier	34	29	41	0.04
BMI, kg/m^2	28±5	27±5	28±4	0.32
Aortic PWV, m/s	8.2±3.2	8.2±3.0	8.2±3.3	0.74
FSRP score, total*	12.3±4.2	11.9±4.2	12.8±4.2	0.07
Systolic blood pressure, mmHg	142±18	140±17	145±19	0.03
Antihypertensive medication use, %	53	53	52	0.91
Diabetes mellitus, %	18	17	20	0.50
Hypertension, %	74	71	77	0.24
Current cigarette smoking, %	2	1	3	0.43
Prevalent cardiovascular disease,† %	4	4	3	0.87
Atrial fibrillation,† %	5	5	5	0.79
Left ventricular hypertrophy, %	4	3	6	0.26
CBF, mL/100g/min				
Whole brain	37.3±7.1	37.3±6.6	37.3±7.7	0.72
Frontal lobes	38.0±8.3	37.7±7.4	38.3±9.4	0.81
Temporal lobes	35.9±8.1	36.3±6.9	35.4±9.6	0.15
Parietal lobes	39.8±10.3	39.6±9.4	40.1±11.4	0.82
Occipital lobes	36.4±10.0	36.9±9.8	35.7±10.3	0.25

Note. Values are presented as mean±standard deviation or frequency. NC indicates normal cognition; MCI, mild cognitive impairment; MOCA, Montreal Cognitive Assessment.; *APOE* indicates apolipoprotein E; BMI, body mass index; PWV, pulse wave velocity; FSRP, Framingham Stroke Risk Profile; CBF, cerebral blood flow; mL/100g/min, milliliters of blood per 100 grams of tissue per minute. *Modified score was included in models excluding points for age (NC, 6.1±2.8; MCI, 6.8±3.2). †Prevalent cardiovascular disease, n=10; atrial fibrillation, n=13; both, n=1; resulting in n=22 with prevalent cardiovascular disease, atrial fibrillation, or both.

2.3.2 Aortic PWV and Cross-Sectional CBF

Main Effect Models

Aortic PWV associations with cross-sectional CBF are presented in **Table 2.2**. Among all participants, aortic PWV related to lower CBF in the whole brain (β=−0.30, *p*-value=0.04) and

occipital lobe (β=−0.49, *p*-value=0.01). Weak evidence (i.e., *p*-value<0.10) of an association between aortic PWV and lower frontal lobe CBF (β=−0.32, *p*-value=0.06) was observed, but these associations did not meet *a priori* significance.

Aortic PWV × *APOE* ε4 associations with cross-sectional CBF associations are presented in **Table 2.3**. The aortic PWV × *APOE* ε4 interaction term related to temporal lobe CBF (β=−1.07, *p*-value=0.002) such that associations between higher aortic PWV and lower CBF were more pronounced among *APOE* ε4 carriers compared with noncarriers.

Table 2.2: Aortic PWV & Cross-Sectional CBF

	Combined (n=268)		NC (n=154)		MCI (n=114)	
	β	*p*-value	β	*p*-value	β	*p*-value
Whole Brain	-0.30	**0.04**	-0.34	0.07	-0.23	0.34
Frontal Lobes	-0.32	0.06	-0.43	**0.04**	-0.20	0.41
Temporal Lobes	-0.16	0.33	-0.36	0.08	0.04	0.90
Parietal Lobes	-0.26	0.23	-0.24	0.37	-0.27	0.42
Occipital Lobes	-0.49	**0.01**	-0.40	0.15	-0.70	**0.02**

Note. PWV indicates pulse wave velocity; CBF, cerebral blood flow; NC, normal cognition; MCI, mild cognitive impairment.

Table 2.3: Aortic PWV × *APOE* ε4 & Cross-Sectional CBF

	Combined (n=268)		NC (n=154)		MCI (n=114)	
	β	*p*-value	β	*p*-value	β	*p*-value
Whole Brain	-0.55	0.08	-1.16	**0.047**	-0.32	0.47
Frontal Lobes	-0.35	0.34	-1.17	0.08	-0.29	0.53
Temporal Lobes	-1.07	**0.002**	-1.81	**0.004**	-1.20	**0.02**
Parietal Lobes	-0.34	0.47	-0.71	0.40	0.17	0.79
Occipital Lobes	-0.44	0.30	-0.64	0.45	-0.19	0.73

Note. PWV indicates pulse wave velocity; *APOE*, apolipoprotein E; CBF, cerebral blood flow; NC, normal cognition; MCI, mild cognitive impairment.

NC Diagnosis Stratified Models

Among participants with NC, aortic PWV related to lower frontal lobe CBF (β=−0.43, *p*-value=0.04; **Table 2.2**; **Figure 2.4**), results that survived exclusion for CVD and atrial fibrillation. Weak evidence (i.e., *p*-value<0.10) of associations between aortic PWV and lower whole brain CBF (β=−0.34, *p*-value=0.07) and temporal lobe CBF (β=−0.36, *p*-value=0.08) were observed, but these associations did not meet *a priori* significance.

The aortic PWV × *APOE* ε4 interaction term related to CBF in the whole brain (β=−1.16, *p*-value=0.047) and temporal lobe (β=−1.81, *p*-value=0.004) such that associations between higher aortic PWV and lower CBF were more pronounced among *APOE* ε4 carriers compared with noncarriers (**Table 2.3**; **Figure 2.5**). Weak evidence (i.e., *p*-value<0.10) of an association between aortic PWV and lower frontal lobe CBF (β=−1.17, *p*-value=0.08) was observed, but these associations did not meet *a priori* significance.

In post hoc analyses examining *APOE* ε4 allele dosage effects, APOE ε4 allele count did not improve model fit, likely because small cell sizes limited power. However, visual inspection of the data suggests an additive effect whereby homozygous carriers of the APOE ε4 allele may have lower CBF in the temporal lobe at higher aortic PWV values than heterozygous APOE ε4 carriers (**Figure 2.6**). When participants with atrial fibrillation and CVD were excluded, results were similar. In post hoc analyses examining the interaction of aortic PWV × hypertension on CBF outcomes, results were null (*p*-value≥0.57).

Figure 2.4: Aortic PWV & Cross-Sectional CBF in NC Participants

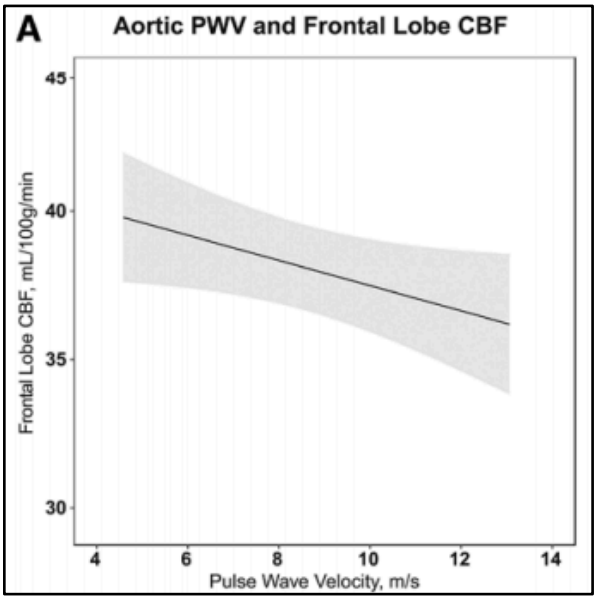

Note. Solid black line reflects fitted linear regression between PWV (x-axis) and frontal lobe CBF outcome (y-axis). Shading reflects 95% confidence interval. PWV indicates pulse wave velocity; CBF, cerebral blood flow.

Figure 2.5: Aortic PWV × *APOE* ε4 & Cross-Sectional Temporal Lobe CBF in NC Participants

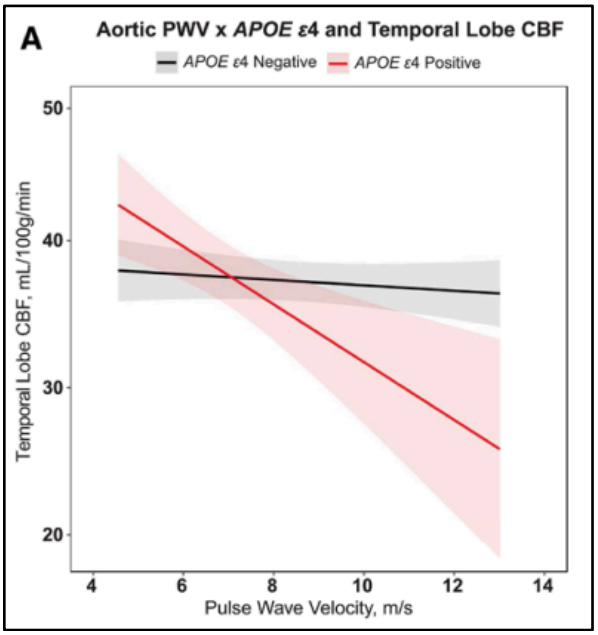

Note. Solid lines reflect fitted linear regression between the interaction of PWV and *APOE* ε4 status (i.e., *APOE* ε4 noncarrier/negative (black) or *APOE* ε4 carrier/positive (red)) (x-axis) on temporal lobe CBF outcome (y-axis). Shading reflects 95% confidence interval. PWV indicates pulse wave velocity; *APOE*, apolipoprotein E; CBF, cerebral blood flow.

Figure 2.6: Aortic PWV × *APOE* ε4 Allele Count & Cross-Sectional Temporal Lobe CBF in NC Participants

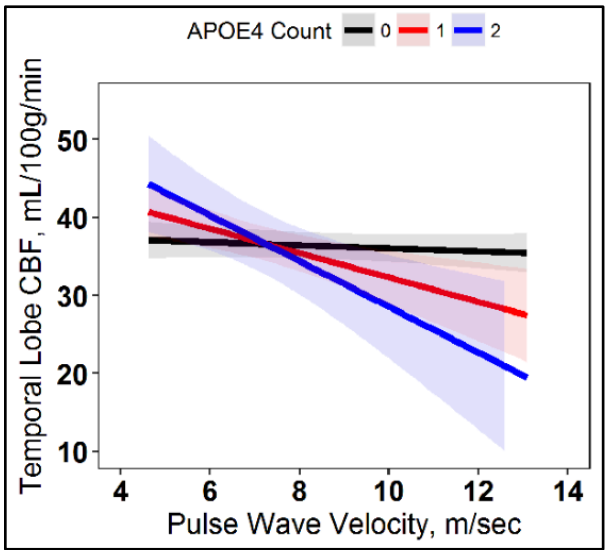

Note. Solid lines reflect fitted linear regression between the interaction of PWV and *APOE* ε4 allele count (i.e., 0 (black), 1 (red), or 2 (blue) allele copies) (x-axis) on temporal lobe CBF outcome (y-axis). Shading reflects 95% confidence interval. PWV indicates pulse wave velocity; *APOE*, apolipoprotein E; CBF, cerebral blood flow.

MCI Diagnosis Stratified Models

Among participants with MCI, aortic PWV related to lower occipital lobe CBF (β=−0.70, *p*-value=0.02), but results were attenuated in a sensitivity analysis excluding participants with atrial fibrillation and CVD (β=−0.54, *p*-value=0.15). Aortic PWV was unrelated to CBF in all remaining regions (*p*-value>0.34, **Table 2**).

The aortic PWV × *APOE* ε4 interaction term related to temporal lobe CBF (β=−1.20, *p*-value=0.02) such that associations between higher aortic PWV and lower CBF were more pronounced among *APOE* ε4 carriers compared with noncarriers. The aortic PWV × *APOE* ε4 interaction term was unrelated to CBF in all remaining regions assessed (*p*-value>0.47, **Table 3**). When participants with atrial fibrillation and CVD were excluded, results were similar. In post-hoc analyses examining aortic PWV × hypertension on CBF outcomes, results were null (*p*-value≥0.44).

2.3.3 Aortic PWV & Longitudinal CBF

Main Effects Analyses

In the combined cohort, baseline aortic PWV was not significantly related to longitudinal CBF in any region (*p*-value>0.18). See **Table 2.4** for PWV main effect results.

Table 2.4. Aortic PWV & Longitudinal CBF

	Combined (n=274)	
	β	*p*-value
Whole Brain	-0.02	0.60
Frontal Lobes	-0.02	0.65
Temporal Lobes	-0.04	0.18
Parietal Lobes	-0.01	0.91
Occipital Lobes	-0.01	0.86

Note. PWV indicates pulse wave velocity; CBF, cerebral blood flow.

Cognitive Diagnosis Subgroup Analyses

Cognitive diagnosis did not appear to modify associations between baseline aortic PWV and longitudinal CBF in any region (*p*-value>0.09). See **Table 2.5** for PWV × diagnosis interaction effects and **Table 2.6** for results stratified by diagnosis.

Table 2.5: Aortic PWV × Diagnosis & Longitudinal CBF

	Combined (n=274)	
	β	*p*-value
Whole Brain	0.06	0.35
Frontal Lobes	0.07	0.35
Temporal Lobes	-0.02	0.75
Parietal Lobes	0.13	0.09
Occipital Lobes	0.08	0.22

Note. PWV indicates pulse wave velocity; CBF, cerebral blood flow.

Table 2.6: Aortic PWV & Longitudinal CBF Stratified by Diagnosis

	NC (n=156)		MCI (n=118)	
	β	*p*-value	β	*p*-value
Whole Brain	-0.01	0.87	-0.002	0.98
Frontal Lobes	0.003	0.96	-0.01	0.88
Temporal Lobes	-0.002	0.97	-0.08	0.14
Parietal Lobes	-0.02	0.77	-0.06	0.44
Occipital Lobes	0.004	0.93	-0.04	0.52

Note. PWV indicates pulse wave velocity; CBF, cerebral blood flow; NC, normal cognition; MCI, mild cognitive impairment.

APOE ε4 Subgroup Analyses

APOE ε4 status modified the relationship between PWV and longitudinal frontal CBF (β=-0.20, *p*-value=0.03) (**Table 2.7**). *APOE* ε4 carriers experienced faster frontal CBF decline at higher PWV values compared to non-carriers. When results were stratified by *APOE* ε4 status, PWV did not significantly relate to longitudinal frontal CBF among *APOE* ε4 carriers (β=-0.16, *p*-value=0.10) or *APOE* ε4 noncarriers (β=0.007, *p*-value=0.89), likely due to limited sample sizes in *APOE* ε4 carrier stratified analyses (**Table 2.8**).

Table 2.7: Aortic PWV × *APOE* ε4 & Longitudinal CBF

	Combined (n=274)	
	β	*p*-value
Whole Brain	-0.13	0.07
Frontal Lobes	-0.20	**0.03**
Temporal Lobes	-0.10	0.10
Parietal Lobes	-0.11	0.25
Occipital Lobes	-0.05	0.51

Note. PWV indicates pulse wave velocity; *APOE*, apolipoprotein E; CBF, cerebral blood flow.

Table 2.8: Aortic PWV & Longitudinal CBF Stratified by APOE ε4 Genetic Status

	APOE ε4 Carrier (n=96)		*APOE* ε4 Noncarrier (n=178)	
	β	*p*-value	β	*p*-value

Whole Brain	-0.09	0.31	-0.01	0.77
Frontal Lobes	-0.16	0.10	0.007	0.89
Temporal Lobes	-0.03	0.68	-0.05	0.14
Parietal Lobes	-0.05	0.65	0.001	0.98
Occipital Lobes	-0.01	-0.87	0.006	0.89

Note. PWV indicates pulse wave velocity; *APOE*, apolipoprotein E; CBF, cerebral blood flow.

2.7 Discussion

Among community-dwelling older adults, higher aortic PWV related cross-sectionally to lower CBF across the brain, including lower frontal lobe CBF in NC participants and lower occipital lobe CBF in MCI participants. Importantly, strongest associations were observed in the interaction of aortic PWV × *APOE* ε4 status on temporal lobe CBF. Among *APOE* ε4 carriers, higher PWV was associated with a more pronounced reduction of CBF in the temporal lobes compared to noncarriers. Moreover, while these associations were present across the combined cohort, they were most pronounced in NC participants. Cross-sectional results suggest temporal lobe perfusion may be selectively vulnerable to age-related aortic stiffness, particularly in the context of *APOE* ε4 genetic risk and in earliest stages of the cognitive aging spectrum.

Longitudinal results demonstrated that associations between aortic PWV and declining CBF is dependent on *APOE* ε4 carrier status. Specifically, modest interactions between PWV and *APOE* ε4 carrier status on frontal lobe CBF indicate that higher PWV is associated with faster decline in frontal lobe CBF among *APOE* ε4 carriers compared to noncarriers. Since longitudinal results were not dependent on cognitive status, any emergent associations between higher aortic stiffness and declining CBF is likely promoted more so by *APOE* ε4 molecular effects (e.g., vulnerable cerebrovasculature) rather than that of emerging neuropathologies associated with clinical symptoms (e.g., AD proteinopathy). The predictive power of aortic stiffness as a marker of cerebral hemodynamic dysregulation may be minimal given the limited associations observed.

This study is among the first to link higher aortic stiffness (i.e., measured centrally in the thoracic aorta) to lower cross-sectional CBF and faster declines in CBF in older adult; demonstrate the importance of *APOE* ε4 genetic risk in promoting significant associations between aortic stiffness and cerebral perfusion; and highlight regional patterns of cerebral hemodynamic vulnerability to aortic stiffness (i.e., temporal lobe cross-sectionally and frontal lobe longitudinally). All associations were determined using gold standard measurements of aortic stiffness and cerebral hemodynamics, and results could not be statistically explained by common cardiovascular risk factors or prevalent CVD, atrial fibrillation, or cerebral atrophy.

Elevated aortic stiffness promotes the dysregulation of blood pressure in aging and increases the transmission of harmful pressure pulsatility into the microcirculation, particularly within high-flow and low-resistance organs like the brain.[70] Consequent changes in cerebral artery structure and function (e.g., wall thickening and stenosis, endothelial dysfunction, BBB dysfunction, capillary rarefaction) can impair hemodynamic regulation and cerebral blood flow, as reported here. Older adults who are carriers of the *APOE* ε4 risk allele may have the highest susceptibility to the effects of aortic stiffness given that the *APOE* ε4 allele promotes worse cerebrovascular integrity and protections because of ε4-associated cerebrovascular damage. It is noteworthy that cell sizes for the subset of *APOE* ε4 carriers are small, so stratified models may be underpowered. In addition to replication, future research is needed to examine the long-term effects of hypertensive risk factor exposure and other common comorbidities closely related to arterial aging (e.g., diabetes) on associations between central and peripheral vascular health.

We provide preliminary evidence of significant interactions between PWV and *APOE* ε4 on temporal lobe hemodynamics cross-sectionally (coupled with more modest evidence of an additive effect of ε4 allele count due to being underpowered with small cell sizes) and frontal lobe hemodynamics longitudinally. *APOE* ε4 carriers may be more susceptible to cerebrovascular injury via elevated aortic PWV. In particular, *APOE* ε4 has been shown to contribute to BBB

dysfunction[193] and cerebrovascular damage before neuronal dysfunction, particularly in medial temporal lobe regions.[160,217] Furthermore, *APOE* ε4 carrier status strengthens vascular disease associations with brain health outcomes,[194,218-220] and *APOE* ε4 carriers have more pronounced reductions in CBF and cerebrovascular reactivity, suggesting more capillary and arteriole damage and dysfunction.[217] Aortic stiffness may thus exert stronger effects in *APOE* ε4 carriers due to their more vulnerable cerebrovasculature and contribute to hypoperfusion in regions most susceptible to early BBB breakdown. The temporal lobe is both selectively susceptible to the earliest markers of vascular dysfunction (e.g., blood pressure dysregulation) and the location at which AD pathology first evolves.[90] Collectively, cerebrovascular vulnerability to central pressure and pulsatility changes may be especially pertinent in the presence of conditions in which autoregulation may be compromised, including chronic risk factors such as hypertension[84,149] or pathological conditions such as cerebral SVD[221] and AD.[222] Further research to better understand our null results is warranted.

Our study has several strengths, including gold standard methods for noninvasively assessing aortic stiffness and regional CBF at rest, stringent quality control procedures, and the use of a core laboratory for processing CMR and brain MRI measurements with blinded raters. The inclusion of older adults with NC and MCI allows us to speculate about the timing of associations between aortic stiffness and CBF across the cognitive spectrum, including prodromal AD. Our sample included predominantly white, well-educated, relatively healthy elders. Although generalizability to other races, ethnicities, ages, and medical conditions is unknown, we speculate that associations reported here would likely be stronger in a cohort with worse cardiovascular health. Multiple comparisons raise the possibility of a false-positive finding and emphasize the need for replication. Finally, we cannot rule out the possibility of residual confounding.

2.8 Conclusions

Among older adults free of clinical dementia, stroke, and heart failure, greater stiffening of the arch of the thoracic aorta was associated with worse cerebral hemodynamics statistically independent of concurrent cardiovascular risk factors, CVD, and atrial fibrillation. Our study highlights the importance of the *APOE* ε4 risk allele in strengthening associations between aortic stiffness and cerebral hypoperfusion and potential vulnerability of frontal and temporal regions. Data support a possible mechanism for central nervous system injury secondary to increased aortic stiffness with age.

CHAPTER 3

Macrovasculature

3.1 Introduction

Given our observed associations between PWV and CBF (see **Chapter 2**), we chose to further investigate potential hemodynamic mediators of these effects. Age-associated increases in pulsatile flow in the brain is thought to be buffered by large arteries in the Circle of Willis (CoW). The CoW is an arterial ring at the base of the brain that connects the primary feeding arteries of the brain (i.e., internal carotid arteries and basilar artery) via communicating artery segments. While the most common theory suggests the CoW evolved in response to CVD to provide compensatory cerebral blood flow,[223] alternative theories suggest the CoW may also have normal physiological roles as a pressure dissipating system, wherein the communicating arteries absorb and redistribute pressure increases related to cardiac pulsatility.[224] Despite its purported roles in collateral circulation and pressure dampening, relatively little is known about the clinical significance of variants in CoW structure.

Our previous data suggests morphological variations in these large arteries predict structural markers of downstream cerebrovascular health, including SVD. In particular, large artery diameters predict white matter damage and enlarged perivascular spaces among older adults (**Figure 3.1**), particularly among older adults at higher risk of AD (**Figure 3.2**). It is thus plausible that the effects of PWV-associated pulsatility on the brain could be mediated by harmful changes to large artery morphology and related changes in vascular resistance to flow.

Figure 3.1: CoW Diameter & SVD

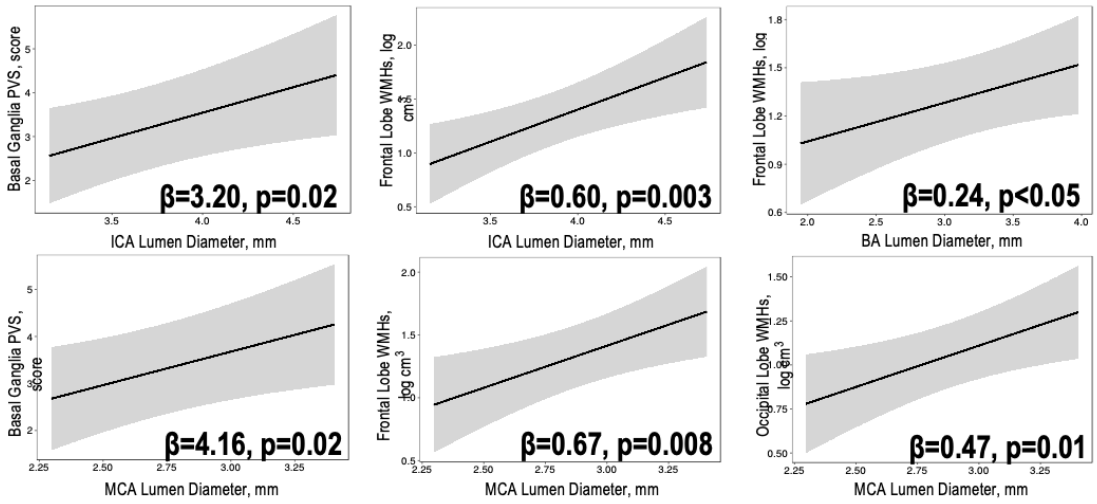

Note. n=126. Solid black line reflects fitted linear regression between artery lumen diameters (x-axis) and WMH outcomes (y-axis) using linear regression models or PVS outcomes (y-axis) using proportional odds regression models, adjusting for age, sex, race/ethnicity, cognitive diagnosis, Framingham Stroke Risk Profile, *APOE* ε4 status, and intracranial volume. Shading reflects 95% confidence interval. CoW indicates Circle of Willis; SVD, small vessel disease, PVS, perivascular spaces; WMH, white matter hyperintensities; ICA, internal carotid artery; BA, basilar artery; MCA, middle cerebral artery.

Figure 3.2: CoW Diameter & SVD by Diagnosis

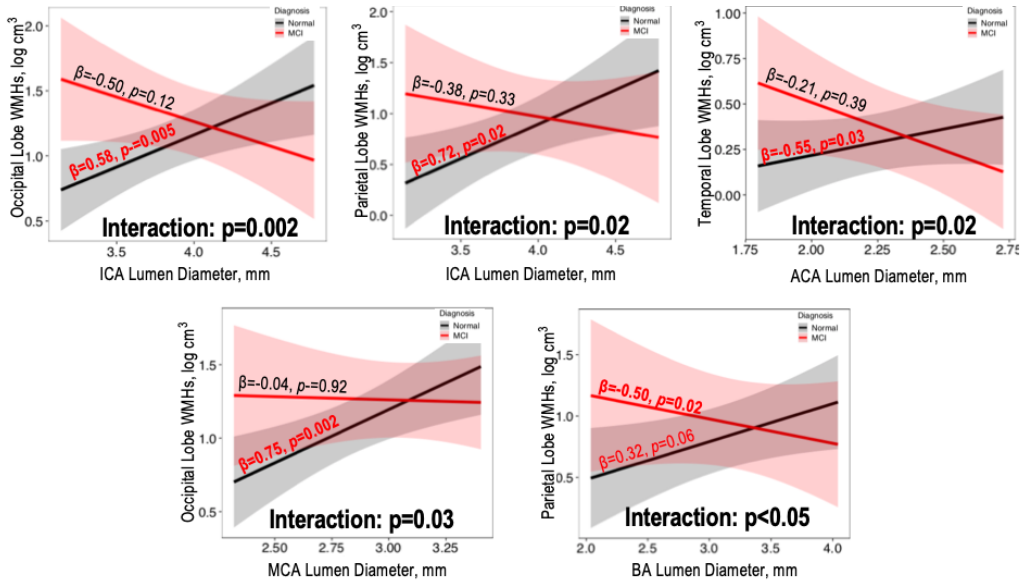

Note. n=126. Solid lines reflect fitted linear regression between the interaction of artery lumen diameter and cognitive diagnosis (i.e., Normal Cognition (black) or Mild Cognitive Impairment (red)) (x-axis) on regional WMH outcomes (y-axis), adjusting for age, sex, race/ethnicity, Framingham Stroke Risk Profile, *APOE* ε4 status, and intracranial volume. Shading reflects 95% confidence interval. CoW indicates Circle of Willis; SVD, small vessel disease, WMH, white matter hyperintensities; ICA, internal carotid artery; ACA, anterior cerebral artery; MCA, middle cerebral artery; BA, basilar artery.

In addition to harmful changes to large artery structure associated with increased pulsatility (e.g., dilatation, hypertrophic remodeling), there is considerable anatomic variation in the number of arteries in the CoW, which may create differential risk profiles for reduced blood flow. In fact, a complete CoW is present in only 14%-45% of individuals, with estimates of CoW patency ranging 14%-45% among autopsy studies[225-228] and 27%-42% among neuroimaging studies.[229,230] Over 50% of the population has a structural variation (e.g., missing, hypoplastic, incompletely developed) in at least one of the communicating arteries when assessed by magnetic resonance imaging, likely since communicating arteries are usually too narrow to enable effective blood flow. Variations are most common in the posterior half of the CoW,[229185] including the posterior communicating artery (PcoA) variant as well as the fetal-type posterior cerebral artery (FTP) variant (20% prevalence). These anomalies may alter CVD occurrence, severity of symptoms, treatment options and recovery from vascular-related cognitive impairment.

3.1.1 Large Artery Mediators of Hemodynamics in the Aging Brain

Since arterial resistance is the major determinant of pressure dissipation and CBF regulation, increases in large artery resistance along the vascular tree, particularly the CoW, may also increase regional vulnerability to hypoperfusion. Four major arteries from the heart feed into the brain: (a) the left and right common carotid arteries that eventually form internal carotid arteries (ICA) in the brain as well as (b) the left and right subclavian arteries that eventually merge to form the basilar artery (BA) in front of the brainstem. The BA branches into posterior cerebral arteries (PCA), which perfuse posterior regions of the brain, and the ICA branches into anterior cerebral arteries (ACA) and middle cerebral arteries (MCA), which perfuse anterior regions of the brain.[231] PCA and ICA segments join together near the base of the skull to form the CoW, a structure whose primary function is thought to be collateral circulation (**Figure 3.3**, Panel A). However, there is considerable variation in CoW anatomy across humans, with only 20-25% of individuals possessing a completely patent structure. The most common abnormalities occurring in the

posterior regions, particularly the PcoA segments connecting anterior and posterior circulation segments (**Figure 3.3**, Panel C).

Figure 3.3: Circle of Willis Structure, Function, & Common Variants

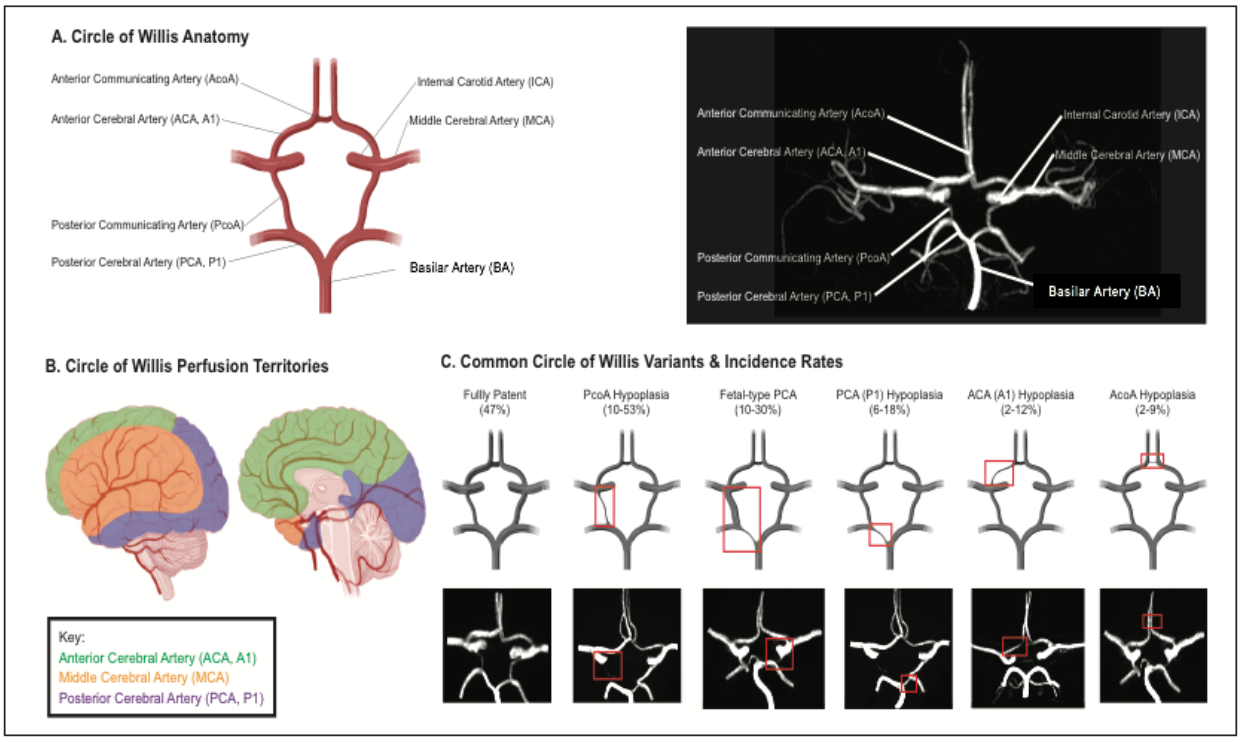

Note. Panel A: The Circle of Willis consists of 7 arterial segments, which are commonly assessed *in vivo* using magnetic resonance angiography. **Panel B:** Each of the 7 segments contributes to distinct perfusion territories across the brain, primarily determined by the ACA/A1, MCA/M1, and PCA/P1 segments. **Panel C:** Circle of Willis variants are present in most adults, most commonly including hypoplastic segments in the posterior circulation; corresponding prevalence data are listed as percentages within parentheses. See **Panel A** for definitions of arterial segment acronyms.

Given the considerable anatomical variability in the CoW and emerging evidence that PcoAs may not pass collateral flow efficiently even when they are present, newer models suggest the CoW may also play a central role in flow and pressure pulsatility dampening[224] under conditions such as hypertension.[232,233] Variations in CoW geometry may create both vulnerabilities in blood flow distribution[234,235] or protective increases in collateral flow.[236] In addition to missing segments, alterations in arterial radius and bifurcation angles at the CoW are strong predictors of hemodynamic stress.[237,238] Typical age-related changes in wall morphology of large arteries,

including stiffening and dilatation,[239] are thought to increase damaging pulsatility into downstream tissue. Indeed, advanced aging and dementia are accompanied by increases in pulsatility in the brain,[240] which promote vascular remodeling, higher resistance, and microvascular damage. More recently, CoW arterial aging (e.g., larger arterial diameters and wall thickening of cerebral large arteries) has been linked to worse clinical outcomes, including worse memory performance[241] and risk of AD.[239] Ultimately, the CoW is one of the largest determinants of innate differences in cerebrovascular resistance among individuals and variations in its structure likely play a critical role in mediating microvascular damage.

The structure of large artery networks also predisposes certain brain areas to high risk of hypoperfusion. Watershed regions, defined as territories supplied by the most distal arterial segments, are the first to be deprived of sufficient blood flow in the event of global hypoperfusion. These regions are highly susceptible to ischemic damage and microinfarcts due the fact that they have the least amount of collateral support from neighboring arterioles. They are primarily located at the junctures of CoW artery perfusion territories and include both cortical watershed regions (e.g., ACA-MCA juncture along the lateral frontal-parietal lobe and MCA-PCA juncture along the lateral temporal lobe) and internal watershed regions (e.g., subcortical white matter along the lateral ventricle and deep MCA arterial systems) (**Figure 3**, Panel B). In contrast to distal perfusion territories, regions supplied by the shortest perfusion branches (e.g., subcortical segments closer to the CoW such as the hippocampus[242,243]) are also especially susceptible to damage. These proximal regions likely have less opportunity to dampen pressure and flow pulsatility, as occurs when blood flow is distributed over the entire cerebrovasculature, and thus experience more severe blood pressure gradients.[244] In addition, age-associated vessel tortuosity may create flow instabilities and generate vortex flow patterns susceptible to embolism and aneurysm rupture.[245,246] The combined effect of these large artery structural variations ultimately contributes to compromises in CBF quality over time and compounds downstream small vessel damage and disease.

Damage from common cardiovascular risk factors, such as hypertension, shifts resistance properties upstream of arterioles and may thus increase the likelihood of prematurely attenuating downstream blood flow. These changes likely increase resistance as initial compensatory responses to vascular damage (e.g., cerebral microvascular remodeling) but may eventually lead to hypoperfusion and microvascular parenchymal damage over time. Thus, upstream large arteries have been increasingly recognized as a major contributor to cerebrovascular regulation, and variabilities in their structure may have larger clinical implications in advanced aging than previously recognized.

3.1.2 Study Aims

In this study, we investigate associations between PWV and large artery morphology, specifically lumen diameter of CoW segments. We further investigate the physiological consequences of the most common CoW variants among aging adults for cerebral hemodynamics, including missing PcoA, missing anterior communicating artery (AcoA), and FTP variants. We examine whether these variants relate to regional CBF alterations. We hypothesize that higher PWV will lead to large artery dilatation (i.e., increased lumen diameter) due to increased pulsatility. Furthermore, given the purported role of communicating arteries in protecting downstream microvasculature from increased pulsatility, we hypothesize that communicating artery variant structures will relate to lower blood flow, particularly in temporal lobe regions vulnerable to hemodynamic stress.

3.2 Methods

3.2.1 Study Cohort

See **Section 2.2.1** for previously described methods for cohort selection. Note, Chapter 3 analyses only included only participants with NC diagnosis and excluded participants for missing, pCASL MRI data, phase contrast magnetic resonance angiography (MRA) data, or covariate data.

3.2.2 CMR Imaging

See **Section 2.2.2** for previously described methods for CMR imaging.

3.2.3 Brain MRI

3.2.3.1 Circle of Willis Evaluation

Participants were scanned at the Vanderbilt University Institute of Imaging Science on a 3T Philips Achieva system (Best, Netherlands) using 8-channel phased-array sensitivity encoding reception. Vessel wall imaging (VWI) (repetition time=1500 ms, echo time=38.5 ms, spatial resolution=0.6x0.6x1.0 mm^3) and MRA images (repetition time=6.8 ms, echo time=3.8 ms, spatial resolution=0.35x0.35x0.35 mm^3) were acquired as part of the larger multimodal neuroimaging protocol.

VWI was used to assess the lumen diameter of the CoW by a board-certified neuroradiologist (Dr. L. Taylor Davis) blinded to clinical information. This novel 3D sequence uses an anti-DRIVE module with appropriately spaced repetition time to keep CSF magnetization near zero, while nulling the blood water signal using a long turbo-spin-echo pulse train, allowing visualization of the vessel walls.[197] CoW basilar artery (BA), supraclinoid ICA (left ICA, right ICA), proximal MCA (left MCA, right MCA), and proximal ACA (left ACA, right ACA) segments were evaluated for inner lumen diameter based off manual measurements of single image slices (see **Figure 3.4**).

Figure 3.4: CoW Lumen Diameter Evaluation on VWI (from Jefferson et al., 2016[197])

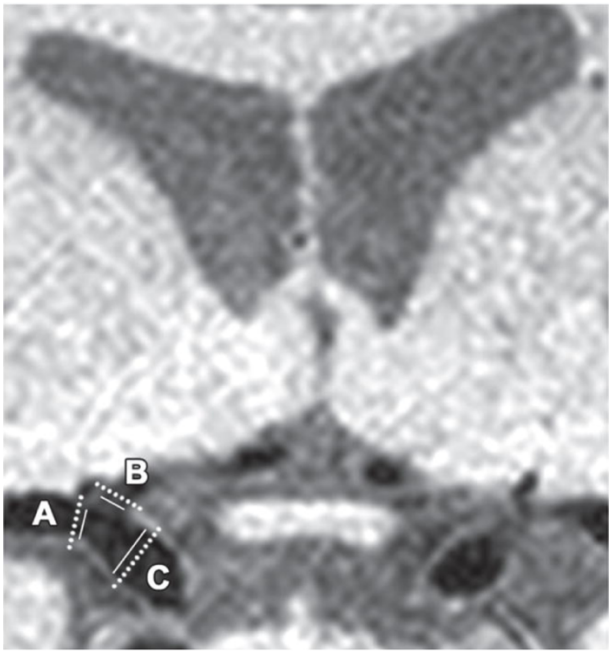

Note. The dashed line illustrates measurement of the outer diameter of the vessel wall and the solid line illustrates measurement of the inner diameter of the vessel wall for representative middle cerebral artery (A), anterior cerebral artery (B), and internal carotid artery (C). CoW indicates Circle of Willis; VWI, vessel wall imaging.

MRA was used to assess the patency of the CoW and all images were reviewed on two separate occasions by a board-certified neuroradiologist (Dr. L. Taylor Davis) blinded to clinical information. CoW communicating artery (i.e., AcoA, left PcoA, right PcoA), P1 (left P1, right P1), and A1 (left A1, right A1) segments were coded based off manual measurements of single image slices as normal (≥0.8 mm), hypoplastic (<0.8 mm), or aplastic (invisible on MRA). All CoW segments that were coded differently between the two measurements were further assessed by a separate reviewer (CWB) using 3D MRA reconstructed images in OsiriX (Geneva, Switzerland). The 3D reconstructed images were used to make a final decision of normal, hypoplastic, or aplastic on all segments in which discrepancies existed. The entire CoW was then further classified as one of 4 variants: missing PcoA (unilateral or bilateral aplastic), missing AcoA (aplastic), full FTP (unilateral or bilateral P1 aplastic), and partial FTP (unilateral or bilateral P1 hypoplasia and normal ipsilateral PcoA) (see **Figure 3.5**).

Figure 3.5: Circle of Willis Patency Evaluation on Magnetic Resonance Angiography

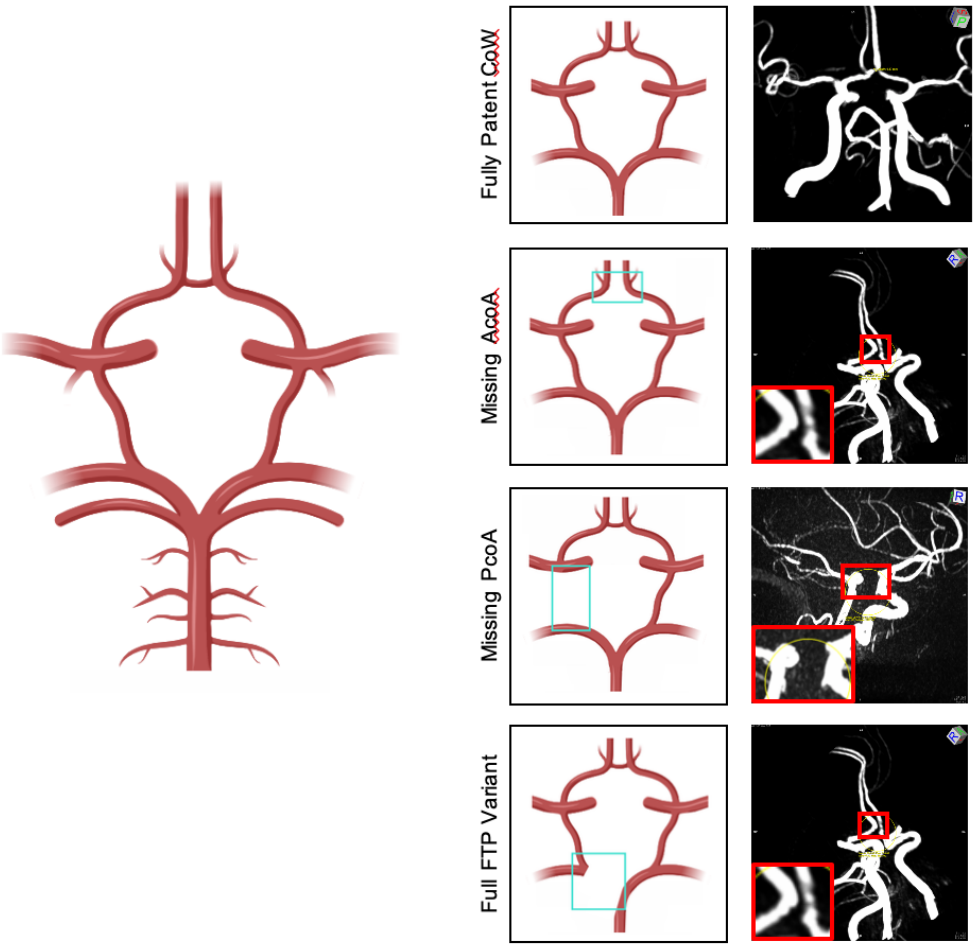

Note. Variants of the Circle of Willis (left) common in the population were classified into 4 groups (right): missing PcoA (unilateral or bilateral aplastic), missing AcoA (aplastic), full FTP (unilateral or bilateral P1 aplastic), and partial FTP (unilateral or bilateral P1 hypoplasia and normal ipsilateral PcoA); CoW indicates Circle of Willis; PcoA, posterior communicating artery; AcoA, anterior communicating artery; FTP, fetal-type posterior cerebral artery.

3.2.3.2 Cerebral Blood Flow

See **Section 2.2.3** for previously described methods for pCASL image collection and processing. Note, T_1-weighted magnetization-prepared rapid gradient echo (isotropic spatial resolution, $1mm^3$) images were post-processed with an established Multi-Atlas Segmentation pipeline[200,201] with parcellation of 4 regions of interest, including frontal, temporal, parietal, and occipital lobes.

3.2.4 Echocardiography

See **Section 2.2.4** for previously described methods for echocardiography.

3.2.5 Genetic Testing

See **Section 2.2.5** for previously described methods for *APOE* e4 genotyping.

3.2.6 Covariate Definitions

See **Section 2.2.6** for previously described methods for defining covariates.

3.2.7 Analytical Plan

Linear regression models with ordinary least square estimates related PWV to VWI-assessed lumen diameters measured across BA and bilateral ICA, MCA, and ACA segments. Models were adjusted for age, sex, race/ethnicity, education, FSRP (excluding points assigned for age), *APOE* ε4 status, and BMI. Significance was set *a priori* at p-value<0.05.

Linear regression models with ordinary least square estimates were also used to relate AcoA, PcoA, full FTP, and partial FTP variants to CBF regions of interest (one test per model), adjusting for age, sex, race/ethnicity, education, FSRP (excluding points assigned for age), *APOE* ε4 status, and regional tissue volume. To determine if outliers were driving the cross-sectional or longitudinal results, additional models were calculated excluding predictor or outcome values >4 standard deviations from the group mean. For all models, follow-up sensitivity analyses were performed excluding participants with prevalent cardiovascular disease or atrial fibrillation to test if these conditions accounted for significant results. All analyses were conducted using R version 3.2.3 (www.r-project.org).

3.3 Results

3.3.1 Participant Characteristics

The cohort was composed of 163 NC participants (73±7 years, 58% male) (**Table 3.1**). In line with the general population, the most common CoW variants occurred at the PcoAs, which had hypoplastic or missing segments in 78% of participants. The second most common variant occurred at the AcoA, which had hypoplastic or missing segments in 58% of participants. In contrast, P1 variants occurred in only 23% of participants, and A1 variants occurred in 10% of participants. Among PcoAs, hypoplastic (42%) and missing (44%) variants occurred at a similar prevalence, while hypoplastic variants were more common among AcoA, P1, and A1 segments. Partial FTP variants (15%) were more common than full FTP variants (8%). Across all segments, unilateral variants were more common than bilateral variants. See **Table 3.2** for more details on the prevalence of CoW variants.

Table 3.1: Participant Characteristics by Communicating Artery Variant

	Combined (n=163)	AcoA & PcoAs Present (n=79)	Missing AcoA (n=14)	Missing PcoA (n=64)	Missing AcoA & PcoA (n=8)	*p*-value
Demographic Characteristics						
Age, years	73±7	72±7	70±9	73±7	74±6	0.40
Sex, % male	58	50	43	71	62	0.06
Race, % Non-Hispanic White	87	90	71	88	75	0.20
Education, years	16±3	16±3	16±2	17±3	18±2	0.42
APOE ε4, % carrier	30	30	29	28	50	0.64
Body mass index, kg/m^2	27.6±5	27.8±5	25.8±4	27.5±5	29.1±4	0.13
Framingham Stroke Risk Profile, total	11.9±4.1	12.1±4.1	11.4±5.1	11.7±4.1	12.9±3.3	0.68
Systolic blood pressure, mmHg	140±17	142±17	136±16	139±19	138±15	0.52
Anti-hypertensive medication usage, %	55	51	57	51	75	0.60
Diabetes, %	16	11	36	17	25	0.12
Cigarette smoking, % current	2	1	7	2	0	0.46
Prevalent cardiovascular disease, %	4	2	0	8	0	0.32
Atrial fibrillation, %	5	5	0	5	12	0.62
Left ventricular hypertrophy, %	3	4	7	2	0	0.63
Grey Matter Volume						
Frontal lobes	226781± 31781	230042± 33330	209526± 32299	226227± 29448	226981± 29193	0.12
Temporal lobes	136272± 15764	137523± 15378	122252± 11396	137417± 15751	137683± 17292	**0.01**
Parietal lobes	129620± 17635	131825± 17271	117127± 15005	129567± 18076	128567± 15722	**0.03**
Occipital lobes	90983±	92650±	81634±	90494±	93565±	**0.004**

	11119	10590	11823	10752	12027	
Cerebral Blood Flow, mL/100g/min						
Frontal lobes	37.4±7.5	38.7±7.0	35.9±8.8	36.0±7.8	38.9±6.5	0.10
Temporal lobes	36.1±6.6	37.1±6.9	35.4±5.0	34.6±6.3	39.1±7.0	0.20
Parietal lobes	39.9±9.9	41.6±10.3	38.9±12.5	38.4±8.5	36.4±8.9	0.27
Occipital lobes	36.7±9.6	39.2±9.0	35.8±13.4	34.1±8.8	34.3±9.4	**0.01**

Note: Descriptive statistics were calculated using mean±standard deviation for continuous variables and frequencies for categorical variables. Between-group characteristics were statistically compared using rank-based Kruskal-Wallis test for continuous variables and Pearson's chi-square test for categorical variables. Framingham Stroke Risk Profile (minus age points) score is 6.2±3.0 for the total cohort. AcoA indicates anterior communicating artery; PcoA, posterior communicating artery; *APOE*, apolipoprotein E; mL/100g/min, milliliters of blood per 100 grams of tissue per minute.

Table 3.2: Prevalence of CoW Variants

Individual Segment	Normal	Variant	
		Hypoplastic[A]	Missing
PcoA	22.1% (69)	41.7% (130)	44.2% (138)
Unilateral PcoA	—	27.2% (85)	23.7% (74)
Bilateral PcoA	—	14.4% (45)	20.5% (64)
AcoA	42.0% (131)	41.3% (129)	16.3% (51)
P1	76.9% (240)	16.7% (52)	7.7% (24)
Unilateral P1	—	14.1% (44)	7.4% (23)
Bilateral P1	—	2.6% (8)	0.3% (1)
A1	89.7% (280)	6.7% (21)	3.5% (11)
Unilateral A1	—	6.7% (21)	3.5% (11)
Bilateral A1	—	0% (0)	0% (0)
FTP Variant	Normal	FTP Variant	
Partial FTP Variant	84.6% (264)	15.4% (48)	
Unilateral Partial FTP	—	12.8% (40)	
Bilateral Partial FTP	—	2.6% (8)	
Full FTP Variant	92.3% (288)	7.7% (24)	
Unilateral Full FTP	—	7.4% (23)	
Bilateral Full FTP	—	0.3% (1)	

Note. PcoA indicates posterior communicating artery; AcoA, anterior communicating artery; P1, P1 segment of poster cerebral artery; A1, A1 segment of the anterior cerebral artery; FTP, fetal-type posterior cerebral artery, wherein there is a hypoplastic (i.e., partial FTP) or missing (i.e., full FTP) P1 segment of the posterior cerebral artery.
[A] Per Iqbal et al. (2013), hypoplastic vessels were encountered either alone or in combination with other anomalies.[247]

3.3.2 PWV & CoW Lumen Diameters

PWV did not relate to CoW lumen diameter across the 7 segments evaluated (p-values>0.17). See **Table 3.3** for details.

Table 3.3: Aortic PWV & CoW Lumen Diameters

	β	95% CI	*p*-value
Left ICA	0.002	0.01	0.91
Right ICA	0.003	0.02	0.86
Left ACA	-0.002	0.01	0.87
Right ACA	0.02	0.01	0.18
Left MCA	0.007	0.01	0.53
Right MCA	-0.01	0.01	0.54
BA	0.03	0.02	0.13

Note. n=150 participants with normal cognition. CI indicates 95% confidence interval; ICA; internal carotid artery; ACA, anterior cerebral artery; MCA, middle cerebral artery; BA, basilar artery.

3.3.3 CoW Variants & CBF

Missing PcoAs were related to frontal lobe (*p*-value=0.04), temporal lobe (*p*-value=0.01), and occipital lobe (*p*-value=0.004) CBF and unrelated to parietal lobe CBF (*p*-value=0.07). Missing AcoA was related to occipital lobe CBF (*p*-value=0.04) and unrelated to frontal lobe, parietal lobe, and temporal lobe CBF (*p*-values>0.19). Neither full FTP nor partial FTP variants related to lobar CBF (*p*-values>0.08). See **Table 3.4** for details.

Table 3.4: CoW Variants & CBF

	β	95% CI	*p*-value
Missing PcoA & CBF ROI			
Frontal Lobe	-2.66	-5.16, -1.60	**0.04**
Parietal Lobe	-3.01	-6.34, 0.31	0.07
Temporal Lobe	-2.82	-5.08, -0.56	**0.01**
Occipital Lobe	-4.35	-7.31, -1.39	**0.004**
Missing AcoA & CBF ROI			
Frontal Lobe	-2.92	-7.34, 1.50	0.19
Parietal Lobe	-3.22	-9.14, 2.69	0.28
Temporal Lobe	-1.88	-5.98, 2.22	0.37
Occipital Lobe	-5.44	-1.07, -1.37	**0.04**
Full FTP Variant & CBF ROI			

Frontal Lobe	-1.15	-5.97, 3.67	0.68
Parietal Lobe	-3.35	-9.67, 2.97	0.30
Temporal Lobe	-1.93	-6.29, 2.44	0.38
Occipital Lobe	-2.22	-7.91, 3.47	0.44
Partial FTP Variant & CBF ROI			
Frontal Lobe	-2.72	-5.81, 3.71	0.08
Parietal Lobe	-0.36	-4.46, 3.75	0.86
Temporal Lobe	-0.69	-3.58, 2.19	0.64
Occipital Lobe	0.06	-3.66, 3.79	0.97

Note. n=163 participants with normal cognition. CoW indicates Circle of Willis; CBF, cerebral blood flow; CI, 95% confidence interval; PcoA, posterior communicating artery; ROI, region of interest; AcoA, anterior communicating artery; FTP, fetal-type posterior cerebral artery.

3.4 Discussion

While PWV failed to predict CoW lumen diameter, suggesting large artery morphological changes likely do not mediate any PWV-CBF associations, differences in CoW variants did appear to relate to downstream microvascular health. Specifically, among community-dwelling older adults free of clinical stroke or dementia, missing PcoA variants are related to lower CBF across brain, including frontal, temporal, and occipital lobes, while missing AcoA variants related to lower parietal lobe CBF. Furthermore, neither partial FTP nor full FTP variants related to CBF outcomes. It is noteworthy that effects reported here are statistically independent of many shared vascular risk factors. Overall results suggest CoW communicating artery variants contribute to subtly different hemodynamic risk profiles, which may place certain individuals at a higher risk for CBF disturbances.

In addition to the CoW's purported role in collateral circulation, it has recently been implicated as a cerebral pressure dampener that acts to reduces hemodynamic stress and protect downstream cerebrovasculature.[224] While the aorta is the primary segment of the central vasculature that absorbs and re-distributes cardiac-generated pulsatile energy, the CoW may serve a similar, secondary function within the cranial cavity. If the CoW acts as a protective pressure diffuser, then

absent segments of the CoW may contribute to compromised CBF. However, the prevailing evolutionary hypothesis of the CoW indicates that its development served to overcome the selective pressure of vascular diseases (e.g., stenosis), implying that it may not play a large role in normal physiology.

Our findings indicate that even among relatively healthy older adults with a low prevalence of cardiovascular disease (4%) compared to the general population over age 65 (24% to 37%),[248] missing communicating arteries may relate to compromised cerebral hemodynamics. While it is not likely that the magnitude of associated CBF reductions would be sufficient to cause outright tissue damage, these unique CoW variants serve to create distinct hemodynamic risk profiles which may be more susceptible to emerging age-related pathology as well as microvascular and tissue dysfunction in vulnerable perfusion areas. A lack of communicating arteries, more so posterior cerebral artery variants (e.g., FTP variants), may expose cerebral microcirculation to high stress that might cause arterial wall and blood brain barrier damage, especially during strenuous conditions.

While we failed to find associations between PWV and CoW morphology as assessed on VWI, it is possible that pulsatility-driven stress and functional changes (more so than outright structural changes) may mediate any downstream effects on CBF. In particular, links between increased pulsatility and markers cellular dysfunction have been well-established in animal models (e.g., endothelial dysfunction[249]) although direction of causality remains unclear. Future work should examine emerging *in vivo* markers of vascular dysfunction as potential mediation candidates, including protein biomarkers of BBB dysfunction and novel neuroimaging measures of vascular reactivity.

There are several strengths of the current project. First, our extensive MRA image review protocol, including double-review by a primary a board-certified neuroradiologist reviewer (Dr. L. Taylor

Davis) and subsequent reconciliation of any discrepancies by a secondary reviewer (Dr. Corey W. Bown), greatly reduces measurement error in CoW assessment. Second, our comprehensive variant coding, including characterization of single segment variants as well as multi-segment variants (i.e., FTP), captures a diverse range of the most commonly observed variants. Our findings thus have large clinical relevance to the general population. Conversely however, it is important to note that the cohort is not reflective of the general population since participants were older, predominantly White, well educated, and relatively healthy as mentioned above. Whether such variables limit the generalizability of our results is unknown, but we purport that in a less healthy cohort with greater vascular risk factors or more compromised cardiac function, the association between communicating artery variants of the CoW and CBF among older adults would likely be stronger. Given the cross-sectional nature of the study, we cannot draw conclusions about causal relationships or CBF trajectory. Furthermore, multiple comparisons raise the possibility of a false positive finding and emphasize the need for replication. Further research is warranted to examine the clinical significance of CoW variations, including the impact of regional CBF compromise on cognition and whether they occur independently or through a shared pathway.

CHAPTER 4[c]

Cognition

4.1 Introduction

Age-related changes in vascular structure and hemodynamics have increasingly been associated with cerebrovascular disease, a leading cause of cognitive impairment.[250-252] Evidence suggests chronic risk factors for cerebrovascular disease, such as hypertension, may impair autoregulatory systems responsible for maintaining constant cerebral perfusion and protecting against mean arterial pressure changes.[84] Systemic vascular changes, such as central arterial stiffening, may further compromise the brain's autoregulatory mechanisms and affect tissue integrity.[253]

Age-related arterial stiffening is postulated to drive end-organ damage through transmission of harmful pulsatile energy to the peripheral microcirculation, a phenomenon associated with microvascular abnormalities in high-flow/low-resistance organs, such as the kidney.[254] The brain, another vulnerable high-flow and low-resistance organ, may also be particularly susceptible to pulsatile energy damage, including increased microvascular remodeling and impaired local blood flow regulation (see Mitchell, 2008[189] for review). Arterial stiffening is often characterized by increased PWV, a noninvasive measure of arterial wall properties. Higher PWV has been linked to worse cognitive performance,[255] faster rates of cognitive decline,[256,257] and MCI,[258] though findings have been inconsistent.[259]

[c] This chapter is adapted from "APOE genotype modifies the association between central arterial stiffening and cognition in older adults" published in *Neurobiology of Aging* and has been reproduced with the permission of the publisher and my co-authors: Dr. Dandan Liu, Dr. Jacquelyn E. Neal, Dr. Elizabeth E. Moore, Dr. Katherine A. Gifford, James G Terry, Sangeeta Nair, Dr. Kimberly R. Pechman, Dr. Katie E. Osborn, Dr. Timothy J. Hohman, Dr. Susan P. Bell, Dr. J. David Sweatt, Dr. Thomas J. Wang, Dr. Joshua A Beckman, Dr. John Jeffrey Carr, and Dr. Angela L. Jefferson.

One of the most well-established risk factors for cognitive decline is the *APOE* ε4, an AD genetic susceptibility marker. *APOE* ε4 is thought to promote AD pathogenesis through its roles in lipid metabolism, accelerating Aβ deposition, and neuroinflammation. However, increasing evidence indicates that *APOE* genotypes also differentially modulate the function of the cerebrovasculature through direct signaling, indirect effects of peripheral and central pathway modulation, and exacerbating the effects of additional vascular risk factors (e.g., hypertension, diabetes).[260] In particular, *APOE* ε4 mediates BBB breakdown[162] and facilitates Aβ accumulation,[161,261] which can induce cerebrovascular dysfunction, including endothelial damage and changes in vascular tone.[262,263] Such *APOE* ε4 vascular effects purportedly occur prior to neuronal dysfunction and degeneration.[160] Accordingly, *APOE* ε4 modifies the association between vascular disease and brain abnormalities[194] and relates to earlier, more progressive cognitive decline.[264] *APOE* ε4 carriers may thus be susceptible to cerebrovascular injury via subclinical central vascular changes, particularly elevated PWV.

Using the best available non-invasive assessment of central arterial stiffening that directly approximates PWV across the proximal aorta, the current study evaluates how *APOE* ε4 interacts with PWV to modify the association between PWV and neuropsychological performance at baseline and longitudinally among community-dwelling older adults free of clinical dementia and stroke. Our hypothesis is that *APOE* ε4 will modify the association between PWV and neuropsychological performance, such that *APOE* ε4 carriers will have stronger associations between elevated PWV and poorer cognitive performance as well as faster cognitive decline when compared to non-carriers. We predict that PWV × *APOE* ε4 associations will be strongest in participants with prodromal dementia (i.e., MCI) because they may be more susceptible to *APOE* ε4 effects. Based on prior findings, we further hypothesize that these effects will be especially prominent in the domains of information processing speed,[257] executive function,[255,265] and episodic memory measures.[70,256,265]

4.2 Methods

4.2.1 Study Cohort

See **Section 2.2.1** for previously described methods for cohort selection. Participants were excluded from the current study for missing baseline PWV, baseline covariate data, or neuropsychological data across all timepoints (**Figure 4.1**).

Figure 4.1: Participant Inclusion & Exclusion Criteria

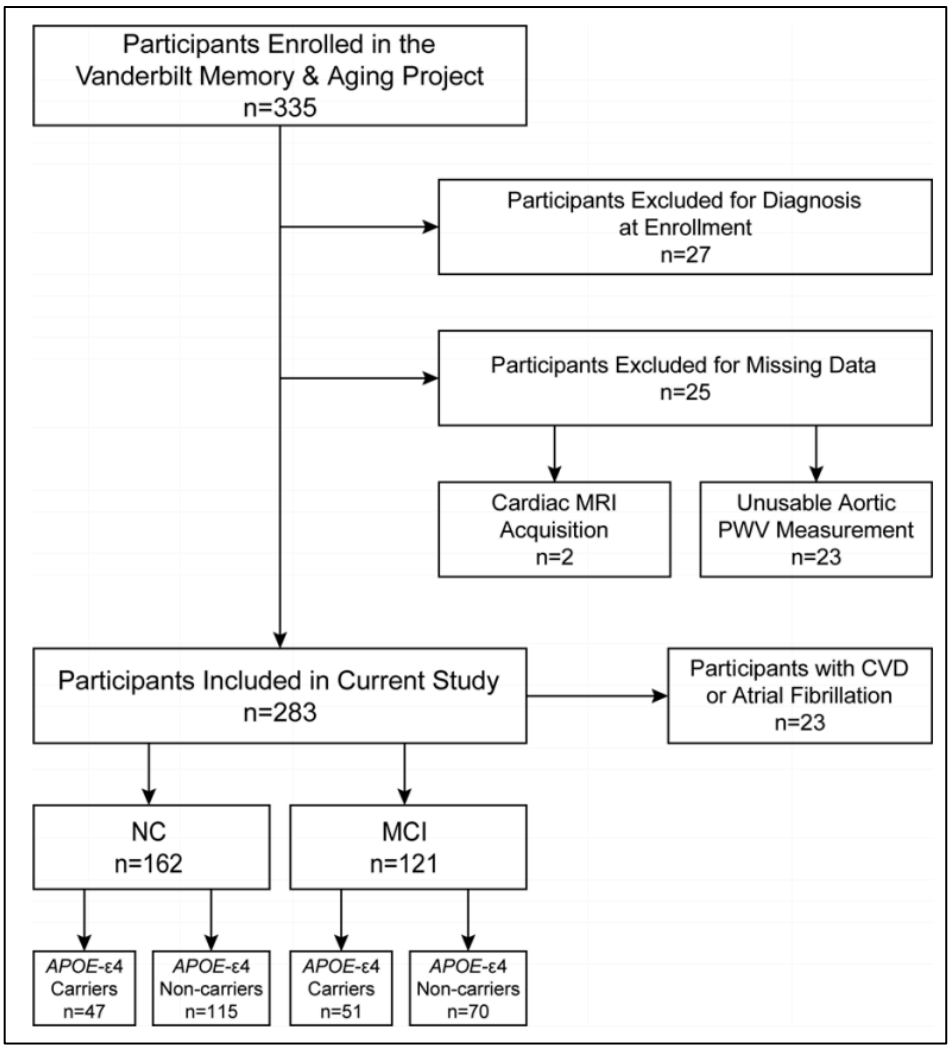

Note. Missing data categories are mutually exclusive. MRI indicates magnetic resonance imaging; PWV, pulse wave velocity; CVD, cardiovascular disease; NC, normal cognition; MCI, mild cognitive impairment; *APOE*, apolipoprotein E.

4.2.2 CMR Imaging

See **Section 2.2.2** for previously described methods for CMR imaging to capture PWV, a gold-standard non-invasive measure of aortic stiffness.

4.2.3 Neuropsychological Assessment

All participants completed a common, comprehensive neuropsychological protocol assessing language, information processing speed, executive functioning, visuospatial skills, and episodic memory (see **Table 4.1** for list of assessment tools). Measures were carefully selected to preclude floor or ceiling effects. Note, these measures were not used as part of the screening or selection of participants into the study.

4.2.4 Echocardiography

See **Section 2.2.4** for previously described methods for echocardiography.

4.2.5 Genetic Testing

See **Section 2.2.5** for previously described methods for *APOE* e4 genotyping.

4.2.6 Covariate Definitions

See **Section 2.2.6** for previously described methods for defining statistical covariates.

4.2.7 Analytical Plan

Before analyses, scatterplots with linear fit and locally weighted smoothing fit were visually inspected for linearity. Covariates were selected *a priori* for their potential to confound the analytical models. Linear regression models with ordinary least square estimates related PWV to neuropsychological test performance (one test per model). Models were adjusted for age,

race/ethnicity, education, *APOE* ε4 status, BMI, and FSRP (excluding points assigned for age). To test hypotheses related to cognitive diagnosis, models were diagnostically stratified (NC, MCI) and then repeated in sensitivity analyses excluding participants with cardiovascular disease or atrial fibrillation to assess whether these conditions accounted for any significant results. To test hypotheses related to *APOE* ε4 status, diagnostically stratified models were repeated with a PWV × *APOE* ε4 interaction term. In post-hoc analyses, significant cross-sectional models were re-analyzed to assess allele dosage effects where *APOE* ε4 status was defined as zero, one, or two ε4 alleles. Lower order terms were retained in the interaction models. Significance was set *a priori* at p-value<0.05.

Linear mixed-effects regression models related baseline PWV to longitudinal neuropsychological performance (one test per model), including an interaction with time to follow-up between baseline and last follow-up visit (in years) as the term of interest. We model the trajectory of cognition using these linear mixed-effect regression models, where terms involving follow-up time capture cognitive decline. Models were adjusted for age, race/ethnicity, education, FSRP score (excluding points assigned for age), BMI, *APOE* ε4 status, and follow-up time. To test hypotheses related to cognitive diagnosis, models were repeated with a PWV × follow-up time × diagnosis interaction term, with follow-up models stratified by diagnosis (NC, MCI). To test hypotheses related to *APOE* ε4 status, models were repeated with a PWV × follow-up time x *APOE* ε4 carrier status interaction term with follow-up models stratified by *APOE* ε4 carrier status (carrier, non-carrier). Lower order terms were included in all interaction models. Significance was set *a priori* at p-value<0.05.

To determine if outliers were driving the cross-sectional or longitudinal results, additional models were calculated excluding predictor or outcome values >4 standard deviations from the group mean. For all models, follow-up sensitivity analyses were performed excluding participants with prevalent cardiovascular disease or atrial fibrillation to test if these conditions accounted for

significant results. To account for the effect of multiple comparisons, the Benjamini-Hochberg procedure[266] was used to control the false discovery rate (FDR); thresholds were set at Q=0.05 for main models and Q=0.10 for *APOE* ε4 interaction models. All analyses were conducted using R version 3.2.3 (www.r-project.org).

4.3 Results

4.3.1 Participant Characteristics

The analytical sample was composed of 283 participants (73±7 years, 59% male), including 162 NC and 121 MCI participants. 283 participants included in the study were seen at baseline with a mean follow-up period of 4.88 years. The mean sample age at baseline was 73 ± 7 years (ranging 60–92 years), 58% were men, and 87% self-identified as non-Hispanic white. At baseline, PWV values ranged 3.5 to 25.5 m/s (8.2±3.2) and did not differ between NC and MCI participant groups (*p*-value=0.87). At least one *APOE* ε4 allele was present in 35% of the cohort, with higher *APOE* ε4 allele prevalence in the MCI (42%) compared to the NC group (29%, *p*-value=0.02). See **Table 4.1** for more details on participant characteristics.

Table 4.1: Baseline Participant Characteristics

	Total (n=283)	NC (n=162)	MCI (n=121)	*p*-value
Demographic Characteristics				
Age, years	73±7	72±7	73±8	0.39
Sex, % male	59	59	58	0.81
Race, % Non-Hispanic White	87	87	86	0.79
Education, years	16±3	16±2	15±3	**<0.001**
MOCA, total	25±3	27±2	23±3	**<0.001**
APOE ε4, % carrier	35	29	42	**0.02**
BMI, kg/m^2	27.6±5	27.4±5	27.8±5	0.24
FSRP, total	12.2±4.2	11.8±4.2	12.8±4.2	0.06
Systolic blood pressures, mmHg	141±18	139±17	144±18	**0.02**
Anti-hypertensive medication usage, %	52	52	52	0.95
Diabetes, %	18	16	21	0.24
Cigarette smoking, % current	2	1	2	0.43
Prevalent cardiovascular disease, %	4	4	3	0.86
Atrial fibrillation, %	5	5	5	0.00
Left ventricular hypertrophy, %	5	4	6	0.41
Aortic PWV, m/s	8.2±3.2	8.2±3.0	8.3±3.4	0.87
Neuropsychological Performance				
Boston Naming Test, 30-Item	26.9±3.0	27.9±2.0	25.6±3.6	**<0.001**
Animal Naming	18.9±5.4	20.8±4.8	16.4±5.1	**<0.001**
WAIS-IV Coding	52.8±13.0	57.4±11.7	46.6±11.9	**<0.001**
DKEFS Number Sequencing, s[a]	41.8±19.4	36.0±12.8	49.6±23.6	**<0.001**
DKEFS Letter-Number Switching, s[a]	115±80	87±35	153±105	**<0.001**
DKEFS Tower Test	14.7±4.7	16.0±4.3	13.0±4.7	**<0.001**
DKEFS Color-Word Inhibition, s[a]	68.5±24.2	59.9±14.1	79.8±29.5	**<0.001**
Letter Fluency (FAS) Test	39.1±11.8	42.9±11.6	33.9±9.8	**<0.001**
Hooper Visual Organization Test	24.5±3.0	25.3±2.5	23.5±3.4	**<0.001**

CVLT-II Total Immediate Recall	40.5±12.2	46.9±9.7	32.0±9.8	**<0.001**
CVLT-II Delayed Recall	8.1±4.4	10.4±3.4	4.9±3.5	**<0.001**
CVLT-II Recognition	2.4±1.0	3.0±0.7	1.6±0.9	**<0.001**
BFLT Total Immediate Recall	114±42	137±30	83±36	**<0.001**
BFLT Delayed Recall	27±11.0	33±7.6	19±10.1	**<0.001**
BFLT Recognition	0.7±0.2	0.8±0.2	0.6±0.2	**<0.001**

Note. NC indicates normal cognition; MCI, mild cognitive impairment; MOCA, Montreal Cognitive Assessment; *APOE*, apolipoprotein E; BMI, body mass index; FSRP, Framingham Stroke Risk Profile; PWV, pulse wave velocity; WAIS-IV, Wechsler Adult Intelligence Scale, 4th edition; DKEFS, Delis-Kaplan Executive Function System; CVLT-II, California Verbal Learning Test, 2nd edition[267]; BFLT-II, Biber Figure Learning Test.
Descriptive statistics by baseline diagnosis were calculated using mean ± standard deviation for continuous variables and frequencies for categorical variables. Between-group characteristics were statistically compared using Wilcoxon test for continuous variables and Pearson test for categorical variables. Bolded values represent significant findings. All neuropsychological performance values are total correct excluding timed tasks measured in seconds (s).
[a] Higher values in speeded test results reflect worse performance.

As expected, the MCI group had worse neuropsychological performances compared to the NC group (*p*-values< 0.001) (**Table 4.1**) and greater annual longitudinal decline across all measures compared to NC participants (**Table 4.2**).

Table 4.2: Annual Change in Neuropsychological Performance

Neuropsychological Test	Total (n=283)	NC (n=162)	MCI (n=121)	*p*-value
Boston Naming Test, 30-Item	26.9±3.0	27.9±2.0	25.6±3.6	**<0.001**
Animal Naming	18.9±5.4	20.8±4.8	16.4±5.1	**<0.001**
WAIS-IV Coding	52.8±13.0	57.4±11.7	46.6±11.9	**<0.001**
DKEFS Number Sequencing, s[a]	41.8±19.4	36.0±12.8	49.6±23.6	**<0.001**
DKEFS Letter-Number Switching, s[a]	115±80	87±35	153±105	**<0.001**
DKEFS Tower Test	14.7±4.7	16.0±4.3	13.0±4.7	**<0.001**
DKEFS Color-Word Inhibition, s[a]	68.5±24.2	59.9±14.1	79.8±29.5	**<0.001**
Letter Fluency (FAS) Test	39.1±11.8	42.9±11.6	33.9±9.8	**<0.001**
Hooper Visual Organization Test	24.5±3.0	25.3±2.5	23.5±3.4	**<0.001**
CVLT-II Total Immediate Recall	40.5±12.2	46.9±9.7	32.0±9.8	**<0.001**
CVLT-II Delayed Recall	8.1±4.4	10.4±3.4	4.9±3.5	**<0.001**
CVLT-II Recognition	2.4±1.0	3.0±0.7	1.6±0.9	**<0.001**
BFLT Total Immediate Recall	114±42	137±30	83±36	**<0.001**
BFLT Delayed Recall	27±11.0	33±7.6	19±10.1	**<0.001**
BFLT Recognition	0.7±0.2	0.8±0.2	0.6±0.2	**<0.001**

Note. NC indicates normal cognition; MCI, Mild Cognitive Impairment; WAIS-IV, Wechsler Adult Intelligence Scale, 4th edition; DKEFS, Delis-Kaplan Executive Function System; CVLT-II, California Verbal Learning Test, 2nd edition[267]; BFLT-II, Biber Figure Learning Test.
Neuropsychological performance values represent the difference between last follow-up visit and baseline visit performances. p-values are presented for comparisons between NC and MCI groups using Wilcoxon test. Bolded values represent significant findings. All neuropsychological performance values are total correct excluding timed tasks measured in seconds (s).
[a] Higher values in speeded test results reflect worse performance.

4.3.2 Aortic PWV & Cross-Sectional Neuropsychological Performance

PWV Main Effects Analyses

In the combined cohort, PWV was unrelated to all neuropsychological performances (*p*-values>0.23). See **Table 4.3** for PWV main effects results in the total sample.

Table 4.3: Aortic PWV & Cross-Sectional Neuropsychological Performance

	β	95% CI	*p*-value
Combined Sample, n=283			
Boston Naming Test, 30-Item	0.01	-0.09, 0.11	0.87
Animal Naming	0.10	-0.08, 0.28	0.27
WAIS-IV Coding	-0.06	-0.49, 0.37	0.79
DKEFS Number Sequencing, s[a]	0.24	-0.43, 0.90	0.49
DKEFS Letter-Number Switching, s[a]	1.69	-1.09, 0.15	0.23
DKEFS Tower Test	-0.02	-0.19, 0.15	0.82
DKEFS Color-Word Inhibition, s[a]	0.28	-0.57, 1.13	0.52
Letter Fluency (FAS) Test	0.24	-0.18, 0.66	0.26
Hooper Visual Organization Test	0.02	-0.09, 0.12	0.78
CVLT-II Total Immediate Recall	0.14	-0.23, 0.52	0.44
CVLT-II Delayed Recall	-0.0003	-0.13, 0.13	>0.99
CVLT-II Recognition	-0.001	-0.03, 0.03	0.96
BFLT Total Immediate Recall	0.26	-0.97, 1.49	0.68
BFLT Delayed Recall	0.06	-0.27, -0.39	0.71
BFLT Recognition	-0.002	-0.01, 0.01	0.67

Note. PWV indicates pulse wave velocity; CI, confidence interval; WAIS-IV, Wechsler Adult Intelligence Scale, 4th edition; DKEFS indicates Delis-Kaplan Executive Function System; CVLT-II, California Verbal Learning Test, 2nd edition[267], BFLT-II, Biber Figure Learning Test.
All neuropsychological performance values are total correct excluding timed tasks measured in seconds (s).
[a] Higher values in speeded test results reflect worse performance.

Cognitive Diagnosis Subgroup Analyses

In results stratified by cognitive diagnosis, PWV was unrelated to all neuropsychological performances among NC participants (*p*-values>0.09) and MCI participants (*p*-values>0.35). See **Table 4.4** for cognitive diagnosis subgroup results.

Table 4.4: Aortic PWV & Cross-Sectional Neuropsychological Performance Stratified by Cognitive Diagnosis

	β	95% CI	*p*-value
NC Participants (n=162)			
Boston Naming Test, 30-Item	0.05	-0.05, 0.15	0.32
Animal Naming	0.14	-0.11, 0.39	0.28
WAIS-IV Coding	0.17	-0.42, 0.76	0.58
DKEFS Number Sequencing, s[a]	0.27	-0.34, 0.88	0.39
DKEFS Letter-Number Switching, s[a]	1.07	-0.58, 2.73	0.20
DKEFS Tower Test	-0.01	-0.25, 0.22	0.93
DKEFS Color-Word Inhibition, s[a]	0.24	-0.50, 0.98	0.52
Letter Fluency (FAS) Test	0.53	-0.09, 1.15	0.09
Hooper Visual Organization Test	0.07	-0.06, 0.20	0.27
CVLT-II Total Immediate Recall	0.08	-0.44, 0.60	0.76
CVLT-II Delayed Recall	-0.02	-0.20, 0.17	0.86
CVLT-II Recognition	-0.01	-0.05, 0.03	0.67
BFLT Total Immediate Recall	0.50	-1.09, 2.08	0.54
BFLT Delayed Recall	0.04	-0.37, 0.45	0.85
BFLT Recognition	-0.004	-0.01, 0.004	0.31
MCI Participants (n=121)			
Boston Naming Test, 30-Item	-0.01	-0.21, 0.18	0.89
Animal Naming	0.09	-0.18, 0.36	0.51
WAIS-IV Coding	-0.31	-0.95, 0.34	0.35
DKEFS Number Sequencing, s[a]	0.13	-1.18, 1.44	0.84
DKEFS Letter-Number Switching, s[a]	2.50	-3.33, 8.32	0.40
DKEFS Tower Test	-0.03	-0.30, 0.25	0.85
DKEFS Color-Word Inhibition, s[a]	0.32	-1.38, 2.02	0.71
Letter Fluency (FAS) Test	-0.12	-0.68, 0.45	0.69
Hooper Visual Organization Test	-0.06	-0.24, 0.13	0.55
CVLT-II Total Immediate Recall	0.24	-0.32, 0.80	0.39
CVLT-II Delayed Recall	0.02	-0.18, 0.22	0.82
CVLT-II Recognition	0.01	-0.04, 0.06	0.57
BFLT Total Immediate Recall	0.22	-1.80, 2.23	0.83

BFLT Delayed Recall	0.16	-0.40, 0.72	0.57
BFLT Recognition	0.003	-0.01, 0.02	0.69

Note. PWV indicates pulse wave velocity; CI, confidence interval; NC, normal cognition; MCI, mild cognitive impairment; WAIS-IV, Wechsler Adult Intelligence Scale, 4th edition; DKEFS, Delis-Kaplan Executive Function System; CVLT-II, California Verbal Learning Test, 2nd edition[267]; BFLT-II, Biber Figure Learning Test.
All neuropsychological performance values are total correct excluding timed tasks measured in seconds (s).
[a] Higher values in speeded test results reflect worse performance.

APOE ε4 Subgroup Analyses

APOE ε4 status modified the relationship between PWV and neuropsychological performance on Boston Naming Test (β=−0.29, 95% CI −0.51 to −0.07, *p*-value=0.01), Delis-Kaplan Executive Function System (DKEFS) Tower Test (β=−0.44, 95% CI −0.82 to −0.07, *p*-value=0.02), and Biber Figure Learning Test (BFLT) Total Immediate Recall (β=−3.07, 95% CI −5.70 to −0.43, *p*-value=0.02) (**Table 4.5**). For each test, *APOE* ε4 carriers experienced worse neuropsychological performances at higher PWV values compared to non-carriers (see **Figure 4.2** for illustrations). Of these *APOE* ε4 interaction results, none survived FDR adjustment. In sensitivity analyses, results were no longer statistically significant after exclusion for cardiovascular disease or atrial fibrillation though effect sizes were comparable to significant observations detected in the primary models. See **Table 4.5** for complete PWV × *APOE* ε4 interaction results. When models were stratified by *APOE* ε4 status, PWV was related to neuropsychological performances on the DKEFS Tower Test among *APOE* ε4 carriers (β=−0.43, 95% CI −0.79 to −0.07, *p*-value=0.02). Among *APOE* ε4 non-carriers, PWV was unrelated to neuropsychological performance (*p*-values>0.14).

Table 4.5: Aortic PWV × *APOE* ε4 & Cross-Sectional Neuropsychological Performance

	β	95% CI	*p*-value
Combined Sample, n=283			
Boston Naming Test, 30-Item	-0.29	-0.51, 0.07	**0.01**
Animal Naming	-0.12	-0.52, 0.27	0.53
WAIS-IV Coding	0.33	-0.61, 1.26	0.49
DKEFS Number Sequencing, s[a]	-0.61	-2.06, 0.83	0.40
DKEFS Letter-Number Switching, s[a]	3.76	-2.23, 9.75	0.22
DKEFS Tower Test	-0.44	-0.82, -0.07	**0.02**

DKEFS Color-Word Inhibition, s[a]	0.29	-1.55, 2.13	0.76
Letter Fluency (FAS) Test	0.11	-0.80, 1.02	0.81
Hooper Visual Organization Test	-0.23	-0.46, 0.004	0.05
CVLT-II Total Immediate Recall	-0.14	-0.94, 0.66	0.73
CVLT-II Delayed Recall	-0.12	-0.40, 0.17	0.42
CVLT-II Recognition	-0.03	-0.10, 0.03	0.32
BFLT Total Immediate Recall	-3.07	-5.70, -0.43	**0.02**
BFLT Delayed Recall	-0.69	-1.40, 0.02	0.06
BFLT Recognition	-0.01	-0.03, 0.002	0.08

Note. PWV indicates pulse wave velocity; *APOE,* apolipoprotein E; CI, confidence interval; WAIS-IV, Wechsler Adult Intelligence Scale, 4th edition; DKEFS, Delis-Kaplan Executive Function System; CVLT-II, California Verbal Learning Test, 2nd edition[267]; BFLT-II, Biber Figure Learning Test.
Bolded values represent significant findings. All neuropsychological performance values are total correct excluding timed tasks measured in seconds (s).
[a] Higher values in speeded test results reflect worse performance.

Figure 4.2: Aortic PWV × *APOE* ε4 & Cross-Sectional Neuropsychological Performance

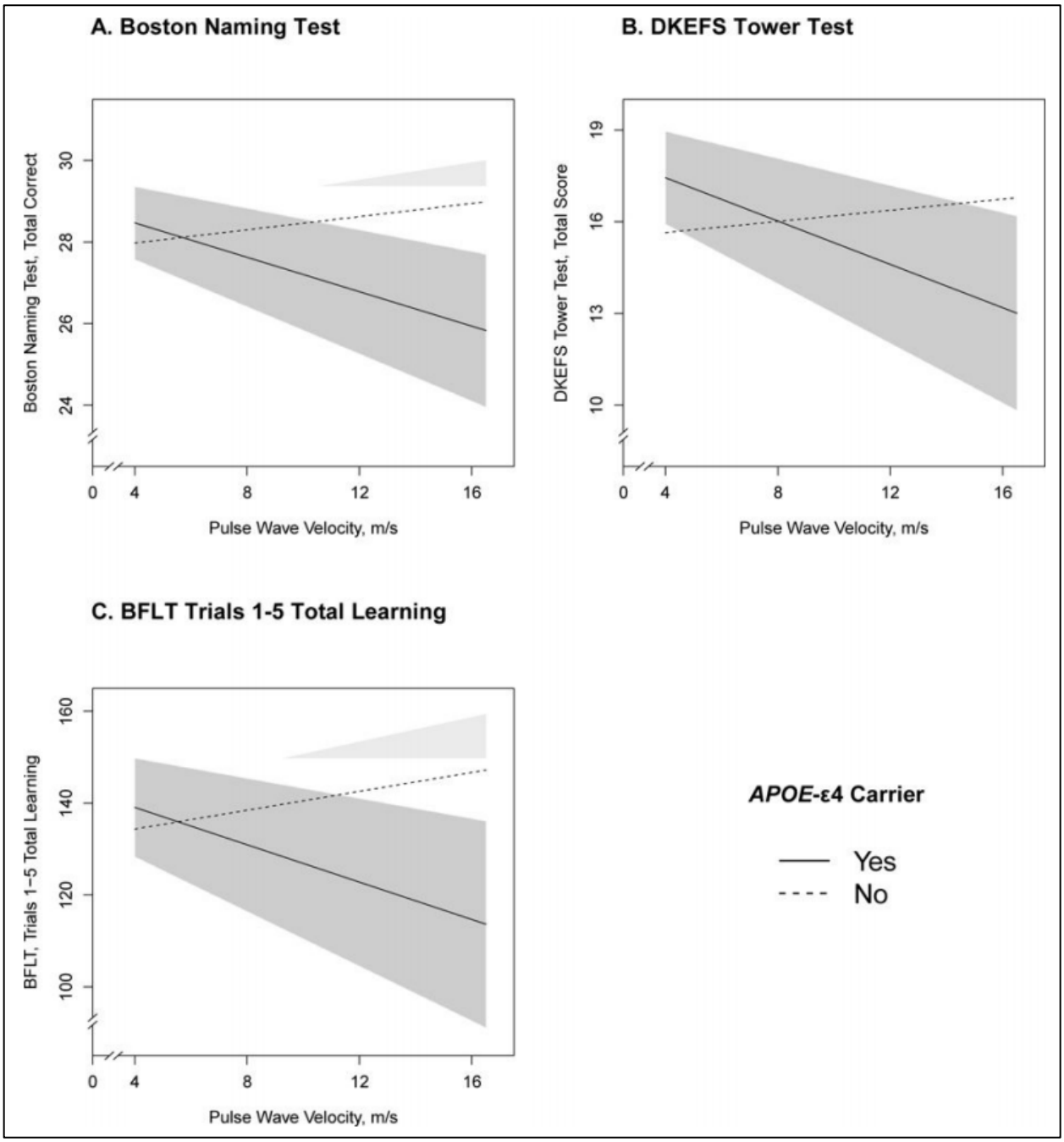

Note. Panel A: *p*-value=0.01. **Panel B:** *p*-value=0.02. **Panel C:** *p*-value=0.02. Lines reflect fitted linear regression models between the interaction of PWV and *APOE* ε4 status (i.e., *APOE* ε4 carrier/positive (solid) or *APOE* ε4 noncarrier/negative (dashed)) (x-axis) on neuropsychological test performance outcomes (y-axis). Shading reflects 95% confidence interval. PWV indicates pulse wave velocity; *APOE,* apolipoprotein E; DKEFS, Delis-Kaplan Executive Function System; BFLT, Biber Figure Learning Test.

When *APOE* ε4 interaction models were stratified by cognitive diagnosis, PWV × *APOE* ε4 was unrelated to neuropsychological performances in the NC cohort (*p*-values>0.09) (**Table 4.6**). In the MCI cohort, *APOE* ε4 significantly modified the relationship between PWV and BFLT Total Immediate Recall (β=−4.11, 95% CI −7.88 to −0.34, *p*-value=0.03) (**Table 4.6**). When adjusting for FDR, this result did not remain significant, but it did persist after exclusion for cardiovascular disease or atrial fibrillation (*p*-value=0.049).

Table 4.6: Aortic PWV × *APOE* ε4 & Cross-Sectional Neuropsychological Performance Stratified by Cognitive Diagnosis

	β	95% CI	*p*-value
NC Participants, n=162			
Boston Naming Test, 30-Item	-0.15	-0.47, 0.18	0.37
Animal Naming	0.43	-0.39, 1.24	0.30
WAIS-IV Coding	0.47	-1.44, 2.38	0.63
DKEFS Number Sequencing, s[a]	0.58	-1.41, 2.57	0.57
DKEFS Letter-Number Switching, s[a]	-0.93	-6.29, 4.43	0.73
DKEFS Tower Test	-0.66	-1.41, 0.10	0.09
DKEFS Color-Word Inhibition, s[a]	-1.88	-4.22, 0.47	0.12
Letter Fluency (FAS) Test	1.10	-0.90, 3.10	0.28
Hooper Visual Organization Test	-1.10	-0.90, 3.10	0.28
CVLT-II Total Immediate Recall	0.82	-0.86, 2.49	0.34
CVLT-II Delayed Recall	0.17	-0.42, 0.76	0.56
CVLT-II Recognition	0.01	-0.12, 0.14	0.86
BFLT Total Immediate Recall	-1.26	-6.37, 3.86	0.63
BFLT Delayed Recall	-0.17	-1.49, 1.15	0.80
BFLT Recognition	-0.005	-0.03, 0.02	0.74
MCI Participants, n=121			
Boston Naming Test, 30-Item	-0.33	-0.69, 0.03	0.07
Animal Naming	-0.30	-0.81, 0.21	0.25
WAIS-IV Coding	0.96	-0.25, 2.17	0.12
DKEFS Number Sequencing, s[a]	-1.05	-3.54, 1.44	0.41
DKEFS Letter-Number Switching, s[a]	5.00	-6.06, 16.07	0.37
DKEFS Tower Test	-0.51	-1.01, 0.003	0.05
DKEFS Color-Word Inhibition, s[a]	0.90	-2.34, 4.13	0.58
Letter Fluency (FAS) Test	-0.002	-1.09, 1.08	>0.99
Hooper Visual Organization Test	-0.23	-0.58, 0.11	0.19

CVLT-II Total Immediate Recall	-0.62	-1.68, 0.44	0.25
CVLT-II Delayed Recall	-0.24	-0.62, 0.14	0.21
CVLT-II Recognition	-0.06	-0.15, 0.04	0.24
BFLT Total Immediate Recall	-4.11	-7.88, -0.34	**0.03**
BFLT Delayed Recall	-0.90	-1.95, 0.15	0.09
BFLT Recognition	-0.02	-0.04, 0.004	0.11

Note. PWV indicates pulse wave velocity; *APOE,* apolipoprotein E; CI, confidence interval; NC, normal cognition; MCI, mild cognitive impairment; WAIS-IV, Wechsler Adult Intelligence Scale, 4th edition; DKEFS, Delis-Kaplan Executive Function System; CVLT-II, California Verbal Learning Test, 2nd edition[267]; BFLT-II, Biber Figure Learning Test.
Bolded values represent significant findings. All neuropsychological performance values are total correct excluding timed tasks measured in seconds (s).
[a] Higher values in speeded test results reflect worse performance.

In follow-up analyses examining *APOE* ε4 allele dosage effects, *APOE* ε4 allele count modified the relationship between PWV and neuropsychological performance in the combined cohort on Boston Naming Test (*p*-value=0.02) (**Table 4.7**). Participants with two copies of the *APOE* ε4 allele performed worse at higher PWV values than participants with one copy of the *APOE* ε4 allele (**Figure 4.3**). This *APOE* ε4 allele count result did not survive FDR adjustment nor did it persist after exclusion for cardiovascular disease or atrial fibrillation or when excluding participants with *APOE* ε2/ε4 genotype. *APOE* ε4 allele dosage did not modify the relationship between PWV and neuropsychological performance in diagnostically stratified results (**Table 4.8**).

Table 4.7: Aortic PWV × *APOE* ε4 Allele Count & Cross-Sectional Neuropsychological Performance

	β	95% CI	*p*-value
Combined Sample, n=283			
Boston Naming Test, 30-Item	-0.22	-0.41, -0.03	**0.02**
Animal Naming	-0.03	-0.37, 0.31	0.87
WAIS-IV Coding	0.39	-0.41, 1.19	0.34
DKEFS Number Sequencing, s[a]	-0.49	-1.72, 0.74	0.43
DKEFS Letter-Number Switching, s[a]	2.09	-3.05, 7.22	0.42
DKEFS Tower Test	-0.27	-0.59, 0.05	0.10
DKEFS Color-Word Inhibition, s[a]	0.45	-1.13, 2.04	0.57
Letter Fluency (FAS) Test	0.22	-0.56, 1.01	0.58
Hooper Visual Organization Test	-0.18	-0.38, 0.02	0.08
CVLT-II Total Immediate Recall	-0.001	-0.69, 0.69	>0.99
CVLT-II Delayed Recall	0.006	-0.25, 0.24	0.96
CVLT-II Recognition	-0.01	-0.07, 0.05	0.79
BFLT Total Immediate Recall	-1.91	-4.17, 0.35	0.10
BFLT Delayed Recall	-0.32	-0.92, 0.29	0.30
BFLT Recognition	-0.01	-0.02, 0.005	0.22

Note. PWV indicates pulse wave velocity; *APOE,* apolipoprotein E; CI, confidence interval; WAIS-IV, Wechsler Adult Intelligence Scale, 4th edition; DKEFS, Delis-Kaplan Executive Function System; CVLT-II, California Verbal Learning Test, 2nd edition[267]; BFLT-II, Biber Figure Learning Test.
Bolded values represent significant findings. All neuropsychological performance values are total correct excluding timed tasks measured in seconds (s).
[a] Higher values in speeded test results reflect worse performance.

Figure 4.3: Aortic PWV × *APOE* ε4 Allele Count & Cross-Sectional Neuropsychological Performance

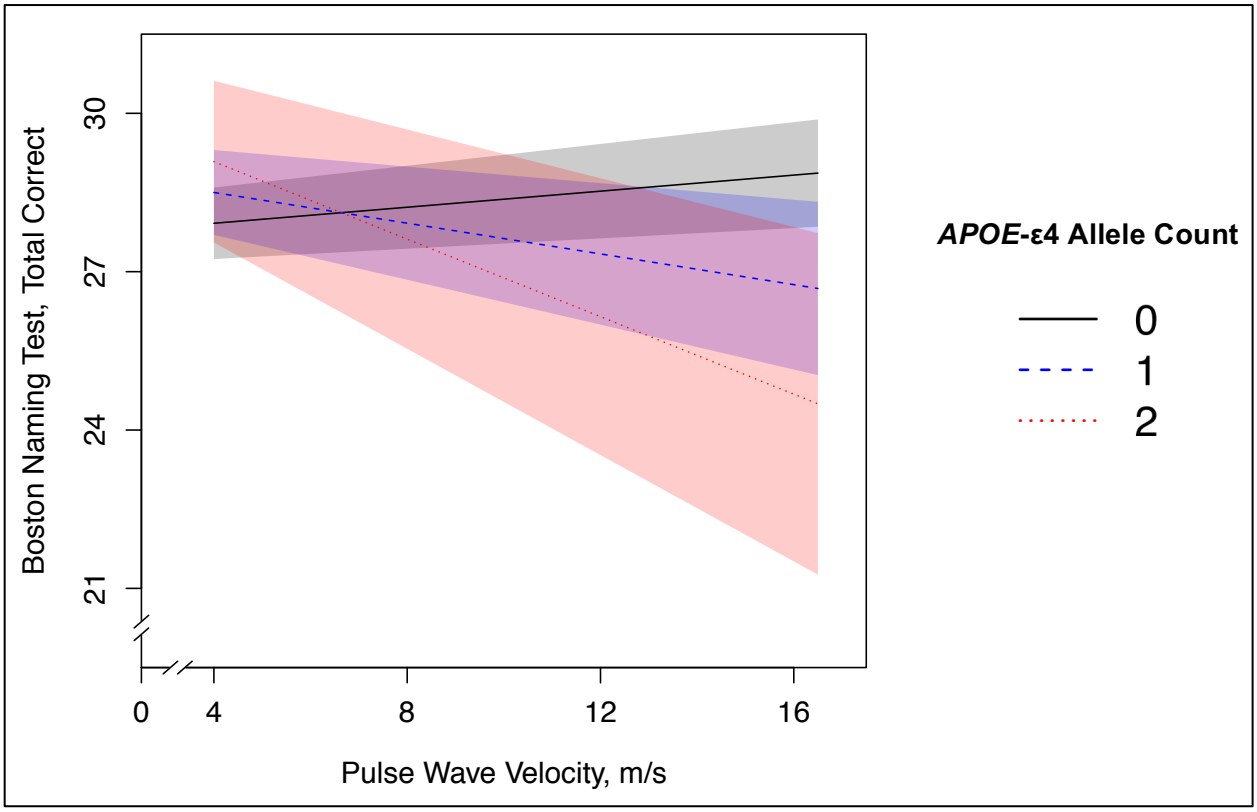

Note. *p*-value=0.02. Lines reflect fitted linear regression between the interaction of PWV and *APOE* ε4 allele count (i.e., 0 (black), 1 (blue), or 2 (red) allele copies) (x-axis) on Boston Naming Test performance outcome (y-axis). Shading reflects 95% confidence intervals. PWV indicates pulse wave velocity; *APOE,* apolipoprotein E.

Table 4.8: Aortic PWV × *APOE* ε4 Allele Count & Cross-Sectional Neuropsychological Performance Stratified by Cognitive Diagnosis

	β	95% CI	*p*-value
NC Participants (n=162)			
Boston Naming Test, 30-Item	-0.07	-0.33, 0.19	0.59
Animal Naming	0.49	-0.15, 1.13	0.13
WAIS-IV Coding	0.64	-0.86, 2.14	0.40
DKEFS Number Sequencing, s[a]	0.33	-1.22, 1.87	0.68
DKEFS Letter-Number Switching, s[a]	-0.70	-4.89, 3.50	0.74
DKEFS Tower Test	-0.45	-1.04, 0.14	0.14
DKEFS Color-Word Inhibition, s[a]	-1.12	-2.97, 0.73	0.23
Letter Fluency (FAS) Test	1.49	-0.08, 3.05	0.06
Hooper Visual Organization Test	-0.08	-0.41, 0.25	0.63
CVLT-II Total Immediate Recall	0.61	-0.70, 1.93	0.36

CVLT-II Delayed Recall	0.16	-0.30, 0.63	0.49
CVLT-II Recognition	0.02	-0.09, 0.12	0.72
BFLT Total Immediate Recall	-0.94	-4.95, 3.07	0.64
BFLT Delayed Recall	-0.20	-1.23, 0.83	0.70
BFLT Recognition	-0.004	-0.02, 0.02	0.70
MCI Participants (n=121)			
Boston Naming Test, 30-Item	-0.26	-0.57, 0.05	0.10
Animal Naming	-0.22	-0.66, 0.22	0.33
WAIS-IV Coding	0.67	-0.39, 1.72	0.21
DKEFS Number Sequencing, s[a]	-0.85	-2.98, 1.28	0.43
DKEFS Letter-Number Switching, s[a]	2.87	-6.63, 12.36	0.55
DKEFS Tower Test	-0.28	-0.72, 0.16	0.21
DKEFS Color-Word Inhibition, s[a]	1.11	-1.67, 3.89	0.43
Letter Fluency (FAS) Test	-0.17	-1.11, 0.77	0.72
Hooper Visual Organization Test	-0.18	-0.48, 0.12	0.24
CVLT-II Total Immediate Recall	0.38	-1.29, 0.53	0.41
CVLT-II Delayed Recall	-0.09	-0.41, 0.23	0.59
CVLT-II Recognition	-0.02	-0.10, 0.06	0.62
BFLT Total Immediate Recall	-2.44	-5.68, 0.81	0.14
BFLT Delayed Recall	-0.32	-1.21, 0.57	0.47
BFLT Recognition	-0.01	-0.03, 0.01	0.28

Note. PWV indicates pulse wave velocity; *APOE,* apolipoprotein E; CI, confidence interval; NC, normal cognition; MCI, mild cognitive impairment; WAIS-IV, Wechsler Adult Intelligence Scale, 4th edition; DKEFS, Delis-Kaplan Executive Function System; CVLT-II, California Verbal Learning Test, 2nd edition[267]; BFLT-II, Biber Figure Learning Test.
All neuropsychological performance values are total correct excluding timed tasks measured in seconds (s).
[a] Higher values in speeded test results reflect worse performance.

4.3.3 Aortic PWV & Longitudinal Neuropsychological Performance

PWV Main Effects Analyses

In the combined cohort, PWV related to longitudinal neuropsychological performance on DKEFS Number Sequencing (β=0.40, *p*-value=0.0002) (**Table 4.9**). Participants experienced faster cognitive decline at higher baseline PWV values. In sensitivity analyses, results remained statistically significant when excluding for outliers (*p*-value=0.001) and participants with cardiovascular disease or atrial fibrillation (*p*-value=0.001).

Table 4.9: Aortic PWV & Longitudinal Neuropsychological Performance

	Nobs	β	*p*-value
Combined Sample (n=283)			
Boston Naming Test, 30-Item	1068	-0.01	0.55
Animal Naming	1069	-0.01	0.55
WAIS-IV Coding	1062	-0.03	0.42
DKEFS Number Sequencing, s[a]	1056	0.40	**0.0002**
DKEFS Letter-Number Switching, s[a]	1023	0.30	0.32
DKEFS Tower Test	1067	0.01	0.56
DKEFS Color-Word Inhibition, s[a]	1036	-0.08	0.75
Letter Fluency (FAS) Test	1068	-0.06	0.08
Hooper Visual Organization Test	1069	-0.02	0.19
CVLT-II Total Immediate Recall	1066	-0.04	0.32
CVLT-II Delayed Recall	1066	-0.02	0.18
CVLT-II Recognition	1065	-0.001	0.68
BFLT Total Immediate Recall	1062	-0.08	0.50
BFLT Delayed Recall	1060	-0.01	0.84
BFLT Recognition	1057	0.0001	0.93

Note. PWV indicates pulse wave velocity; Nobs, Number of observations; WAIS-IV, Wechsler Adult Intelligence Scale, 4th edition; DKEFS, Delis-Kaplan Executive Function System; CVLT-II, California Verbal Learning Test, 2nd edition[267]; BFLT-II, Biber Figure Learning Test.
Bolded values represent significant findings. All neuropsychological performance values are total correct excluding timed tasks measured in seconds (s).
[a] Higher values in speeded test results reflect worse performance.

Cognitive Diagnosis Subgroup Analyses

Cognitive diagnosis did not appear to modify associations between PWV and longitudinal neuropsychological performance (*p*-values>0.15) (**Table 4.10**).

While weak evidence (i.e., *p*-value~0.10) of an interaction between aortic PWV and cognitive diagnosis on DKEFS Number Sequencing was observed (β=0.30, *p*-value=0.15), these associations did not meet *a priori* significance; results stratified by cognitive diagnosis indicated that PWV was associated with longitudinal DKEFS Number Sequencing performance in both NC (β=0.30, *p*-value=0.003) and MCI participants (β=0.60, *p*-value=0.02) (**Table 4.11**).

Table 4.10: Aortic PWV × Diagnosis & Longitudinal Neuropsychological Performance

	Nobs	β	*p*-value
Combined Sample (n=283)			
Boston Naming Test, 30-Item	1068	-0.02	0.65
Animal Naming	1069	0.01	0.77
WAIS-IV Coding	1062	0.05	0.55
DKEFS Number Sequencing, s[a]	1056	0.30	0.15
DKEFS Letter-Number Switching, s[a]	1023	0.80	0.28
DKEFS Tower Test	1067	-0.04	0.25
DKEFS Color-Word Inhibition, s[a]	1036	-0.80	0.28
Letter Fluency (FAS) Test	1068	-0.06	0.43
Hooper Visual Organization Test	1069	-0.02	0.59
CVLT-II Total Immediate Recall	1066	-0.09	0.27
CVLT-II Delayed Recall	1066	-0.004	0.90
CVLT-II Recognition	1065	-0.004	0.52
BFLT Total Immediate Recall	1062	-0.10	0.65
BFLT Delayed Recall	1060	-0.04	0.53
BFLT Recognition	1057	-0.001	0.63

Note. PWV indicates pulse wave velocity; Nobs, number of observations; WAIS-IV, Wechsler Adult Intelligence Scale, 4th edition; DKEFS, Delis-Kaplan Executive Function System; CVLT-II, California Verbal Learning Test, 2nd edition[267]; BFLT-II, Biber Figure Learning Test.
Bolded values represent significant findings. All neuropsychological performance values are total correct excluding timed tasks measured in seconds (s).
[a] Higher values in speeded test results reflect worse performance.

Table 4.11: Aortic PWV & Longitudinal Neuropsychological Performance Stratified by Cognitive Diagnosis

	Nobs	β	*p*-value
NC Participants (n=162)			
Boston Naming Test, 30-Item	666	-0.01	0.48
Animal Naming	667	-0.04	0.12
WAIS-IV Coding	664	-0.05	0.19
DKEFS Number Sequencing, s[a]	662	0.30	**0.003**
DKEFS Letter-Number Switching, s[a]	659	0.16	0.35
DKEFS Tower Test	667	0.03	0.18
DKEFS Color-Word Inhibition, s[a]	645	0.20	**0.01**
Letter Fluency (FAS) Test	667	-0.05	0.16
Hooper Visual Organization Test	667	-0.01	0.15
CVLT-II Total Immediate Recall	669	-0.002	0.97
CVLT-II Delayed Recall	669	-0.01	0.40

CVLT-II Recognition	667	0.0004	0.90
BFLT Total Immediate Recall	665	-0.03	0.84
BFLT Delayed Recall	664	0.02	0.64
BFLT Recognition	664	0.001	0.32
MCI Participants (n=121)			
Boston Naming Test, 30-Item	402	-0.02	0.61
Animal Naming	402	-0.03	0.50
WAIS-IV Coding	398	0.004	0.97
DKEFS Number Sequencing, s[a]	394	0.60	**0.02**
DKEFS Letter-Number Switching, s[a]	364	1	0.31
DKEFS Tower Test	400	-0.01	0.70
DKEFS Color-Word Inhibition, s[a]	391	-0.50	0.35
Letter Fluency (FAS) Test	401	-0.09	0.32
Hooper Visual Organization Test	402	-0.03	0.46
CVLT-II Total Immediate Recall	397	-0.10	0.11
CVLT-II Delayed Recall	397	-0.02	0.31
CVLT-II Recognition	398	-0.004	0.56
BFLT Total Immediate Recall	397	-0.14	0.50
BFLT Delayed Recall	396	-0.04	0.52
BFLT Recognition	393	-0.0003	0.87

Note. PWV indicates pulse wave velocity; Nobs, number of observations; NC, normal cognition; MCI, mild cognitive impairment; WAIS-IV, Wechsler Adult Intelligence Scale, 4th edition; DKEFS= Delis-Kaplan Executive Function System; CVLT-II= California Verbal Learning Test, 2nd edition[267]; BFLT-II= Biber Figure Learning Test.
Bolded values represent significant findings. All neuropsychological performance values are total correct excluding timed tasks measured in seconds (s).
[a] Higher values in speeded test results reflect worse performance.

APOE ε4 Subgroup Analyses

APOE ε4 status modified the relationship between PWV and longitudinal neuropsychological performance on Hooper Visual Organization Test (β=-0.09, *p*-value=0.03) (**Table 4.12**). *APOE* ε4 carriers experienced faster cognitive decline at higher PWV values compared to non-carriers. When models were stratified by *APOE* ε4 status, PWV related to longitudinal neuropsychological performances on Hooper Visual Organization Test among *APOE* ε4 carriers (β=-0.11, *p*-value=0.03) (**Table 4.13**). Among *APOE* ε4 noncarriers, PWV did not relate to longitudinal neuropsychological performances on Hooper Visual Organization Test (*p*-values>0.17). In sensitivity analyses, *APOE* ε4 carrier stratified results remained statistically significant after

exclusion for cardiovascular disease or atrial fibrillation (β=-0.12, *p*-value=0.03) and when excluding for outliers (β=-0.11, p=0.03).

While weak evidence (i.e., *p*-value<0.10) of an interaction between aortic PWV and *APOE* ε4 status on Boston Naming Test (β=-0.08, *p*-value=0.08) (**Table 4.12**) was observed, these associations did not meet *a priori* significance; results stratified by *APOE* ε4 status indicated that PWV was not associated with longitudinal Boston Naming Test performance in either *APOE* ε4 carriers (β=-0.08, *p*-value=0.18) or *APOE* ε4 noncarriers (β=-0.01, *p*-value=0.56) (**Table 4.13**). Weak evidence (i.e., *p*-value~0.10) of an interaction between aortic PWV and *APOE* ε4 status on DKEFS Number Sequencing (β=0.40, *p*-value=0.11) (**Table 4.12**) was observed (β=0.30, *p*-value=0.15), and results stratified by *APOE* ε4 status indicated that PWV was associated with longitudinal DKEFS Number Sequencing performance in both *APOE* ε4 carriers (β=0.70, *p*-value=0.02) and *APOE* ε4 noncarriers (β=0.40, *p*-value=0.001) (**Table 4.13**).

Table 4.12: Aortic PWV × *APOE* ε4 & Longitudinal Neuropsychological Performance

	Nobs	β	*p*-value
Combined Sample, n=283			
Boston Naming Test, 30-Item	1068	-0.08	0.08
Animal Naming	1069	0.03	0.57
WAIS-IV Coding	1062	-0.09	0.41
DKEFS Number Sequencing, s[a]	1056	0.40	0.11
DKEFS Letter-Number Switching, s[a]	1023	-0.90	0.32
DKEFS Tower Test	1067	0.01	0.89
DKEFS Color-Word Inhibition, s[a]	1036	-0.70	0.28
Letter Fluency (FAS) Test	1068	-0.13	0.16
Hooper Visual Organization Test	1069	-0.09	**0.03**
CVLT-II Total Immediate Recall	1066	-0.04	0.67
CVLT-II Delayed Recall	1066	0.01	0.81
CVLT-II Recognition	1065	-0.003	0.68
BFLT Total Immediate Recall	1062	-0.09	0.76
BFLT Delayed Recall	1060	-0.04	0.64
BFLT Recognition	1057	-0.001	0.70

Note. PWV indicates pulse wave velocity; *APOE*, apolipoprotein E; Nobs, number of observations; WAIS-IV, Wechsler Adult Intelligence Scale, 4th edition; DKEFS, Delis-Kaplan Executive Function System; CVLT-II, California Verbal Learning Test, 2nd edition[267]; BFLT-II, Biber Figure Learning Test.
Bolded values represent significant findings. All neuropsychological performance values are total correct excluding timed tasks measured in seconds (s).
[a] Higher values in speeded test results reflect worse performance.

Table 4.13: Aortic PWV & Longitudinal Neuropsychological Performance Stratified by *APOE* ε4 Genetic Status

	Nobs	β	*p*-value
APOE ε4 Carriers (n=98)			
Boston Naming Test, 30-Item	365	-0.08	0.18
Animal Naming	365	-0.02	0.76
WAIS-IV Coding	363	-0.13	0.38
DKEFS Number Sequencing, s[a]	359	0.70	**0.02**
DKEFS Letter-Number Switching, s[a]	342	-0.20	0.84
DKEFS Tower Test	365	0.01	0.75
DKEFS Color-Word Inhibition, s[a]	356	-0.80	0.42
Letter Fluency (FAS) Test	365	-0.18	0.11
Hooper Visual Organization Test	366	-0.11	**0.03**
CVLT-II Total Immediate Recall	363	-0.09	0.45
CVLT-II Delayed Recall	363	-0.01	0.45
CVLT-II Recognition	364	-0.004	0.64
BFLT Total Immediate Recall	362	-0.20	0.54
BFLT Delayed Recall	362	-0.06	0.49
BFLT Recognition	362	-0.001	0.52
APOE ε4 Noncarriers (n=185)			
Boston Naming Test, 30-Item	703	-0.01	0.56
Animal Naming	704	-0.05	**0.02**
WAIS-IV Coding	699	-0.04	0.19
DKEFS Number Sequencing, s[a]	697	0.40	**0.001**
DKEFS Letter-Number Switching, s[a]	681	0.60	**0.03**
DKEFS Tower Test	702	-0.001	0.98
DKEFS Color-Word Inhibition, s[a]	680	0.15	0.07
Letter Fluency (FAS) Test	703	-0.07	0.06
Hooper Visual Organization Test	703	-0.01	0.18
CVLT-II Total Immediate Recall	703	-0.04	0.25
CVLT-II Delayed Recall	703	-0.02	0.09
CVLT-II Recognition	701	-0.002	0.55
BFLT Total Immediate Recall	700	-0.17	0.08
BFLT Delayed Recall	698	-0.02	0.58

BFLT Recognition	696	-0.0003	0.62

Note. PWV indicates pulse wave velocity; *APOE*, apolipoprotein E; Nobs, number of observations; WAIS-IV, Wechsler Adult Intelligence Scale, 4th edition; DKEFS, Delis-Kaplan Executive Function System; CVLT-II, California Verbal Learning Test, 2nd edition[267]; BFLT-II, Biber Figure Learning Test.
Bolded values represent significant findings. All neuropsychological performance values are total correct excluding timed tasks measured in seconds (s).
[a] Higher values in speeded test results reflect worse performance.

4.4 Discussion

Among community-dwelling older adults free of clinical stroke or dementia, PWV demonstrated cross-sectional associations with cognitive performance dependent on *APOE* ε4 carrier status. Specifically, modest interactions between PWV and *APOE* ε4 carrier status on multiple cognitive domains indicate that higher PWV is associated with worse lexical retrieval, visuospatial memory encoding, and executive function performance among *APOE* ε4 carriers compared to noncarriers. Moreover, among *APOE* ε4 carriers, the association between PWV and executive function performance may be most pronounced (regardless of ε4 allele dosage), while the association between PWV and lexical retrieval performance may be most pronounced among homozygous *APOE* ε4 carriers specifically. Finally, interactions between PWV and *APOE* ε4 carrier status on visuospatial memory encoding performance may be most pronounced among MCI participants. Cross-sectional results suggest *APOE* ε4 carriers experience pronounced lexical retrieval and executive function deficits at higher PWV values, and in the context of prodromal AD*, APOE* ε4 carriers additionally experience pronounced visuospatial memory encoding deficits at higher PWV values.

Longitudinally, higher PWV at study entry relates to faster decline in processing speed over the mean 4.9-year follow-up period; weak evidence suggests these widespread associations may be even more pronounced among NC participants and *APOE* ε4 noncarriers (i.e., healthy aging phenotype). In addition, higher PWV is associated with faster decline in visuoperceptual skills among *APOE* ε4 carriers compared to noncarriers. Longitudinal results suggest higher baseline

aortic stiffness is associated with faster declines in processing speed among all participants (particularly in healthy agers) and faster declines in visuoperceptual processing among *APOE* ε4 carriers specifically.

Taken together, results suggest that aortic stiffness among older adults may be predictive of faster declines in processing speed, a hallmark of cognitive aging and key cognitive resource underlying performance in various cognitive domains. Importantly, processing speed is supported by both frontal grey matter and global white matter, both of which are significantly vulnerable to microvascular damage, cerebral ischemic vulnerability, and thus the hemodynamic stress theoretically perpetuated by aortic stiffness. Second, results suggest that among individuals at genetic risk for AD (i.e., *APOE* ε4 carriers), higher aortic stiffness may be a marker of worse lexical retrieval and executive function (i.e., cognitive processes supported by frontotemporal networks of the brain) and potentially predictive of faster declines in visuoperceptual processing. Notably, our measure of visuoperceptual skills (i.e., HVOT) is multifactorial and supported by numerous core processes, including executive functioning (i.e., a primary driver of HVOT performance in NC participants), lexical retrieval (i.e., a primary driver of HVOT performance in MCI participants), and perceptual integration. Thus, it is plausible that the effects of the interaction between aortic stiffness and *APOE* ε4 may be more localized to frontotemporal networks at baseline, and these early stiffness-related network alterations may be a harbinger of visuoperceptual processing declines as the effects of aortic stiffness worsen over time. It is noteworthy that all reported effects are statistically independent of many shared vascular risk factors, only modestly attenuated by cardiovascular disease or atrial fibrillation, and equivalent to over 3 years of accelerated cognitive aging when comparing the effect of one year of aging to the effect of PWV × *APOE* ε4 on cognition in cross-sectional results at baseline.

In theoretical models, age-related central arterial stiffening results in increased PWV, transmission of damaging pulsatile energy, and microvascular dysfunction, including decreased blood flow to

high-demand organs as purported by Mitchell (2008).[189] The impact of cerebral hypoperfusion may have the greatest impact in distal vascular territories where tissue is farthest from blood supply, in regions susceptible to mechanical stress due to supply from the most direct perfusion branches (i.e., watershed regions, including grey matter border zones and internal white matter tracts), or in the most metabolically active regions that are particularly sensitive to hemodynamic deficits, such as frontal cortex.[268] Watershed microinfarct pathologies associated with cerebral hypoperfusion have been linked primarily to deficits in core cognitive abilities, including processing speed,[269] working memory,[270] and visuospatial abilities[270] in community-dwelling older adults. Thus, the longitudinal implication of processing speed and *APOE* ε4-dependent visuoperceptual processing (as well as multiple component processes of visuoperceptual processing in cross-sectional analyses) is consistent with previous evidence. The additional implication of memory encoding tasks in cross-sectional findings further fits into this framework, as memory encoding processes are highly dependent on medial temporal lobe structures that are both susceptible to reduced oxygen/glucose and age-related cerebrovascular dysfunction (e.g., BBB breakdown). Lastly, executive function is highly dependent on regions and tracts particularly vulnerable to hypoperfusion, including frontal cortex, parieto-occipital cortex, and white matter.[253]

The presence of *APOE* ε4 may intensify the effects of age-related aortic stiffness to produce detectable neuropsychological changes due to *APOE* ε4-related vascular dysfunction (e.g., BBB dysfunction and increased susceptibility of microvasculature to hemodynamic stress; compromises in protective autoregulatory mechanisms due to elevated systolic blood pressure and emerging neuropathology). Thus, the *APOE* ε4 genetic backdrop may allow associations between aortic stiffness and worse brain health to emerge at PWV levels that may not be as harmful or clinically manifest among *APOE* ε4 noncarriers. Recent cerebrovascular regulation studies in advanced aging and MCI suggest that if cerebrovascular responses to central vascular changes are compromised, then the brain may experience lower perfusion levels and compromised autoregulation, changes that are related to end-organ damage.[67,221] If cerebrovascular responses to

central vascular changes are compromised, then end-organ damage in the brain may yield worse cognitive and behavioral outcomes.

A majority of findings were weakened in the sensitivity analyses excluding participants with prevalent cardiovascular disease or atrial fibrillation. Such attenuation suggests PWV and *APOE* ε4 status may relate to cognition in more pathological cardiovascular states, such that cardiovascular disease or atrial fibrillation are potential contributors.[271] Cardiovascular disease conditions impair structural integrity and vessel health, while rhythm issues, such as atrial fibrillation, increase stroke risk by elevating clotting factors and relate to hippocampal atrophy,[272] cognitive impairment, and dementia.[273] However, it is important to note that effect sizes from the primary models and the sensitivity models excluding cardiovascular disease or atrial fibrillation were comparable suggesting the null sensitivity models might be explained by decreased power due to fewer available participants.

There are several strengths of the current project. First, direct CMR assessment of PWV across the aortic arch greatly reduces measurement error introduced by traditional measures (e.g., carotid-femoral PWV), which reflect mixed vascular properties along the arterial tree. CMR more accurately assesses the aortic path, which is uniquely implicated in peripheral health since it contributes an estimated 60–70% of total systemic compliance.[274] Second, our comprehensive neuropsychological protocol captures a diverse range of outcomes. Third, *APOE* ε4 genotyping and aortic PWV data were processed in batch in a core laboratory by technicians blinded to clinical information. Conversely, it is important to note that the cohort is not reflective of the general population since participants were older, predominantly White, well educated, and relatively healthy with a low prevalence of CVD (4%) compared to the general population over age 65 (24% to 37%).[248] Furthermore, participant drop-out over time occurred more frequently among MCI participants, limiting the sample sizes in this diagnostic group. Whether such variables limit the generalizability of our results is unknown, but we purport that in a less healthy cohort with greater

vascular risk factors, more compromised cardiac function, or more cognitively impaired, the association between PWV and cognition among older adults would likely be stronger.

Results provide evidence that pulse-wave velocity assessment could be a useful tool to identify individuals at high risk of cognitive decline or early stages of cognitive decline and to implement interventions aimed at slowing the progression to dementia.[265] However, limited longitudinal effects suggest the aortic stiffness may not exert extensive direct effects on brain health among older adults. Measures of aortic stiffness may thus be more useful as a marker of accumulated vascular damage among older adults and should be examined at earlier age ranges (e.g., mid-life) to further investigate if any direct casual effects exist. Follow-up analyses will facilitate future examination of PWV and *APOE* ε4 interactions on the rate of cognitive decline as well as the underlying pathophysiology of subclinical vascular changes to declining cognition, particularly microvascular integrity and hemodynamic disturbances in the brain.

CHAPTER 5

Summary & Conclusions

5.1 Overarching Summary

Longitudinal results indicate that CMR measurements of aortic stiffness are predictive of declines in information processing speed (associated with global white matter integrity[275]) among all participants and further predictive of declines in frontal lobe CBF and visuoperceptual skills (associated with occipito-temporal networks[276,277]) among *APOE* ε4 carriers during a nearly 5-year mean follow-up period. Longitudinal results did not depend significantly on cognitive diagnosis (i.e., NC vs. MCI), suggesting that cognitive and hemodynamic vulnerability to aortic stiffness among older adults (i.e., aged 65+) may not be related to emerging AD neuropathology. The lack of associations between aortic stiffness and perfusion over time in the combined cohort may indicate that observed vulnerabilities of processing speeds domains likely occur through perfusion-independent arterial aging pathways (e.g., endothelial dysfunction, BBB dysfunction, neurotoxic inflammation and oxidative stress); they may also reflect the fact that our perfusion measures did not capture white matter, which is the primary anatomical driver of processing speed performance.

Importantly, our most pronounced longitudinal associations occurred among *APOE* ε4 carriers, which supports our hypotheses that *APOE* ε4 and aortic stiffness combine synergistically to exacerbate brain aging outcomes.[260] While vulnerability of the frontal lobe to vascular dysfunction is well-established in vascular dementia, the implication of occipito-temporal network dysfunction (i.e., declines in visuoperceptual skills) was somewhat surprising. However, these cognitive associations may be partially explained by the regionally-specific cerebrovascular effects that *APOE* ε4 is purported to exert, including BBB dysfunction in temporal lobes[162,278] and greater CBF declines in frontal, parietal, and temporal cortices in normal aging.[196] Thus, aortic stiffness and *APOE* ε4 synergistic effects appears to be most relevant for CVD-vulnerable frontal-

subcortical cerebrovascular function as well as *APOE* ε4-vulnerable temporal network neurovascular function. The lack of anatomical alignment between frontal perfusion and occipito-temporal network dysfunction results is likely explained either through independent aortic stiffness damage pathways (e.g., SVD in frontal regions vs. BBB dysfunction in temporal regions) or through observations that hypoperfusion-related frontal and parieto-occipital white matter changes are particularly associated with hippocampal atrophy.[279]

Cross-sectional findings indicate that higher aortic stiffness is associated with subtle global blood flow reductions, including more pronounced associations in the temporal lobe among *APOE* ε4 carriers without cognitive impairment (i.e., NC). However, aortic stiffness associations with cognitive impairment (i.e., lexical retrieval, executive function, visuospatial memory encoding) were most pronounced among *APOE* ε4 carriers with early-stage AD (i.e., MCI). These results support the early involvement of *APOE* ε4 in temporal lobe cerebrovascular dysfunction among cognitively unimpaired older adults (as described above) and provide additional evidence for the necessity of AD-related pathological changes to promote cognitive dysfunction, in particular a three-way synergistic interplay between systemic vascular risk (i.e., aortic stiffness), *APOE* ε4 neurotoxic effects (e.g., directly through neuroinflammation pathways, indirectly through *APOE* ε4-associated cerebrovascular dysfunction), and AD-related pathological processes and proteins (e.g., Aβ, tau).[260] The particular vulnerability of the temporal lobe perfusion in cross-sectional results compared to frontal lobe in longitudinal results may reflect either that aortic stiffness exerts its strongest effects on temporal lobe hemodynamics earlier in the lifespan (i.e., prior to study enrollment) or that aortic stiffness and temporal lobe hemodynamic dysregulation may co-occur downstream of a tertiary variable (discussed further below). Previous literature suggests the temporal lobe cerebrovasculature may experience overlapping vulnerability to blood pressure-related hypoxic-ischemic injury, AD-related BBB breakdown, and cortical microinfarcts, but additional research is needed to clarify temporal sequencing of these earliest-stage changes as well as their cause-effect relationships. Regardless, longitudinal results suggest some utility of aortic

stiffness in predicting declines in frontal-associated cerebral perfusion and cognitive networks among *APOE* ε4+ older adults, although associations were limited.

Investigations into the potential roles of the cerebral macrovasculature in mediating hemodynamic dysfunction revealed that, while theoretical models suggest aortic stiffness may promote cerebral hypoperfusion through increased vascular remodeling and resistance to flow, aortic stiffness is not significantly related to large artery wall remodeling (i.e., thicker walls, narrow lumens). Findings support emerging evidence that microvascular function (e.g., endothelial dysfunction, BBB dysfunction) may play the largest role in associations between aortic stiffness and worse cerebrovascular and cognitive aging. Future research investigating the causal or intermediate roles of microcirculatory changes along our purported damage pathways is needed. Interestingly, exploratory investigations into the role of other macrovascular characteristics in age-related cerebrovascular dysfunction revealed that differences in CoW patency are associated with compromises in cerebral hemodynamics. Specifically, common communicating artery variant structures were associated with frontal and occipital lobe hypoperfusion. While these early-stage findings warrant further investigation, results suggest CoW structural variants may represent another type of pre-existing risk factor for worse arterial aging (i.e., beyond *APOE* ε4 genetic risk) that place certain individuals at higher risk for hypoperfusion with higher aortic stiffness. Multiple interpretations likely exist for the observed results and additional research is needed to investigate the involvement of other hemodynamic characteristics promoted by atypical arterial structures (e.g., changes in time-to-peak, pressure variability, and non-laminar flow profiles) and more detailed risk stratification to understand the relevance of these factors across subpopulations as well as how they interact with existing comorbidities commonly found in older adult populations.

5.2 Overarching Discussion

As detailed in **Chapter 2**, a direct pathway from aortic stiffness to compromised neurovascular health, including CBF and related neuropsychological functions, may exist due to increased transmission of harmful pulsatile energy into the microvasculature, which compromises both their structural integrity and function. While a direct pathway between cardiovascular changes and brain health is plausible, cardiovascular dysfunction may also relate to worse brain health as a consequence of emerging neuropathology (i.e., a brain to heart pathway). Several reports indicate that evolving pathology and neurodegeneration in the AD brain may drive disruptions of autonomic control circuits responsible for heart rate and blood pressure control. Indeed, autonomic dysfunction has been repeatedly described in AD patients [280-286], including impaired cardiovagal parasympathetic function [287,288] and vasomotor sympathetic dysfunction [289]. Although Braak and Braak staging criteria do not include evaluation of the brainstem, a central regulator of autonomic function, its early involvement in AD suggests emerging relevance [290]. AD pathophysiology may cause a disruption of essential brainstem circuitry responsible for cardiovascular control, upstream autonomic control centers responsible for integrating peripheral signals and regulating the brainstem (e.g., hypothalamus and insula) [291,292], and cortical modulators of these autonomic circuits [293]. Moreover, cholinergic signaling pathways associated with cerebral and peripheral nerve dysfunction may be particularly vulnerable in AD [282,294]. Ultimately, varied abnormalities in brain structures and networks subserving autonomic regulation may impair cardiovascular function in AD, accounting for previously reported connections between cardiovascular function and abnormal brain changes [61-63,66,67,295].

It is also possible that the link between cardiovascular and brain dysfunction is an epiphenomenon. In support of this hypothesis, pleiotropy between AD and cardiovascular risk-associated genes has been increasingly established. For example, variants in the presenilin-1 gene, the same gene associated with early-onset AD, have been reported in idiopathic dilated cardiomyopathy [296]. These variants appear to reduce protein expression of the presenilin 1 protein, likely compromising

its direct roles in calcium signaling [297,298] and excitation-contraction coupling [296] rather than amyloid processing. More recent genetic studies have indicated that the polygenetic component of AD is also enriched for cardiovascular risk factors, particularly lipid-associated factors potentially linked to BBB damage and pathological cholesterol metabolism in the brain [299,300]. In addition to a common genetic profile affecting the heart and brain, studies of cardiovascular protein abnormalities in AD have further demonstrated a common molecular profile. In AD patients, biochemically similar Aβ deposits have been shown to co-exist in the heart and brain, and myocardial Aβ deposits appear to contribute to early diastolic dysfunction, as defined by impaired left ventricular relaxation [301]. While cardiovascular amyloid is likely common in advanced age [302-304], cardiovascular $A\beta_{40}$ and $A\beta_{42}$ expression is particularly increased in AD [301]. The possibility that Aβ aggregates may directly drive cardiomyocyte defects is strengthened by findings that myocardial Aβ oligomers promote changes in calcium homeostasis that likely mediate cardiomyocyte toxicity and contractile dysfunction in idiopathic dilated cardiomyopathy [296]. Future genetic, biochemical, and molecular studies will likely continue to shed light on the shared mechanisms underlying declines in heart and brain health, as well as whether these declines occur independently or through a shared pathway.

5.3 Clinical Significance

Arterial stiffness has been known as a sign of cardiovascular risk since the 19th century. Despite this, accurate measurement and clinical utility have only emerged in recent times. Arterial stiffness and its hemodynamic consequences are now established as predictors of adverse cardiovascular outcome. The present research findings provide some evidence that aortic PWV may serve as a novel and accessible biomarker of early-stage cerebrovascular dysregulation in aging, including the occurrence of subtle cerebral hemodynamic dysregulation and cognitive dysfunction. Central arterial stiffness may predict age-related cerebrovascular dysfunction earlier and with greater ability than other measures of central arterial aging, including systolic blood pressure, pulse

pressure, and augmentation index. Our results add to this body of literature to support CMR-assessed PWV as a potential predictor of brain-related outcomes in aging adults, particularly carriers of the *APOE* ε4 risk allele. Aortic PWV may thus serve as a useful clinical screening tool with novel (although limited) predictive value for age-related cerebrovascular dysfunction.

As a screening tool to identify worse cerebrovascular aging in its early stages, aortic PWV evaluations would promote earlier diagnostic evaluation; more effective risk factor management or intervention at earlier stages; and more comprehensive tracking of vascular disease course and intervention efficacy within both patient populations and research studies. When using the most common techniques for central arterial stiffness assessment (e.g., distal pressure sensors like mechanotransducers or high-fidelity applanation tonometers; distension waves obtained from the high-definition echotracking devices), there is a need to consider methodological confounds, including comorbidities that may delay or attenuate the pressure waveform (e.g., aortic, iliac, or proximal femoral stenosis) or make distance measurements inaccurate (e.g., metabolic syndrome, obesity, diabetes, peripheral artery disease). Since these distal pressure sensor techniques are based on peripheral pulse pressure, they are ultimately a poor reflection of central aortic pressure.[305] Furthermore, while ultrasound-based and MR-based methods require estimation of aortic wall thickness and diameter for indirect measurement of aortic stiffness, this is not a concern with CMR assessment of aortic stiffness. While assessment of aortic PWV via cardiac imaging provides a more accurate assessment of true aortic PWV compared to carotid-femoral PWV (thereby avoiding many of the transit time and distance measurement limitations), cardiac imaging is often underutilized due to perceived costs, limiting patient factors and comfort, and longer examination periods.[306] Thus, using both carotid-femoral PWV as an initial screening tool in conjunction with cardiac imaging may help provide more accessible initial detection coupled with high-sensitivity refinement of clinical diagnosis, prognosis, and subsequent treatment plans. Screening for higher aortic stiffness among *APOE* ε4 carriers may help predict cerebrovascular dysfunction, a well-known early-stage contributor to accelerated cognitive aging in healthy and ADRD populations.

Earlier and more sensitive identification of patients at high-risk for cerebrovascular dysfunction may in turn facilitate improved patient outcomes with respect to cognitive aging.

5.4 Future Directions

5.4.1 Immediate Follow-up Questions within Human Datasets

Numerous opportunities for extending our research findings using immediately available data exist, including (1) assessing whether hemodynamic patterns account for associations between aortic stiffness and cognition (e.g., the degree to which stiffness-cognition associations are attenuated by inclusion of perfusion covariates or creating mediation models with perfusion as the mediator variable of interest); (2) assessing alternative mediators of stiffness-cognition associations, such as fluid biomarkers of BBB dysfunction and neuroinflammation; (3) further deconvolving aortic stiffness associations with brain health variables by examining contributions of other hallmarks of arterial aging (e.g., hypertension) and comorbidities known to modify the effects of aortic stiffness (e.g., diabetes); (4) more in-depth risk factor characterization (e.g., interactions between aortic stiffness and sex) to further refine high-risk identification; (5) investigating aortic stiffness effects on interrelated characteristics of early-stage hemodynamic dysfunction (e.g., mean blood pressure vs. pulsatility, hypoperfusion, cerebrovascular reactivity, temporal flow characteristics such as time-to-peak); and (6) further investigating the implications of exploratory CoW-CBF research findings (**Chapter 3**) within the larger framework of systemic arterial aging (e.g., introducing communicating artery variants as a potential modifier of associations between aortic stiffness and cerebral perfusion; developing a data-driven approach to determine which variant structures may be most relevant to risk of microcirculatory damage and dysfunction).

5.4.2 Long-term Follow-up Questions within Human Datasets

Outside of the data currently available within the Vanderbilt Memory & Aging Project, significant questions still need to be resolved to understand the casual vs. correlative roles of aortic stiffness and the magnitude of its potential effects on brain health, including (1) the effects of aortic stiffness over the lifespan, particularly in mid-life where the effects of many systemic vascular variables are expected to be greatest; (2) the relative contributions of aortic stiffness to cerebral perfusion and cognition compared to alternative biomarkers of arterial aging-related damage that may demonstrate more predictive value as intermediate endpoints (e.g., measures of impedance matching between aorta and carotids; true flow pulsatility, which is the purported direct mechanism of damage to microcirculation); (3) the effects of different AD biomarker profiles (e.g., CSF fluid protein abnormalities) across time on observed associations; and (4) potential effects of aortic stiffness on more subtle and sensitive measures of neuronal dysfunction (i.e., prior to tissue infarction or CVD). Developing a deeper understanding of the effects (or unrelated cooccurrence) of aortic stiffness with early cerebrovascular dysfunction will require a sophisticated approach to identifying high-risk baseline or age-related differences in demographics (e.g., *APOE* ε4 genetic risk, CoW variant structures, sex, cardiovascular comorbidities, racial/ethnic differences, and other factors related to social determinants of health), high-risk exposure windows (e.g., older age, midlife), and the correct downstream targets to develop intervention strategies in the case that aortic stiffness does directly promote accelerated brain aging.

REFERENCES

1. 2022 Alzheimer's disease facts and figures. *Alzheimers Dement*. 2022; 18: 700-789.

2. Rajan KB, Weuve J, Barnes LL, McAninch EA, Wilson RS and Evans DA. Population estimate of people with clinical Alzheimer's disease and mild cognitive impairment in the United States (2020-2060). *Alzheimers Dement*. 2021; 17: 1966-1975.

3. Ferri CP, Prince M, Brayne C, Brodaty H, Fratiglioni L, Ganguli M, Hall K, Hasegawa K, Hendrie H, Huang Y, Jorm A, Mathers C, Menezes PR, Rimmer E and Scazufca M. Global prevalence of dementia: a Delphi consensus study. *Lancet (London, England)*. 2005; 366: 2112-7.

4. Gorelick PB, Scuteri A, Black SE, Decarli C, Greenberg SM, Iadecola C, Launer LJ, Laurent S, Lopez OL, Nyenhuis D, Petersen RC, Schneider JA, Tzourio C, Arnett DK, Bennett DA, Chui HC, Higashida RT, Lindquist R, Nilsson PM, Roman GC, Sellke FW and Seshadri S. Vascular contributions to cognitive impairment and dementia: a statement for healthcare professionals from the american heart association/american stroke association. *Stroke*. 2011; 42: 2672-2713.

5. Snyder HM, Corriveau RA, Craft S, Faber JE, Greenberg SM, Knopman D, Lamb BT, Montine TJ, Nedergaard M, Schaffer CB, Schneider JA, Wellington C, Wilcock DM, Zipfel GJ, Zlokovic B, Bain LJ, Bosetti F, Galis ZS, Koroshetz W and Carrillo MC. Vascular contributions to cognitive impairment and dementia including Alzheimer's disease. *Alzheimer's & dementia : the journal of the Alzheimer's Association*. 2015; 11: 710-717.

6. Corriveau RA, Bosetti F, Emr M, Gladman JT, Koenig JI, Moy CS, Pahigiannis K, Waddy SP and Koroshetz W. The Science of Vascular Contributions to Cognitive Impairment and Dementia (VCID): A Framework for Advancing Research Priorities in the Cerebrovascular Biology of Cognitive Decline. *Cell Mol Neurobiol*. 2016; 36: 281-288.

7. Williamson JD, Pajewski NM, Auchus AP, Bryan RN, Chelune G, Cheung AK, Cleveland ML, Coker LH, Crowe MG, Cushman WC, Cutler JA, Davatzikos C, Desiderio L, Erus G, Fine LJ, Gaussoin SA, Harris D, Hsieh MK, Johnson KC, Kimmel PL, Tamura MK, Launer LJ, Lerner AJ, Lewis CE, Martindale-Adams J, Moy CS, Nasrallah IM, Nichols LO, Oparil S, Ogrocki PK, Rahman M, Rapp SR, Reboussin DM, Rocco MV, Sachs BC, Sink KM, Still CH, Supiano MA, Snyder JK, Wadley VG, Walker J, Weiner DE, Whelton PK, Wilson VM, Woolard N, Wright JT, Jr. and Wright CB. Effect of Intensive vs Standard Blood Pressure Control on Probable Dementia: A Randomized Clinical Trial. *Journal of the American Medical Association*. 2019; 321: 553-561.

8. de Havenon A, Anadani M, Prabhakaran S, Wong KH, Yaghi S and Rost N. Increased Blood Pressure Variability and the Risk of Probable Dementia or Mild Cognitive Impairment: A Post Hoc Analysis of the SPRINT MIND Trial. *J Am Heart Assoc*. 2021; 10: e022206.

9. Mancia G. Prognostic value of long-term blood pressure variability: the evidence is growing. *Hypertension*. 2011; 57: 141-3.

10. Crook T, Bartus RT, Ferris SH, Whitehouse P, Cohen GD and Gershon S. Age-associated memory impairment: Proposed diagnostic criteria and measures of clinical change — report of a national institute of mental health work group. *Developmental Neuropsychology*. 1986; 2: 261-276.

11. Crook T, Bahar H and Sudilovsky A. Age-associated memory impairment: diagnostic criteria and treatment strategies. *International journal of neurology*. 1987; 21-22: 73-82.

12. Ward A, Arrighi HM, Michels S and Cedarbaum JM. Mild cognitive impairment: disparity of incidence and prevalence estimates. *Alzheimers Dement*. 2012; 8: 14-21.

13. O'Hara R, Derouesné C, Fountoulakis KN and Yesavage JA. Therapeutic approaches to age-associated neurocognitive disorders. *Dialogues Clin Neurosci*. 2001; 3: 191-213.

14. Ritchie K, Artero S and Touchon J. Classification criteria for mild cognitive impairment: a population-based validation study. *Neurology*. 2001; 56: 37-42.

15. Hanninen T, Koivisto K, Reinikainen KJ, Helkala EL, Soininen H, Mykkanen L, Laakso M and Riekkinen PJ. Prevalence of ageing-associated cognitive decline in an elderly population. *Age Ageing*. 1996; 25: 201-5.

16. Albert MS, DeKosky ST, Dickson D, Dubois B, Feldman HH, Fox NC, Gamst A, Holtzman DM, Jagust WJ, Petersen RC, Snyder PJ, Carrillo MC, Thies B and Phelps CH. The diagnosis of mild cognitive impairment due to Alzheimer's disease: recommendations from the National Institute on Aging-Alzheimer's Association workgroups on diagnostic guidelines for Alzheimer's disease. *Alzheimers Dement*. 2011; 7: 270-279.

17. Casagrande M, Marselli G, Agostini F, Forte G, Favieri F and Guarino A. The complex burden of determining prevalence rates of mild cognitive impairment: A systematic review. *Frontiers in psychiatry*. 2022; 13: 960648.

18. Manly JJ, Jones RN, Langa KM, Ryan LH, Levine DA, McCammon R, Heeringa SG and Weir D. Estimating the Prevalence of Dementia and Mild Cognitive Impairment in the US: The 2016 Health and Retirement Study Harmonized Cognitive Assessment Protocol Project. *JAMA Neurol*. 2022; 79: 1242-1249.

19. Wilson RS, Weir DR, Leurgans SE, Evans DA, Hebert LE, Langa KM, Plassman BL, Small BJ and Bennett DA. Sources of variability in estimates of the prevalence of Alzheimer's disease in the United States. *Alzheimers Dement*. 2011; 7: 74-9.

20. Rajan KB, Weuve J, Wilson RS, Barnes LL, McAninch EA and Evans DA. Temporal changes in the likelihood of dementia and MCI over 18 years in a population sample. *Neurology*. 2020; 94: e292-e298.

21. Wolters FJ and Ikram MA. Epidemiology of Vascular Dementia. *Arteriosclerosis, thrombosis, and vascular biology*. 2019; 39: 1542-1549.

22. Chauhan G, Adams HHH, Satizabal CL, Bis JC, Teumer A, Sargurupremraj M, Hofer E, Trompet S, Hilal S, Smith AV, Jian X, Malik R, Traylor M, Pulit SL, Amouyel P, Mazoyer B, Zhu YC, Kaffashian S, Schilling S, Beecham GW, Montine TJ, Schellenberg GD, Kjartansson O, Guðnason V, Knopman DS, Griswold ME, Windham BG, Gottesman RF, Mosley TH, Schmidt R, Saba Y, Schmidt H, Takeuchi F, Yamaguchi S, Nabika T, Kato N, Rajan KB, Aggarwal NT, De Jager PL, Evans DA, Psaty BM, Rotter JI, Rice K, Lopez OL, Liao J, Chen C, Cheng CY, Wong TY, Ikram MK, van der Lee SJ, Amin N, Chouraki V, DeStefano AL, Aparicio HJ, Romero JR, Maillard P, DeCarli C, Wardlaw JM, Hernández M, Luciano M, Liewald D, Deary IJ, Starr JM, Bastin ME, Muñoz Maniega S, Slagboom PE, Beekman M, Deelen J, Uh HW, Lemmens R, Brodaty H, Wright MJ, Ames D, Boncoraglio GB, Hopewell JC, Beecham AH, Blanton SH, Wright CB, Sacco RL, Wen W, Thalamuthu A, Armstrong NJ, Chong E, Schofield PR, Kwok JB, van der Grond J, Stott DJ, Ford I, Jukema JW, Vernooij MW, Hofman A, Uitterlinden AG, van der Lugt A, Wittfeld K, Grabe HJ, Hosten N, von Sarnowski B, Völker U, Levi C, Jimenez-Conde J, Sharma P, Sudlow CLM, Rosand J, Woo D, Cole JW, Meschia JF, Slowik A, Thijs V, Lindgren A, Melander O, Grewal RP, Rundek T, Rexrode K, Rothwell PM, Arnett DK, Jern C, Johnson JA, Benavente OR, Wasssertheil-Smoller S, Lee JM, Wong Q, Mitchell BD, Rich SS, McArdle PF, Geerlings MI, van der Graaf Y, de Bakker PIW, Asselbergs FW, Srikanth V, Thomson R, McWhirter R, Moran C, Callisaya M, Phan T, Rutten-Jacobs LCA, Bevan S, Tzourio C, Mather KA, Sachdev PS, van Duijn CM, Worrall BB, Dichgans M, Kittner SJ, Markus HS, Ikram MA, Fornage M, Launer LJ, Seshadri S, Longstreth WT, Jr. and Debette S. Genetic and lifestyle risk factors for MRI-defined brain infarcts in a population-based setting. *Neurology*. 2019; 92: e486-503.

23. Larrabee GJ and Crook TH, 3rd. Estimated prevalence of age-associated memory impairment derived from standardized tests of memory function. *International psychogeriatrics*. 1994; 6: 95-104.

24. Kapasi A, DeCarli C and Schneider JA. Impact of multiple pathologies on the threshold for clinically overt dementia. *Acta Neuropathol*. 2017; 134: 171-186.

25. Brenowitz WD, Hubbard RA, Keene CD, Hawes SE, Longstreth WT, Jr., Woltjer RL and Kukull WA. Mixed neuropathologies and estimated rates of clinical progression in a large autopsy sample. *Alzheimers Dement*. 2017; 13: 654-662.

26. Gottesman RF, Albert MS, Alonso A, Coker LH, Coresh J, Davis SM, Deal JA, McKhann GM, Mosley TH, Sharrett AR, Schneider ALC, Windham BG, Wruck LM and Knopman DS. Associations Between Midlife Vascular Risk Factors and 25-Year Incident Dementia in the Atherosclerosis Risk in Communities (ARIC) Cohort. *JAMA Neurol*. 2017; 74: 1246-1254.

27. Petrovitch H, White LR, Izmirilian G, Ross GW, Havlik RJ, Markesbery W, Nelson J, Davis DG, Hardman J, Foley DJ and Launer LJ. Midlife blood pressure and neuritic plaques, neurofibrillary tangles, and brain weight at death: the HAAS. Honolulu-Asia aging Study. *Neurobiol Aging*. 2000; 21: 57-62.

28. Conner SC, Pase MP, Carneiro H, Raman MR, McKee AC, Alvarez VE, Walker JM, Satizabal CL, Himali JJ, Stein TD, Beiser A and Seshadri S. Mid-life and late-life vascular risk

factor burden and neuropathology in old age. *Annals of clinical and translational neurology*. 2019.

29. Jellinger KA and Attems J. Challenges of multimorbidity of the aging brain: a critical update. *Journal of neural transmission (Vienna, Austria : 1996)*. 2015; 122: 505-21.

30. Kalaria RN and Sepulveda-Falla D. Cerebral Small Vessel Disease in Sporadic and Familial Alzheimer Disease. *The American journal of pathology*. 2021; 191: 1888-1905.

31. Schneider JA, Arvanitakis Z, Bang W and Bennett DA. Mixed brain pathologies account for most dementia cases in community-dwelling older persons. *Neurology*. 2007; 69: 2197-2204.

32. Jellinger KA and Attems J. Incidence of cerebrovascular lesions in Alzheimer's disease: a postmortem study. *Acta Neuropathol*. 2003; 105: 14-7.

33. Vermeer SE, Prins ND, den Heijer T, Hofman A, Koudstaal PJ and Breteler MM. Silent brain infarcts and the risk of dementia and cognitive decline. *The New England Journal of Medicine*. 2003; 348: 1215-1222.

34. Zekry D, Duyckaerts C, Moulias R, Belmin J, Geoffre C, Herrmann F and Hauw JJ. Degenerative and vascular lesions of the brain have synergistic effects in dementia of the elderly. *Acta Neuropathol*. 2002; 103: 481-7.

35. Snowdon DA, Greiner LH, Mortimer JA, Riley KP, Greiner PA and Markesbery WR. Brain infarction and the clinical expression of Alzheimer disease. The Nun Study. *Journal of American Medical Association*. 1997; 277: 813-817.

36. Esiri MM, Nagy Z, Smith MZ, Barnetson L and Smith AD. Cerebrovascular disease and threshold for dementia in the early stages of Alzheimer's disease. *Lancet*. 1999; 354: 919-20.

37. Østergaard L, Engedal TS, Moreton F, Hansen MB, Wardlaw JM, Dalkara T, Markus HS and Muir KW. Cerebral small vessel disease: Capillary pathways to stroke and cognitive decline. *Journal of Cerebral Blood Flow & Metabolism*. 2016; 36: 302-325.

38. Sweeney MD, Montagne A, Sagare AP, Nation DA, Schneider LS, Chui HC, Harrington MG, Pa J, Law M, Wang DJJ, Jacobs RE, Doubal FN, Ramirez J, Black SE, Nedergaard M, Benveniste H, Dichgans M, Iadecola C, Love S, Bath PM, Markus HS, Al-Shahi Salman R, Allan SM, Quinn TJ, Kalaria RN, Werring DJ, Carare RO, Touyz RM, Williams SCR, Moskowitz MA, Katusic ZS, Lutz SE, Lazarov O, Minshall RD, Rehman J, Davis TP, Wellington CL, González HM, Yuan C, Lockhart SN, Hughes TM, Chen CLH, Sachdev P, O'Brien JT, Skoog I, Pantoni L, Gustafson DR, Biessels GJ, Wallin A, Smith EE, Mok V, Wong A, Passmore P, Barkof F, Muller M, Breteler MMB, Román GC, Hamel E, Seshadri S, Gottesman RF, van Buchem MA, Arvanitakis Z, Schneider JA, Drewes LR, Hachinski V, Finch CE, Toga AW, Wardlaw JM and Zlokovic BV. Vascular dysfunction-The disregarded partner of Alzheimer's disease. *Alzheimers Dement*. 2019; 15: 158-167.

39. Kalaria RN. Neuropathological diagnosis of vascular cognitive impairment and vascular dementia with implications for Alzheimer's disease. *Acta Neuropathol*. 2016; 131: 659-85.

40. Carare RO, Aldea R, Agarwal N, Bacskai BJ, Bechman I, Boche D, Bu G, Bulters D, Clemens A, Counts SE, de Leon M, Eide PK, Fossati S, Greenberg SM, Hamel E, Hawkes CA, Koronyo-Hamaoui M, Hainsworth AH, Holtzman D, Ihara M, Jefferson A, Kalaria RN, Kipps CM, Kanninen KM, Leinonen V, McLaurin J, Miners S, Malm T, Nicoll JAR, Piazza F, Paul G, Rich SM, Saito S, Shih A, Scholtzova H, Snyder H, Snyder P, Thormodsson FR, van Veluw SJ, Weller RO, Werring DJ, Wilcock D, Wilson MR, Zlokovic BV and Verma A. Clearance of interstitial fluid (ISF) and CSF (CLIC) group-part of Vascular Professional Interest Area (PIA): Cerebrovascular disease and the failure of elimination of Amyloid-β from the brain and retina with age and Alzheimer's disease-Opportunities for Therapy. *Alzheimer's & dementia (Amsterdam, Netherlands)*. 2020; 12: e12053.

41. Iturria-Medina Y, Sotero RC, Toussaint PJ, Mateos-Perez JM and Evans AC. Early role of vascular dysregulation on late-onset Alzheimer's disease based on multifactorial data-driven analysis. *Nat Commun*. 2016; 7: 11934.

42. Guo LH, Alexopoulos P and Perneczky R. Heart-type fatty acid binding protein and vascular endothelial growth factor: cerebrospinal fluid biomarker candidates for Alzheimer's disease. *European archives of psychiatry and clinical neuroscience*. 2013; 263: 553-60.

43. Erqou S, Thompson A, Di Angelantonio E, Saleheen D, Kaptoge S, Marcovina S and Danesh J. Apolipoprotein(a) isoforms and the risk of vascular disease: systematic review of 40 studies involving 58,000 participants. *Journal of the American College of Cardiology*. 2010; 55: 2160-7.

44. Clarke DD and Sokoloff L. Regulation of Cerebral Metabolic Rate. In: G. J. Siegel, B. W. Agranoff, R. W. Albers, S. K. Fisher and M. D. Uhler, eds. *Basic Neurochemistry: Molecular, Cellular and Medical Aspects 6th edition* Philadelphia: Lippincott-Raven; 1999.

45. Rolfe DF and Brown GC. Cellular energy utilization and molecular origin of standard metabolic rate in mammals. *Physiological reviews*. 1997; 77: 731-58.

46. Mergenthaler P, Lindauer U, Dienel GA and Meisel A. Sugar for the brain: the role of glucose in physiological and pathological brain function. *Trends in neurosciences*. 2013; 36: 587-97.

47. Williams LR and Leggett RW. Reference values for resting blood flow to organs of man. *Clinical Physics and Physiological Measurement*. 1989; 10: 187-217.

48. Xing CY, Tarumi T, Liu J, Zhang Y, Turner M, Riley J, Tinajero CD, Yuan LJ and Zhang R. Distribution of cardiac output to the brain across the adult lifespan. *J Cereb Blood Flow Metab*. 2017; 37: 2848-2856.

49. Lassen NA. Autoregulation of Cerebral Blood Flow. *Circ Res*. 1964; 15: Suppl:201-4.

50. Warnert EA, Murphy K, Hall JE and Wise RG. Noninvasive assessment of arterial compliance of human cerebral arteries with short inversion time arterial spin labeling. *J Cereb Blood Flow Metab*. 2015; 35: 461-8.

51. Manfre L, Giarratano E, Maggio A, Banco A, Vaccaro G and Lagalla R. MR imaging of the brain: findings in asymptomatic patients with thalassemia intermedia and sickle cell-thalassemia disease. *AJR American journal of roentgenology*. 1999; 173: 1477-80.

52. Motomiya M and Karino T. Flow patterns in the human carotid artery bifurcation. *Stroke*. 1984; 15: 50-6.

53. Blackwell DL and Villarroel MA. Tables of Summary Health Statistics for U.S. Adults: 2017 National Health Interview Survey. National Center for Health Statistics. 2018.

54. Benjamin EJ, Virani SS, Callaway CW, Chamberlain AM, Chang AR, Cheng S, Chiuve SE, Cushman M, Delling FN, Deo R, de Ferranti SD, Ferguson JF, Fornage M, Gillespie C, Isasi CR, Jimenez MC, Jordan LC, Judd SE, Lackland D, Lichtman JH, Lisabeth L, Liu S, Longenecker CT, Lutsey PL, Mackey JS, Matchar DB, Matsushita K, Mussolino ME, Nasir K, O'Flaherty M, Palaniappan LP, Pandey A, Pandey DK, Reeves MJ, Ritchey MD, Rodriguez CJ, Roth GA, Rosamond WD, Sampson UKA, Satou GM, Shah SH, Spartano NL, Tirschwell DL, Tsao CW, Voeks JH, Willey JZ, Wilkins JT, Wu JH, Alger HM, Wong SS and Muntner P. Heart disease and stroke statistics-2018 update: A report from the American Heart Association. *Circulation*. 2018; 137: e67-e492.

55. Gottesman RF, Schneider AL, Albert M, Alonso A, Bandeen-Roche K, Coker L, Coresh J, Knopman D, Power MC, Rawlings A, Sharrett AR, Wruck LM and Mosley TH. Midlife hypertension and 20-year cognitive change: the atherosclerosis risk in communities neurocognitive study. *JAMA Neurol*. 2014; 71: 1218-27.

56. Hoth KF, Poppas A, Moser DJ, Paul RH and Cohen RA. Cardiac dysfunction and cognition in older adults with heart failure. *Cognitive and Behavioral Neurology*. 2008; 21: 65-72.

57. Sauve MJ, Lewis WR, Blankenbiller M, Rickabaugh B and Pressler SJ. Cognitive impairments in chronic heart failure: a case controlled study. *J Card Fail*. 2009; 15: 1-10.

58. Hammond CA, Blades NJ, Chaudhry SI, Dodson JA, Longstreth WT, Jr., Heckbert SR, Psaty BM, Arnold AM, Dublin S, Sitlani CM, Gardin JM, Thielke SM, Nanna MG, Gottesman RF, Newman AB and Thacker EL. Long-Term Cognitive Decline After Newly Diagnosed Heart Failure: Longitudinal Analysis in the CHS (Cardiovascular Health Study). *Circ Heart Fail*. 2018; 11: e004476.

59. Cermakova P, Eriksdotter M, Lund L, Winblad B, Religa P and Religa D. Heart failure and Alzheimer's disease. *Journal of Internal Medicine*. 2015; 277: 406-425.

60. Jefferson AL and Benjamin EJ. Cardiovascular disease, cognitive decline, and dementia. In: L. O. Wahlund, T. Erkinjuntti and S. Gauthier, eds. *Vascular cognitive impairment in clinical practice* Cambridge, UK: Cambridge University Press; 2009: 166-177.

61. Jefferson AL, Poppas A, Paul RH and Cohen RA. Systemic hypoperfusion is associated with executive dysfunction in geriatric cardiac patients. *Neurobiol Aging*. 2007; 28: 477-483.

62. Jefferson AL, Himali JJ, Beiser AS, Au R, Massaro JM, Seshadri S, Gona P, Salton CJ, DeCarli C, O'Donnell CJ, Benjamin EJ, Wolf PA and Manning WJ. Cardiac index is associated with brain aging: The Framingham Heart Study. *Circulation*. 2010; 122: 690-7.

63. Jefferson AL, Beiser AS, Himali JJ, Seshadri S, O'Donnell CJ, Manning WJ, Wolf PA, Au R and Benjamin EJ. Low cardiac index is associated with incident dementia and Alzheimer disease: The Framingham Heart Study. *Circulation*. 2015; 131: 1333-1339.

64. Okonkwo OC, Cohen RA, Gunstad J and Poppas A. Cardiac output, blood pressure variability, and cognitive decline in geriatric cardiac patients. *J Cardiopulm Rehabil Prev*. 2011; 31: 290-7.

65. Sabayan B, van Buchem MA, Sigurdsson S, Zhang Q, Harris TB, Gudnason V, Arai AE and Launer LJ. Cardiac hemodynamics are linked with structural and functional features of brain aging: the age, gene/environment susceptibility (AGES)-Reykjavik Study. *J Am Heart Assoc*. 2015; 4: e001294.

66. Kresge HA, Khan OA, Wegener MA, Liu D, Terry JG, Nair S, Cambronero FE, Gifford KA, Osborn KE, Hohman TJ, Pechman KR, Bell SP, Wang TJ, Carr JJ and Jefferson AL. Subclinical compromise in cardiac strain relates to lower cognitive performances in older adults. *J Am Heart Assoc*. 2018; 7: e007562.

67. Jefferson AL, Liu D, Gupta DK, Pechman KR, Watchmaker JM, Gordon EA, Rane S, Bell SP, Mendes LA, Davis LT, Gifford KA, Hohman TJ, Wang TJ and Donahue MJ. Lower cardiac index levels relate to lower cerebral blood flow in older adults. *Neurology*. 2017; 89: 2327-2334.

68. Strandgaard S, Olesen J, Skinhoj E and Lassen NA. Autoregulation of brain circulation in severe arterial hypertension. *British medical journal*. 1973; 1: 507-10.

69. Singer J, Trollor JN, Baune BT, Sachdev PS and Smith E. Arterial stiffness, the brain and cognition: a systematic review. *Ageing research reviews*. 2014; 15: 16-27.

70. Mitchell GF, van Buchem MA, Sigurdsson S, Gotal JD, Jonsdottir MK, Kjartansson O, Garcia M, Aspelund T, Harris TB, Gudnason V and Launer LJ. Arterial stiffness, pressure and flow pulsatility and brain structure and function: the Age, Gene/Environment Susceptibility--Reykjavik study. *Brain*. 2011; 134: 3398-3407.

71. de Havenon A, Wong KH, Elkhetali A, McNally JS, Majersik JJ and Rost NS. Carotid Artery Stiffness Accurately Predicts White Matter Hyperintensity Volume 20 Years Later: A Secondary Analysis of the Atherosclerosis Risk in the Community Study. *AJNR Am J Neuroradiol*. 2019; 40: 1369-1373.

72. Palta P, Sharrett AR, Wei J, Meyer ML, Kucharska-Newton A, Power MC, Deal JA, Jack CR, Knopman D, Wright J, Griswold M, Tanaka H, Mosley TH and Heiss G. Central Arterial Stiffness Is Associated With Structural Brain Damage and Poorer Cognitive Performance: The ARIC Study. *J Am Heart Assoc*. 2019; 8: e011045.

73. Jefferson AL, Cambronero FE, Liu D, Moore EE, Neal JE, Terry JG, Nair S, Pechman KR, Rane S, Davis LT, Gifford KA, Hohman TJ, Bell SP, Wang TJ, Beckman JA and Carr JJ. Higher aortic stiffness is related to lower cerebral blood flow and preserved cerebrovascular reactivity in older adults. *Circulation*. 2018; 138: 1951-1962.

74. Iulita MF, Noriega de la Colina A and Girouard H. Arterial stiffness, cognitive impairment and dementia: confounding factor or real risk? *Journal of neurochemistry*. 2018; 144: 527-548.

75. Salthouse TA. The processing-speed theory of adult age differences in cognition. *Psychological Review*. 1996; 103: 403-428.

76. Martin AJ, Friston KJ, Colebatch JG and Frackowiak RS. Decreases in regional cerebral blood flow with normal aging. *J Cereb Blood Flow Metab*. 1991; 11: 684-9.

77. Lee C, Lopez OL, Becker JT, Raji C, Dai W, Kuller LH and Gach HM. Imaging cerebral blood flow in the cognitively normal aging brain with arterial spin labeling: implications for imaging of neurodegenerative disease. *J Neuroimaging*. 2009; 19: 344-52.

78. Donahue MJ, Hussey E, Rane S, Wilson T, van Osch M, Hartkamp N, Hendrikse J and Ally BA. Vessel-encoded arterial spin labeling (VE-ASL) reveals elevated flow territory asymmetry in older adults with substandard verbal memory performance. *Journal of Magnetic Resonance Imaging*. 2014; 39: 377-386.

79. Asllani I, Habeck C, Borogovac A, Brown TR, Brickman AM and Stern Y. Separating function from structure in perfusion imaging of the aging brain. *Hum Brain Mapp*. 2009; 30: 2927-35.

80. Chen JJ, Rosas HD and Salat DH. Age-associated reductions in cerebral blood flow are independent from regional atrophy. *Neuroimage*. 2011; 55: 468-78.

81. Huang CW, Hsu SW, Chang YT, Huang SH, Huang YC, Lee CC, Chang WN, Lui CC, Chen NC and Chang CC. Cerebral Perfusion Insufficiency and Relationships with Cognitive Deficits in Alzheimer's Disease: A Multiparametric Neuroimaging Study. *Scientific reports*. 2018; 8: 1541.

82. Wirth M, Pichet Binette A, Brunecker P, Kobe T, Witte AV and Floel A. Divergent regional patterns of cerebral hypoperfusion and gray matter atrophy in mild cognitive impairment patients. *Journal of Cerebral Blood Flow & Metabolism*. 2017; 37: 814-824.

83. Putcha D, Brickhouse M, O'Keefe K, Sullivan C, Rentz D, Marshall G, Dickerson B and Sperling R. Hippocampal hyperactivation associated with cortical thinning in Alzheimer's disease signature regions in non-demented elderly adults. *J Neurosci*. 2011; 31: 17680-8.

84. Immink RV, van den Born BJ, van Montfrans GA, Koopmans RP, Karemaker JM and van Lieshout JJ. Impaired cerebral autoregulation in patients with malignant hypertension. *Circulation*. 2004; 110: 2241-5.

85. Zlokovic BV. Neurovascular pathways to neurodegeneration in Alzheimer's disease and other disorders. *Nature reviews Neuroscience*. 2011; 12: 723-38.

86. Iturria-Medina Y, Hachinski V and Evans AC. The vascular facet of late-onset Alzheimer's disease: an essential factor in a complex multifactorial disorder. *Current opinion in neurology*. 2017; 30: 623-629.

87. Ruitenberg A, den Heijer T, Bakker SL, van Swieten JC, Koudstaal PJ, Hofman A and Breteler MM. Cerebral hypoperfusion and clinical onset of dementia: the Rotterdam Study. *Ann Neurol*. 2005; 57: 789-794.

88. Alsop DC, Dai W, Grossman M and Detre JA. Arterial spin labeling blood flow MRI: its role in the early characterization of Alzheimer's disease. *J Alzheimers Dis*. 2010; 20: 871-80.

89. Chen W, Song X, Beyea S, D'Arcy R, Zhang Y and Rockwood K. Advances in perfusion magnetic resonance imaging in Alzheimer's disease. *Alzheimers Dement*. 2011; 7: 185-96.

90. Braak H and Braak E. Neuropathological stageing of Alzheimer-related changes. *Acta Neuropathol*. 1991; 82: 239-259.

91. Scahill RI, Schott JM, Stevens JM, Rossor MN and Fox NC. Mapping the evolution of regional atrophy in Alzheimer's disease: unbiased analysis of fluid-registered serial MRI. *Proc Natl Acad Sci U S A*. 2002; 99: 4703-7.

92. Benedictus MR, Binnewijzend MAA, Kuijer JPA, Steenwijk MD, Versteeg A, Vrenken H, Scheltens P, Barkhof F, van der Flier WM and Prins ND. Brain volume and white matter hyperintensities as determinants of cerebral blood flow in Alzheimer's disease. *Neurobiol Aging*. 2014; 35: 2665-2670.

93. Zonneveld HI, Loehrer EA, Hofman A, Niessen WJ, van der Lugt A, Krestin GP, Ikram MA and Vernooij MW. The bidirectional association between reduced cerebral blood flow and brain atrophy in the general population. *J Cereb Blood Flow Metab*. 2015; 35: 1882-7.

94. Suter OC, Sunthorn T, Kraftsik R, Straubel J, Darekar P, Khalili K and Miklossy J. Cerebral hypoperfusion generates cortical watershed microinfarcts in Alzheimer disease. *Stroke*. 2002; 33: 1986-1992.

95. Petrovitch H, Ross GW, Steinhorn SC, Abbott RD, Markesbery W, Davis D, Nelson J, Hardman J, Masaki K, Vogt MR, Launer L and White LR. AD lesions and infarcts in demented and non-demented Japanese-American men. *Ann Neurol*. 2005; 57: 98-103.

96. Montine TJ, Koroshetz WJ, Babcock D, Dickson DW, Galpern WR, Glymour MM, Greenberg SM, Hutton ML, Knopman DS, Kuzmichev AN, Manly JJ, Marder KS, Miller BL, Phelps CH, Seeley WW, Sieber BA, Silverberg NB, Sutherland M, Torborg CL, Waddy SP, Zlokovic BV and Corriveau RA. Recommendations of the Alzheimer's disease-related dementias conference. *Neurology*. 2014; 83: 851-860.

97. Montagne A, Barnes SR, Sweeney MD, Halliday MR, Sagare AP, Zhao Z, Toga AW, Jacobs RE, Liu CY, Amezcua L, Harrington MG, Chui HC, Law M and Zlokovic BV. Blood-brain barrier breakdown in the aging human hippocampus. *Neuron*. 2015; 85: 296-302.

98. Paul J, Strickland S and Melchor JP. Fibrin deposition accelerates neurovascular damage and neuroinflammation in mouse models of Alzheimer's disease. *J Exp Med*. 2007; 204: 1999-2008.

99. Zipser BD, Johanson CE, Gonzalez L, Berzin TM, Tavares R, Hulette CM, Vitek MP, Hovanesian V and Stopa EG. Microvascular injury and blood-brain barrier leakage in Alzheimer's disease. *Neurobiol Aging*. 2007; 28: 977-86.

100. Lepelletier FX, Mann DM, Robinson AC, Pinteaux E and Boutin H. Early changes in extracellular matrix in Alzheimer's disease. *Neuropathology and applied neurobiology*. 2017; 43: 167-182.

101. Zlokovic BV. The blood-brain barrier in health and chronic neurodegenerative disorders. *Neuron*. 2008; 57: 178-201.

102. Hutchings M and Weller RO. Anatomical relationships of the pia mater to cerebral blood vessels in man. *Journal of neurosurgery*. 1986; 65: 316-25.

103. Bakker EN, Bacskai BJ, Arbel-Ornath M, Aldea R, Bedussi B, Morris AW, Weller RO and Carare RO. Lymphatic clearance of the brain: Perivascular, paravascular and significance for neurodegenerative diseases. *Cell Mol Neurobiol*. 2016; 36: 181-94.

104. Weller RO, Subash M, Preston SD, Mazanti I and Carare RO. Perivascular drainage of amyloid-beta peptides from the brain and its failure in cerebral amyloid angiopathy and Alzheimer's disease. *Brain pathology (Zurich, Switzerland)*. 2008; 18: 253-66.

105. Hawkes CA, Sullivan PM, Hands S, Weller RO, Nicoll JA and Carare RO. Disruption of arterial perivascular drainage of amyloid-beta from the brains of mice expressing the human APOE epsilon4 allele. *PLoS One*. 2012; 7: e41636.

106. Carare RO, Bernardes-Silva M, Newman TA, Page AM, Nicoll JA, Perry VH and Weller RO. Solutes, but not cells, drain from the brain parenchyma along basement membranes of capillaries and arteries: significance for cerebral amyloid angiopathy and neuroimmunology. *Neuropathology and applied neurobiology*. 2008; 34: 131-44.

107. Tarasoff-Conway JM, Carare RO, Osorio RS, Glodzik L, Butler T, Fieremans E, Axel L, Rusinek H, Nicholson C, Zlokovic BV, Frangione B, Blennow K, Menard J, Zetterberg H, Wisniewski T and de Leon MJ. Clearance systems in the brain-implications for Alzheimer disease. *Nature reviews Neurology*. 2015; 11: 457-70.

108. Iliff JJ, Wang M, Liao Y, Plogg BA, Peng W, Gundersen GA, Benveniste H, Vates GE, Deane R, Goldman SA, Nagelhus EA and Nedergaard M. A paravascular pathway facilitates CSF flow through the brain parenchyma and the clearance of interstitial solutes, including amyloid beta. *Sci Transl Med*. 2012; 4: 147ra111.

109. Iliff JJ and Nedergaard M. Is there a cerebral lymphatic system? *Stroke*. 2013; 44: S93-5.

110. Weller RO. Pathology of cerebrospinal fluid and interstitial fluid of the CNS: significance for Alzheimer disease, prion disorders and multiple sclerosis. *J Neuropathol Exp Neurol*. 1998; 57: 885-94.

111. Weller RO, Massey A, Kuo YM and Roher AE. Cerebral amyloid angiopathy: accumulation of A beta in interstitial fluid drainage pathways in Alzheimer's disease. *Annals of the New York Academy of Sciences*. 2000; 903: 110-7.

112. Shibata M, Yamada S, Kumar SR, Calero M, Bading J, Frangione B, Holtzman DM, Miller CA, Strickland DK, Ghiso J and Zlokovic BV. Clearance of Alzheimer's amyloid-ss(1-40) peptide from brain by LDL receptor-related protein-1 at the blood-brain barrier. *J Clin Invest*. 2000; 106: 1489-99.

113. Donahue JE, Flaherty SL, Johanson CE, Duncan JA, 3rd, Silverberg GD, Miller MC, Tavares R, Yang W, Wu Q, Sabo E, Hovanesian V and Stopa EG. RAGE, LRP-1, and amyloid-beta protein in Alzheimer's disease. *Acta Neuropathol*. 2006; 112: 405-15.

114. ElAli A, Theriault P, Prefontaine P and Rivest S. Mild chronic cerebral hypoperfusion induces neurovascular dysfunction, triggering peripheral beta-amyloid brain entry and aggregation. *Acta Neuropathol Commun*. 2013; 1: 75.

115. Salvadores N, Searcy JL, Holland PR and Horsburgh K. Chronic cerebral hypoperfusion alters amyloid-beta peptide pools leading to cerebral amyloid angiopathy, microinfarcts and haemorrhages in Tg-SwDI mice. *Clin Sci (Lond)*. 2017; 131: 2109-2123.

116. Wisniewski HM and Wegiel J. Beta-amyloid formation by myocytes of leptomeningeal vessels. *Acta Neuropathol*. 1994; 87: 233-41.

117. Cai Z, Liu Z, Xiao M, Wang C and Tian F. Chronic Cerebral Hypoperfusion Promotes Amyloid-Beta Pathogenesis via Activating beta/gamma-Secretases. *Neurochemical research*. 2017; 42: 3446-3455.

118. Mattsson N, Tosun D, Insel PS, Simonson A, Jack CR, Jr., Beckett LA, Donohue M, Jagust W, Schuff N and Weiner MW. Association of brain amyloid-beta with cerebral perfusion and structure in Alzheimer's disease and mild cognitive impairment. *Brain*. 2014; 137: 1550-61.

119. Sakono M and Zako T. Amyloid oligomers: formation and toxicity of Abeta oligomers. *The FEBS journal*. 2010; 277: 1348-58.

120. Attems J. Sporadic cerebral amyloid angiopathy: pathology, clinical implications, and possible pathomechanisms. *Acta Neuropathol*. 2005; 110: 345-59.

121. Biron KE, Dickstein DL, Gopaul R and Jefferies WA. Amyloid triggers extensive cerebral angiogenesis causing blood brain barrier permeability and hypervascularity in Alzheimer's disease. *PLoS One*. 2011; 6: e23789.

122. Jucker M and Walker LC. Self-propagation of pathogenic protein aggregates in neurodegenerative diseases. *Nature*. 2013; 501: 45-51.

123. Hampel H, Hardy J, Blennow K, Chen C, Perry G, Kim SH, Villemagne VL, Aisen P, Vendruscolo M, Iwatsubo T, Masters CL, Cho M, Lannfelt L, Cummings JL and Vergallo A. The Amyloid-β Pathway in Alzheimer's Disease. *Molecular psychiatry*. 2021; 26: 5481-5503.

124. Thal DR, Rub U, Orantes M and Braak H. Phases of A beta-deposition in the human brain and its relevance for the development of AD. *Neurology*. 2002; 58: 1791-800.

125. Song HL, Shim S, Kim DH, Won SH, Joo S, Kim S, Jeon NL and Yoon SY. β-Amyloid is transmitted via neuronal connections along axonal membranes. *Ann Neurol*. 2014; 75: 88-97.

126. Nath S, Agholme L, Kurudenkandy FR, Granseth B, Marcusson J and Hallbeck M. Spreading of neurodegenerative pathology via neuron-to-neuron transmission of β-amyloid. *J Neurosci*. 2012; 32: 8767-77.

127. Pignataro A and Middei S. Trans-Synaptic Spread of Amyloid-β in Alzheimer's Disease: Paths to β-Amyloidosis. *Neural plasticity*. 2017; 2017: 5281829.

128. Whittington A, Sharp DJ and Gunn RN. Spatiotemporal Distribution of β-Amyloid in Alzheimer Disease Is the Result of Heterogeneous Regional Carrying Capacities. *Journal of nuclear medicine : official publication, Society of Nuclear Medicine*. 2018; 59: 822-827.

129. Zhang H, Cao Y, Ma L, Wei Y and Li H. Possible Mechanisms of Tau Spread and Toxicity in Alzheimer's Disease. *Frontiers in cell and developmental biology*. 2021; 9: 707268.

130. Levin F, Jelistratova I, Betthauser TJ, Okonkwo O, Johnson SC, Teipel SJ and Grothe MJ. In vivo staging of regional amyloid progression in healthy middle-aged to older people at risk of Alzheimer's disease. *Alzheimer's research & therapy*. 2021; 13: 178.

131. Mattsson N, Palmqvist S, Stomrud E, Vogel J and Hansson O. Staging β-Amyloid Pathology With Amyloid Positron Emission Tomography. *JAMA Neurol*. 2019; 76: 1319-1329.

132. Villeneuve S, Rabinovici GD, Cohn-Sheehy BI, Madison C, Ayakta N, Ghosh PM, La Joie R, Arthur-Bentil SK, Vogel JW, Marks SM, Lehmann M, Rosen HJ, Reed B, Olichney J, Boxer AL, Miller BL, Borys E, Jin LW, Huang EJ, Grinberg LT, DeCarli C, Seeley WW and Jagust W. Existing Pittsburgh Compound-B positron emission tomography thresholds are too high: statistical and pathological evaluation. *Brain*. 2015; 138: 2020-33.

133. Palmqvist S, Schöll M, Strandberg O, Mattsson N, Stomrud E, Zetterberg H, Blennow K, Landau S, Jagust W and Hansson O. Earliest accumulation of β-amyloid occurs within the default-mode network and concurrently affects brain connectivity. *Nat Commun*. 2017; 8: 1214.

134. Castillo-Carranza DL, Nilson AN, Van Skike CE, Jahrling JB, Patel K, Garach P, Gerson JE, Sengupta U, Abisambra J, Nelson P, Troncoso J, Ungvari Z, Galvan V and Kayed R. Cerebral Microvascular Accumulation of Tau Oligomers in Alzheimer's Disease and Related Tauopathies. *Aging Dis*. 2017; 8: 257-266.

135. Bennett RE, Robbins AB, Hu M, Cao X, Betensky RA, Clark T, Das S and Hyman BT. Tau induces blood vessel abnormalities and angiogenesis-related gene expression in P301L transgenic mice and human Alzheimer's disease. *Proc Natl Acad Sci U S A*. 2018; 115: E1289-e1298.

136. Williams S, Chalmers K, Wilcock GK and Love S. Relationship of neurofibrillary pathology to cerebral amyloid angiopathy in Alzheimer's disease. *Neuropathology and applied neurobiology*. 2005; 31: 414-21.

137. Kim HJ, Park S, Cho H, Jang YK, San Lee J, Jang H, Kim Y, Kim KW, Ryu YH, Choi JY, Moon SH, Weiner MW, Jagust WJ, Rabinovici GD, DeCarli C, Lyoo CH, Na DL and Seo SW. Assessment of Extent and Role of Tau in Subcortical Vascular Cognitive Impairment Using 18F-AV1451 Positron Emission Tomography Imaging. *JAMA Neurol*. 2018.

138. Qiu L, Ng G, Tan EK, Liao P, Kandiah N and Zeng L. Chronic cerebral hypoperfusion enhances Tau hyperphosphorylation and reduces autophagy in Alzheimer's disease mice. *Scientific reports*. 2016; 6: 23964.

139. Raz L, Bhaskar K, Weaver J, Marini S, Zhang Q, Thompson JF, Espinoza C, Iqbal S, Maphis NM, Weston L, Sillerud LO, Caprihan A, Pesko JC, Erhardt EB and Rosenberg GA. Hypoxia promotes tau hyperphosphorylation with associated neuropathology in vascular dysfunction. *Neurobiology of disease*. 2018.

140. Merlini M, Wanner D and Nitsch RM. Tau pathology-dependent remodelling of cerebral arteries precedes Alzheimer's disease-related microvascular cerebral amyloid angiopathy. *Acta Neuropathol*. 2016; 131: 737-52.

141. Blair LJ, Frauen HD, Zhang B, Nordhues BA, Bijan S, Lin YC, Zamudio F, Hernandez LD, Sabbagh JJ, Selenica ML and Dickey CA. Tau depletion prevents progressive blood-brain barrier damage in a mouse model of tauopathy. *Acta Neuropathol Commun*. 2015; 3: 8.

142. Rivera-Rivera LA, Turski P, Johnson KM, Hoffman C, Berman SE, Kilgas P, Rowley HA, Carlsson CM, Johnson SC and Wieben O. 4D flow MRI for intracranial hemodynamics assessment in Alzheimer's disease. *J Cereb Blood Flow Metab*. 2016; 36: 1718-1730.

143. Park L, Anrather J, Zhou P, Frys K, Pitstick R, Younkin S, Carlson GA and Iadecola C. NADPH-oxidase-derived reactive oxygen species mediate the cerebrovascular dysfunction induced by the amyloid beta peptide. *J Neurosci*. 2005; 25: 1769-77.

144. Park L, Zhou P, Pitstick R, Capone C, Anrather J, Norris EH, Younkin L, Younkin S, Carlson G, McEwen BS and Iadecola C. Nox2-derived radicals contribute to neurovascular and behavioral dysfunction in mice overexpressing the amyloid precursor protein. *Proc Natl Acad Sci U S A*. 2008; 105: 1347-52.

145. Lourenco CF, Ledo A, Barbosa RM and Laranjinha J. Neurovascular uncoupling in the triple transgenic model of Alzheimer's disease: Impaired cerebral blood flow response to neuronal-derived nitric oxide signaling. *Experimental neurology*. 2017; 291: 36-43.

146. Tarantini S, Tran CHT, Gordon GR, Ungvari Z and Csiszar A. Impaired neurovascular coupling in aging and Alzheimer's disease: Contribution of astrocyte dysfunction and endothelial impairment to cognitive decline. *Experimental gerontology*. 2017; 94: 52-58.

147. Bar KJ, Boettger MK, Seidler N, Mentzel HJ, Terborg C and Sauer H. Influence of galantamine on vasomotor reactivity in Alzheimer's disease and vascular dementia due to cerebral microangiopathy. *Stroke*. 2007; 38: 3186-92.

148. den Abeelen AS, Lagro J, van Beek AH and Claassen JA. Impaired cerebral autoregulation and vasomotor reactivity in sporadic Alzheimer's disease. *Current Alzheimer research*. 2014; 11: 11-7.

149. Jennings JR, Muldoon MF, Ryan C, Price JC, Greer P, Sutton-Tyrrell K, van der Veen FM and Meltzer CC. Reduced cerebral blood flow response and compensation among patients with untreated hypertension. *Neurology*. 2005; 64: 1358-65.

150. Kim YS, Immink RV, Stok WJ, Karemaker JM, Secher NH and van Lieshout JJ. Dynamic cerebral autoregulatory capacity is affected early in Type 2 diabetes. *Clinical Science*. 2008; 115: 255-62.

151. Schroeter ML, Cutini S, Wahl MM, Scheid R and Yves von Cramon D. Neurovascular coupling is impaired in cerebral microangiopathy--An event-related Stroop study. *Neuroimage*. 2007; 34: 26-34.

152. Tanzi RE. The genetics of Alzheimer disease. *Cold Spring Harb Perspect Med*. 2012; 2.

153. Sienski G, Narayan P, Bonner JM, Kory N, Boland S, Arczewska AA, Ralvenius WT, Akay L, Lockshin E, He L, Milo B, Graziosi A, Baru V, Lewis CA, Kellis M, Sabatini DM, Tsai LH and Lindquist S. APOE4 disrupts intracellular lipid homeostasis in human iPSC-derived glia. *Sci Transl Med*. 2021; 13.

154. Fernandez CG, Hamby ME, McReynolds ML and Ray WJ. The Role of APOE4 in Disrupting the Homeostatic Functions of Astrocytes and Microglia in Aging and Alzheimer's Disease. *Front Aging Neurosci*. 2019; 11: 14.

155. Yamazaki Y, Shinohara M, Yamazaki A, Ren Y, Asmann YW, Kanekiyo T and Bu G. ApoE (Apolipoprotein E) in Brain Pericytes Regulates Endothelial Function in an Isoform-Dependent Manner by Modulating Basement Membrane Components. *Arteriosclerosis, thrombosis, and vascular biology*. 2020; 40: 128-144.

156. Schmechel DE, Saunders AM, Strittmatter WJ, Crain BJ, Hulette CM, Joo SH, Pericak-Vance MA, Goldgaber D and Roses AD. Increased amyloid beta-peptide deposition in cerebral cortex as a consequence of apolipoprotein E genotype in late-onset Alzheimer disease. *Proc Natl Acad Sci U S A*. 1993; 90: 9649-9653.

157. Michels L, Warnock G, Buck A, Macauda G, Leh SE, Kaelin AM, Riese F, Meyer R, O'Gorman R, Hock C, Kollias S and Gietl AF. Arterial spin labeling imaging reveals widespread

and Abeta-independent reductions in cerebral blood flow in elderly apolipoprotein epsilon-4 carriers. *J Cereb Blood Flow Metab*. 2016; 36: 581-95.

158. Wang R, Fratiglioni L, Laukka EJ, Lovden M, Kalpouzos G, Keller L, Graff C, Salami A, Backman L and Qiu C. Effects of vascular risk factors and APOE epsilon4 on white matter integrity and cognitive decline. *Neurology*. 2015; 84: 1128-35.

159. Sengillo JD, Winkler EA, Walker CT, Sullivan JS, Johnson M and Zlokovic BV. Deficiency in mural vascular cells coincides with blood-brain barrier disruption in Alzheimer's disease. *Brain Pathol*. 2013; 23: 303-10.

160. Bell RD, Winkler EA, Singh I, Sagare AP, Deane R, Wu Z, Holtzman DM, Betsholtz C, Armulik A, Sallstrom J, Berk BC and Zlokovic BV. Apolipoprotein E controls cerebrovascular integrity via cyclophilin A. *Nature*. 2012; 485: 512-6.

161. Holtzman DM, Fagan AM, Mackey B, Tenkova T, Sartorius L, Paul SM, Bales K, Ashe KH, Irizarry MC and Hyman BT. Apolipoprotein E facilitates neuritic and cerebrovascular plaque formation in an Alzheimer's disease model. *Ann Neurol*. 2000; 47: 739-747.

162. Halliday MR, Rege SV, Ma Q, Zhao Z, Miller CA, Winkler EA and Zlokovic BV. Accelerated pericyte degeneration and blood-brain barrier breakdown in apolipoprotein E4 carriers with Alzheimer's disease. *Journal of Cerebral Blood Flow and Metabolism*. 2016; 36: 216-27.

163. Kalogeris T, Baines CP, Krenz M and Korthuis RJ. Cell biology of ischemia/reperfusion injury. *International review of cell and molecular biology*. 2012; 298: 229-317.

164. Cozzolino O, Marchese M, Trovato F, Pracucci E, Ratto GM, Buzzi MG, Sicca F and Santorelli FM. Understanding Spreading Depression from Headache to Sudden Unexpected Death. *Front Neurol*. 2018; 9: 19.

165. Kunz A and Iadecola C. Cerebral vascular dysregulation in the ischemic brain. *Handb Clin Neurol*. 2009; 92: 283-305.

166. Muramatsu K, Fukuda A, Togari H, Wada Y and Nishino H. Vulnerability to cerebral hypoxic-ischemic insult in neonatal but not in adult rats is in parallel with disruption of the blood-brain barrier. *Stroke*. 1997; 28: 2281-8; discussion 2288-9.

167. Devonshire IM, Papadakis NG, Port M, Berwick J, Kennerley AJ, Mayhew JE and Overton PG. Neurovascular coupling is brain region-dependent. *Neuroimage*. 2012; 59: 1997-2006.

168. Nishino A, Tajima Y, Takuwa H, Masamoto K, Taniguchi J, Wakizaka H, Kokuryo D, Urushihata T, Aoki I, Kanno I, Tomita Y, Suzuki N, Ikoma Y and Ito H. Long-term effects of cerebral hypoperfusion on neural density and function using misery perfusion animal model. *Sci Rep*. 2016; 6: 25072.

169. Ekstrom A. How and when the fMRI BOLD signal relates to underlying neural activity: the danger in dissociation. *Brain Res Rev*. 2010; 62: 233-44.

170. Dugan LL and Choi DW. Hypoxia-Ischemia and Brain infarction. In: G. J. Siegel, B. W. Agranoff and R. W. Albers, eds. *Basic Neurochemistry: Molecular, Cellular and Medical Aspects 6th edition* Philadelphia: Lippincott-Raven; 1999.

171. Petito CK, Olarte JP, Roberts B, Nowak TS, Jr. and Pulsinelli WA. Selective glial vulnerability following transient global ischemia in rat brain. *J Neuropathol Exp Neurol*. 1998; 57: 231-8.

172. Mifsud G, Zammit C, Muscat R, Di Giovanni G and Valentino M. Oligodendrocyte pathophysiology and treatment strategies in cerebral ischemia. *CNS neuroscience & therapeutics*. 2014; 20: 603-12.

173. Pantoni L, Garcia JH and Gutierrez JA. Cerebral white matter is highly vulnerable to ischemia. *Stroke*. 1996; 27: 1641-6; discussion 1647.

174. Cheng GW, Mok KK, Yeung SH, Kofler J, Herrup K and Tse KH. Apolipoprotein E ε4 Mediates Myelin Breakdown by Targeting Oligodendrocytes in Sporadic Alzheimer Disease. *J Neuropathol Exp Neurol*. 2022; 81: 717-730.

175. Baron JC, Yamauchi H, Fujioka M and Endres M. Selective neuronal loss in ischemic stroke and cerebrovascular disease. *J Cereb Blood Flow Metab*. 2014; 34: 2-18.

176. Kirino T. Delayed neuronal death in the gerbil hippocampus following ischemia. *Brain research*. 1982; 239: 57-69.

177. Pulsinelli WA, Brierley JB and Plum F. Temporal profile of neuronal damage in a model of transient forebrain ischemia. *Ann Neurol*. 1982; 11: 491-8.

178. Payabvash S, Souza LC, Wang Y, Schaefer PW, Furie KL, Halpern EF, Gonzalez RG and Lev MH. Regional ischemic vulnerability of the brain to hypoperfusion: the need for location specific computed tomography perfusion thresholds in acute stroke patients. *Stroke*. 2011; 42: 1255-60.

179. Takano K, Latour LL, Formato JE, Carano RA, Helmer KG, Hasegawa Y, Sotak CH and Fisher M. The role of spreading depression in focal ischemia evaluated by diffusion mapping. *Ann Neurol*. 1996; 39: 308-18.

180. Brennan KC, Beltrán-Parrazal L, López-Valdés HE, Theriot J, Toga AW and Charles AC. Distinct vascular conduction with cortical spreading depression. *Journal of neurophysiology*. 2007; 97: 4143-51.

181. Shabir O, Pendry B, Lee L, Eyre B, Sharp PS, Rebollar MA, Drew D, Howarth C, Heath PR, Wharton SB, Francis SE and Berwick J. Assessment of neurovascular coupling and cortical spreading depression in mixed mouse models of atherosclerosis and Alzheimer's disease. *eLife*. 2022; 11.

182. Hossmann KA. Viability thresholds and the penumbra of focal ischemia. *Ann Neurol*. 1994; 36: 557-65.

183. O'Rourke MF and Hashimoto J. Mechanical factors in arterial aging: a clinical perspective. *Journal of the American College of Cardiology*. 2007; 50: 1-13.

184. Rajeev V, Fann DY, Dinh QN, Kim HA, De Silva TM, Lai MKP, Chen CL, Drummond GR, Sobey CG and Arumugam TV. Pathophysiology of blood brain barrier dysfunction during chronic cerebral hypoperfusion in vascular cognitive impairment. *Theranostics*. 2022; 12: 1639-1658.

185. Frauenknecht K, Plaschke K and Sommer C. Transient oligemia is associated with long-term changes in binding densities of cortical inhibitory GABAA receptors in the rat brain. *Brain research*. 2009; 1271: 95-102.

186. Koike MA, Green KN, Blurton-Jones M and Laferla FM. Oligemic hypoperfusion differentially affects tau and amyloid-{beta}. *The American journal of pathology*. 2010; 177: 300-10.

187. Mitchell GF, Parise H, Benjamin EJ, Larson MG, Keyes MJ, Vita JA, Vasan RS and Levy D. Changes in arterial stiffness and wave reflection with advancing age in healthy men and women: the Framingham Heart Study. *Hypertension*. 2004; 43: 1239-1245.

188. Mitchell GF, Hwang SJ, Vasan RS, Larson MG, Pencina MJ, Hamburg NM, Vita JA, Levy D and Benjamin EJ. Arterial stiffness and cardiovascular events: the Framingham Heart Study. *Circulation*. 2010; 121: 505-511.

189. Mitchell GF. Effects of central arterial aging on the structure and function of the peripheral vasculature: implications for end-organ damage. *J Appl Physiol (1985)*. 2008; 105: 1652-1660.

190. Xu TY, Staessen JA, Wei FF, Xu J, Li FH, Fan WX, Gao PJ, Wang JG and Li Y. Blood flow pattern in the middle cerebral artery in relation to indices of arterial stiffness in the systemic circulation. *American journal of hypertension*. 2012; 25: 319-24.

191. Tarumi T, Shah F, Tanaka H and Haley AP. Association between central elastic artery stiffness and cerebral perfusion in deep subcortical gray and white matter. *American journal of hypertension*. 2011; 24: 1108-13.

192. Whitlock MC and Hundley WG. Noninvasive imaging of flow and vascular function in disease of the aorta. *JACC: Cardiovascular imaging*. 2015; 8: 1094-1106.

193. Alata W, Ye Y, St-Amour I, Vandal M and Calon F. Human apolipoprotein E varepsilon4 expression impairs cerebral vascularization and blood-brain barrier function in mice. *Journal of Cerebral Blood Flow Metabolism*. 2015; 35: 86-94.

194. DeCarli C, Reed T, Miller BL, Wolf PA, Swan GE and Carmelli D. Impact of apolipoprotein E epsilon4 and vascular disease on brain morphology in men from the NHLBI twin study. *Stroke*. 1999; 30: 1548-53.

195. Wierenga CE, Clark LR, Dev SI, Shin DD, Jurick SM, Rissman RA, Liu TT and Bondi MW. Interaction of age and APOE genotype on cerebral blood flow at rest. *Journal of Alzheimers Disease : JAD*. 2013; 34: 921-35.

196. Thambisetty M, Beason-Held L, An Y, Kraut MA and Resnick SM. APOE epsilon4 genotype and longitudinal changes in cerebral blood flow in normal aging. *Arch Neurol*. 2010; 67: 93-8.

197. Jefferson AL, Gifford KA, Acosta LM, Bell SP, Donahue MJ, Taylor Davis L, Gottlieb J, Gupta DK, Hohman TJ, Lane EM, Libon DJ, Mendes LA, Niswender K, Pechman KR, Rane S, Ruberg FL, Ru Su Y, Zetterberg H and Liu D. The Vanderbilt Memory & Aging Project: Study design and baseline cohort overview. *J Alzheimers Dis*. 2016; 52: 539-559.

198. Morris JC. The Clinical Dementia Rating (CDR): Current version and scoring rules. *Neurology*. 1993; 43: 2412-2414.

199. Cambronero FE, Liu D, Neal JE, Moore EE, Gifford KA, Terry JG, Nair S, Pechman KR, Osborn KE, Hohman TJ, Bell SP, Sweatt JD, Wang TJ, Beckman JA, Carr JJ and Jefferson AL. APOE genotype modifies the association between central arterial stiffening and cognition in older adults. *Neurobiol Aging*. 2018; 67: 120-127.

200. Asman AJ and Landman BA. Non-local statistical label fusion for multi-atlas segmentation. *Medical Image Analysis*. 2013; 17: 194-208.

201. Harrigan RL, Yvernault BC, Boyd BD, Damon SM, Gibney KD, Conrad BN, Phillips NS, Rogers BP, Gao Y and Landman BA. Vanderbilt University Institute of Imaging Science Center for Computational Imaging XNAT: A multimodal data archive and processing environment. *Neuroimage*. 2016; 124: 1097-101.

202. Donahue MJ, Faraco CC, Strother MK, Chappell MA, Rane S, Dethrage LM, Hendrikse J and Siero JC. Bolus arrival time and cerebral blood flow responses to hypercarbia. *Journal of Cerebral Blood Flow & Metabolism*. 2014; 34: 1243-1252.

203. Jenkinson M and Smith S. A global optimisation method for robust affine registration of brain images. *Medical Image Analysis*. 2001; 5: 143-156.

204. Alsop DC, Detre JA, Golay X, Gunther M, Hendrikse J, Hernandez-Garcia L, Lu H, MacIntosh BJ, Parkes LM, Smits M, van Osch MJ, Wang DJ, Wong EC and Zaharchuk G. Recommended implementation of arterial spin-labeled perfusion MRI for clinical applications: A consensus of the ISMRM perfusion study group and the European consortium for ASL in dementia. *Magnetic resonance in medicine*. 2015; 73: 102-116.

205. Jenkinson M, Beckmann CF, Behrens TE, Woolrich MW and Smith SM. FSL. *Neuroimage*. 2012; 62: 782-790.

206. Lang RM, Badano LP, Mor-Avi V, Afilalo J, Armstrong A, Ernande L, Flachskampf FA, Foster E, Goldstein SA, Kuznetsova T, Lancellotti P, Muraru D, Picard MH, Rietzschel ER, Rudski L, Spencer KT, Tsang W and Voigt JU. Recommendations for cardiac chamber

quantification by echocardiography in adults: an update from the American Society of Echocardiography and the European Association of Cardiovascular Imaging. *Journal of the American Society of Echocardiography*. 2015; 28: 1-39 e14.

207. Espeseth T, Westlye LT, Walhovd KB, Fjell AM, Endestad T, Rootwelt H and Reinvang I. Apolipoprotein E ε4-related thickening of the cerebral cortex modulates selective attention. *Neurobiol Aging*. 2012; 33: 304-322.e1.

208. Abondio P, Sazzini M, Garagnani P, Boattini A, Monti D, Franceschi C, Luiselli D and Giuliani C. The Genetic Variability of APOE in Different Human Populations and Its Implications for Longevity. *Genes*. 2019; 10.

209. Wisdom NM, Mignogna J and Collins RL. Variability in Wechsler Adult Intelligence Scale-IV subtest performance across age. *Archives of clinical neuropsychology : the official journal of the National Academy of Neuropsychologists*. 2012; 27: 389-97.

210. Prabhavathi K, Selvi KT, Poornima KN and Sarvanan A. Role of biological sex in normal cardiac function and in its disease outcome - a review. *Journal of Clinical Diagnostic Research*. 2014; 8: Be01-4.

211. McCarrey AC, An Y, Kitner-Triolo MH, Ferrucci L and Resnick SM. Sex differences in cognitive trajectories in clinically normal older adults. *Psychology and aging*. 2016; 31: 166-75.

212. Chen Y, Lv C, Li X, Zhang J, Chen K, Liu Z, Li H, Fan J, Qin T, Luo L and Zhang Z. The positive impacts of early-life education on cognition, leisure activity, and brain structure in healthy aging. *Aging*. 2019; 11: 4923-4942.

213. Leigh JA, Alvarez M and Rodriguez CJ. Ethnic Minorities and Coronary Heart Disease: an Update and Future Directions. *Current atherosclerosis reports*. 2016; 18: 9.

214. Wolf PA, D'Agostino RB, Belanger AJ and Kannel WB. Probability of stroke: a risk profile from the Framingham Study. *Stroke*. 1991; 22: 312-318.

215. D'Agostino RB, Wolf PA, Belanger AJ and Kannel WB. Stroke risk profile: Adjustment for antihypertensive medication. The Framingham Study. *Stroke*. 1994; 25: 40-43.

216. Rawle MJ, Davis D, Bendayan R and Wong A. Apolipoprotein-E (Apoe) ε4 and cognitive decline over the adult life course. *Translational Psychiatry*. 2018; 8: 18.

217. Suri S, Mackay CE, Kelly ME, Germuska M, Tunbridge EM, Frisoni GB, Matthews PM, Ebmeier KP, Bulte DP and Filippini N. Reduced cerebrovascular reactivity in young adults carrying the APOE epsilon4 allele. *Alzheimer's & dementia : the journal of the Alzheimer's Association*. 2015; 11: 648-57.e1.

218. Peila R, Rodriguez BL and Launer LJ. Type 2 diabetes, APOE gene, and the risk for dementia and related pathologies: The Honolulu-Asia Aging Study. *Diabetes*. 2002; 51: 1256-62.

219. Matsuzaki T, Sasaki K, Tanizaki Y, Hata J, Fujimi K, Matsui Y, Sekita A, Suzuki SO, Kanba S, Kiyohara Y and Iwaki T. Insulin resistance is associated with the pathology of Alzheimer disease: the Hisayama study. *Neurology*. 2010; 75: 764-70.

220. Walker KA, Power MC, Hoogeveen RC, Folsom AR, Ballantyne CM, Knopman DS, Windham BG, Selvin E, Jack CR, Jr. and Gottesman RF. Midlife Systemic Inflammation, Late-Life White Matter Integrity, and Cerebral Small Vessel Disease: The Atherosclerosis Risk in Communities Study. *Stroke*. 2017; 48: 3196-3202.

221. Brickman AM, Guzman VA, Gonzalez-Castellon M, Razlighi Q, Gu Y, Narkhede A, Janicki S, Ichise M, Stern Y, Manly JJ, Schupf N and Marshall RS. Cerebral autoregulation, beta amyloid, and white matter hyperintensities are interrelated. *Neuroscience letters*. 2015; 592: 54-58.

222. Niwa K, Kazama K, Younkin L, Younkin SG, Carlson GA and Iadecola C. Cerebrovascular autoregulation is profoundly impaired in mice overexpressing amyloid precursor protein. *American journal of physiology Heart and circulatory physiology*. 2002; 283: H315-23.

223. Riggs HE and Rupp C. Variation in form of circle of Willis. The relation of the variations to collateral circulation: anatomic analysis. *Arch Neurol*. 1963; 8: 8-14.

224. Vrselja Z, Brkic H, Mrdenovic S, Radic R and Curic G. Function of circle of Willis. *J Cereb Blood Flow Metab*. 2014; 34: 578-84.

225. De Silva KR, Silva R, Gunasekera WS and Jayesekera RW. Prevalence of typical circle of Willis and the variation in the anterior communicating artery: A study of a Sri Lankan population. *Annals of Indian Academy of Neurology*. 2009; 12: 157-61.

226. Kapoor K, Singh B and Dewan LI. Variations in the configuration of the circle of Willis. *Anatomical science international*. 2008; 83: 96-106.

227. Klimek-Piotrowska W, Rybicka M, Wojnarska A, Wójtowicz A, Koziej M and Hołda MK. A multitude of variations in the configuration of the circle of Willis: an autopsy study. *Anatomical science international*. 2016; 91: 325-33.

228. Hashemi SM, Mahmoodi R and Amirjamshidi A. Variations in the Anatomy of the Willis' circle: A 3-year cross-sectional study from Iran (2006-2009). Are the distributions of variations of circle of Willis different in different populations? Result of an anatomical study and review of literature. *Surgical neurology international*. 2013; 4: 65.

229. Li Q, Li J, Lv F, Li K, Luo T and Xie P. A multidetector CT angiography study of variations in the circle of Willis in a Chinese population. *Journal of clinical neuroscience : official journal of the Neurosurgical Society of Australasia*. 2011; 18: 379-83.

230. Krabbe-Hartkamp MJ, van der Grond J, de Leeuw FE, de Groot JC, Algra A, Hillen B, Breteler MM and Mali WP. Circle of Willis: morphologic variation on three-dimensional time-of-flight MR angiograms. *Radiology*. 1998; 207: 103-11.

231. Hendrikse J, van der Grond J, Lu H, van Zijl PC and Golay X. Flow territory mapping of the cerebral arteries with regional perfusion MRI. *Stroke*. 2004; 35: 882-887.

232. Kontos HA, Wei EP, Navari RM, Levasseur JE, Rosenblum WI and Patterson JL, Jr. Responses of cerebral arteries and arterioles to acute hypotension and hypertension. *Am J Physiol*. 1978; 234: H371-83.

233. Willie CK and Ainslie PN. Cool head, hot brain: cerebral blood flow distribution during exercise. *J Physiol*. 2011; 589: 2657-8.

234. Zhang C, Li S, Pu F, Fan Y and Li D. The effect of anatomic variations of circle of Willis on cerebral blood distribution during posture change from supination to standing: a model study. *Bio-medical materials and engineering*. 2014; 24: 2371-80.

235. Zhang C, Wang L, Li X, Li S, Pu F, Fan Y and Li D. Modeling the circle of Willis to assess the effect of anatomical variations on the development of unilateral internal carotid artery stenosis. *Bio-medical materials and engineering*. 2014; 24: 491-9.

236. Shahan CP, Gray RI, Croce MA and Fabian TC. Impact of circle of Willis anatomy in traumatic blunt cerebrovascular injury-related stroke. *Trauma surgery & acute care open*. 2017; 2: e000086.

237. Alnaes MS, Isaksen J, Mardal KA, Romner B, Morgan MK and Ingebrigtsen T. Computation of hemodynamics in the circle of Willis. *Stroke*. 2007; 38: 2500-5.

238. Liu X, Gao Z, Xiong H, Ghista D, Ren L, Zhang H, Wu W, Huang W and Hau WK. Three-dimensional hemodynamics analysis of the circle of Willis in the patient-specific nonintegral arterial structures. *Biomechanics and modeling in mechanobiology*. 2016; 15: 1439-1456.

239. Gutierrez J, Honig L, Elkind MS, Mohr JP, Goldman J, Dwork AJ, Morgello S and Marshall RS. Brain arterial aging and its relationship to Alzheimer dementia. *Neurology*. 2016; 86: 1507-15.

240. Chung CP, Lee HY, Lin PC and Wang PN. Cerebral Artery Pulsatility is Associated with Cognitive Impairment and Predicts Dementia in Individuals with Subjective Memory Decline or Mild Cognitive Impairment. *J Alzheimers Dis*. 2017; 60: 625-632.

241. Gutierrez J, Kulick E, Park Moon Y, Dong C, Cheung K, Ahmet B, Stern Y, Alperin N, Rundek T, Sacco RL, Wright CB and Elkind MSV. Brain Arterial Diameters and Cognitive Performance: The Northern Manhattan Study. *Journal of the International Neuropsychological Society : JINS*. 2018; 24: 335-346.

242. Jack CR, Jr., Nichols DA, Sharbrough FW, Marsh WR and Petersen RC. Selective posterior cerebral artery Amytal test for evaluating memory function before surgery for temporal lobe seizure. *Radiology*. 1988; 168: 787-93.

243. Momjian-Mayor I and Baron JC. The pathophysiology of watershed infarction in internal carotid artery disease: review of cerebral perfusion studies. *Stroke*. 2005; 36: 567-77.

244. Blanco PJ, Muller LO and Spence JD. Blood pressure gradients in cerebral arteries: a clue to pathogenesis of cerebral small vessel disease. 2017; 2: 108-117.

245. Valen-Sendstad K, Piccinelli M and Steinman DA. High-resolution computational fluid dynamics detects flow instabilities in the carotid siphon: implications for aneurysm initiation and rupture? *J Biomech*. 2014; 47: 3210-6.

246. Fukushima T, Homma T, Harakawa K, Sakata N and Azuma T. Vortex generation in pulsatile flow through arterial bifurcation models including the human carotid artery. *J Biomech Eng*. 1988; 110: 166-71.

247. Iqbal S. A comprehensive study of the anatomical variations of the circle of willis in adult human brains. *Journal of clinical and diagnostic research : JCDR*. 2013; 7: 2423-7.

248. Blackwell DL, Lucas JW and Clarke TC. Summary health statistics for U.S. adults: national health interview survey, 2012. *Vital Health Stat 10*. 2014: 1-161.

249. Kostov K. The Causal Relationship between Endothelin-1 and Hypertension: Focusing on Endothelial Dysfunction, Arterial Stiffness, Vascular Remodeling, and Blood Pressure Regulation. *Life (Basel, Switzerland)*. 2021; 11.

250. Kalaria RN. Cerebrovascular disease and mechanisms of cognitive impairment: evidence from clinicopathological studies in humans. *Stroke*. 2012; 43: 2526-34.

251. Pantoni L. Cerebral small vessel disease: from pathogenesis and clinical characteristics to therapeutic challenges. *The Lancet Neurology*. 2010; 9: 689-701.

252. Pantoni L, Poggesi A and Inzitari D. Cognitive decline and dementia related to cerebrovascular diseases: some evidence and concepts. *Cerebrovasc Dis*. 2009; 27 Suppl 1: 191-6.

253. Maillard P, Mitchell GF, Himali JJ, Beiser A, Tsao CW, Pase MP, Satizabal CL, Vasan RS, Seshadri S and DeCarli C. Effects of arterial stiffness on brain integrity in young adults from the Framingham Heart Study. *Stroke*. 2016; 47: 1030-1036.

254. Triantafyllou A, Anyfanti P, Gavriilaki E, Zabulis X, Gkaliagkousi E, Petidis K, Triantafyllou G, Gkolias V, Pyrpasopoulou A and Douma S. Association between retinal vessel caliber and arterial stiffness in a population comprised of normotensive to early-stage hypertensive individuals. *Am J Hypertens*. 2014; 27: 1472-8.

255. Zhong W, Cruickshanks KJ, Schubert CR, Carlsson CM, Chappell RJ, Klein BE, Klein R and Acher CW. Pulse wave velocity and cognitive function in older adults. *Alzheimer disease and associated disorders*. 2014; 28: 44-49.

256. Waldstein SR, Rice SC, Thayer JF, Najjar SS, Scuteri A and Zonderman AB. Pulse pressure and pulse wave velocity are related to cognitive decline in the Baltimore Longitudinal Study of Aging. *Hypertension*. 2008; 51: 99-104.

257. Watson NL, Sutton-Tyrrell K, Rosano C, Boudreau RM, Hardy SE, Simonsick EM, Najjar SS, Launer LJ, Yaffe K, Atkinson HH, Satterfield S and Newman AB. Arterial stiffness and cognitive decline in well-functioning older adults. *J Gerontol A Biol Sci Med Sci*. 2011; 66: 1336-42.

258. Meyer ML, Palta P, Tanaka H, Deal JA, Wright J, Knopman DS, Griswold ME, Mosley TH and Heiss G. Association of Central Arterial Stiffness and Pressure Pulsatility with Mild Cognitive Impairment and Dementia: The Atherosclerosis Risk in Communities Study-Neurocognitive Study (ARIC-NCS). *J Alzheimers Dis*. 2017; 57: 195-204.

259. Poels MM, van Oijen M, Mattace-Raso FU, Hofman A, Koudstaal PJ, Witteman JC and Breteler MM. Arterial stiffness, cognitive decline, and risk of dementia: the Rotterdam study. *Stroke*. 2007; 38: 888-892.

260. Tai LM, Thomas R, Marottoli FM, Koster KP, Kanekiyo T, Morris AW and Bu G. The role of APOE in cerebrovascular dysfunction. *Acta Neuropathol*. 2016; 131: 709-23.

261. Castellano JM, Kim J, Stewart FR, Jiang H, DeMattos RB, Patterson BW, Fagan AM, Morris JC, Mawuenyega KG, Cruchaga C, Goate AM, Bales KR, Paul SM, Bateman RJ and Holtzman DM. Human apoE isoforms differentially regulate brain amyloid-beta peptide clearance. *Sci Transl Med*. 2011; 3: 89ra57.

262. Thomas T, Thomas G, McLendon C, Sutton T and Mullan M. beta-Amyloid-mediated vasoactivity and vascular endothelial damage. *Nature*. 1996; 380: 168-71.

263. Thomas T, McLendon C, Sutton ET and Thomas G. beta-Amyloid-induced cerebrovascular endothelial dysfunction. *Annals New York Academy of Sciences*. 1997; 826: 447-51.

264. Martins CA, Oulhaj A, de Jager CA and Williams JH. APOE alleles predict the rate of cognitive decline in Alzheimer disease: a nonlinear model. *Neurology*. 2005; 65: 1888-93.

265. Alvarez-Bueno C, Cunha PG, Martinez-Vizcaino V, Pozuelo-Carrascosa DP, Visier-Alfonso ME, Jimenez-Lopez E and Cavero-Redondo I. Arterial Stiffness and Cognition Among Adults: A Systematic Review and Meta-Analysis of Observational and Longitudinal Studies. *J Am Heart Assoc*. 2020; 9: e014621.

266. Benjamini Y and Hochberg Y. Controlling the false discovery rate: A practical and powerful approach to multiple testing. *J R Stat Soc Series B Stat Methodol*. 1995; 57: 289-300.

267. Delis DC, Kramer J, Kaplan E and Ober B. *California Verbal Learning Test–II, Second Edition*. San Antonio, TX: The Psychological Corporation; 2000.

268. Kochunov P, Ramage AE, Lancaster JL, Robin DA, Narayana S, Coyle T, Royall DR and Fox P. Loss of cerebral white matter structural integrity tracks the gray matter metabolic decline in normal aging. *Neuroimage*. 2009; 45: 17-28.

269. Arvanitakis Z, Leurgans SE, Barnes LL, Bennett DA and Schneider JA. Microinfarct pathology, dementia, and cognitive systems. *Stroke*. 2011; 42: 722-727.

270. Kapasi A, Leurgans SE, James BD, Boyle PA, Arvanitakis Z, Nag S, Bennett DA, Buchman AS and Schneider JA. Watershed microinfarct pathology and cognition in older persons. *Neurobiol Aging*. 2018; 70: 10-17.

271. Jefferson AL. Vascular risk factors and midlife cognition: rethinking the exposure window. *Circulation*. 2014; 129: 1548-1550.

272. Knecht S, Oelschlager C, Duning T, Lohmann H, Albers J, Stehling C, Heindel W, Breithardt G, Berger K, Ringelstein EB, Kirchhof P and Wersching H. Atrial fibrillation in stroke-free patients is associated with memory impairment and hippocampal atrophy. *European heart journal*. 2008; 29: 2125-32.

273. Forti P, Maioli F, Pisacane N, Rietti E, Montesi F and Ravaglia G. Atrial fibrillation and risk of dementia in non-demented elderly subjects with and without mild cognitive impairment. *Neurological research*. 2006; 28: 625-629.

274. Stergiopulos N, Segers P and Westerhof N. Use of pulse pressure method for estimating total arterial compliance in vivo. *The American journal of physiology*. 1999; 276: H424-8.

275. Magistro D, Takeuchi H, Nejad KK, Taki Y, Sekiguchi A, Nouchi R, Kotozaki Y, Nakagawa S, Miyauchi CM, Iizuka K, Yokoyama R, Shinada T, Yamamoto Y, Hanawa S, Araki T, Hashizume H, Sassa Y and Kawashima R. The Relationship between Processing Speed and Regional White Matter Volume in Healthy Young People. *PLoS One*. 2015; 10: e0136386.

276. Moritz CH, Johnson SC, McMillan KM, Haughton VM and Meyerand ME. Functional MRI neuroanatomic correlates of the Hooper Visual Organization Test. *Journal of the International Neuropsychological Society*. 2004; 10: 939-947.

277. Irani F. Visuoperceptual. In: J. S. Kreutzer, J. DeLuca and B. Caplan, eds. *Encyclopedia of Clinical Neuropsychology* New York, NY: Springer; 2011.

278. Montagne A, Nation DA, Sagare AP and Barisano G. APOE4 leads to blood-brain barrier dysfunction predicting cognitive decline. 2020; 581: 71-76.

279. de Leeuw FE, Barkhof F and Scheltens P. White matter lesions and hippocampal atrophy in Alzheimer's disease. *Neurology*. 2004; 62: 310-2.

280. Elmstahl S, Petersson M, Lilja B, Samuelsson SM, Rosen I and Bjuno L. Autonomic cardiovascular responses to tilting in patients with Alzheimer's disease and in healthy elderly women. *Age Ageing*. 1992; 21: 301-7.

281. Vitiello B, Veith RC, Molchan SE, Martinez RA, Lawlor BA, Radcliffe J, Hill JL and Sunderland T. Autonomic dysfunction in patients with dementia of the Alzheimer type. *Biological psychiatry*. 1993; 34: 428-33.

282. Femminella GD, Rengo G, Komici K, Iacotucci P, Petraglia L, Pagano G, de Lucia C, Canonico V, Bonaduce D, Leosco D and Ferrara N. Autonomic dysfunction in Alzheimer's disease: tools for assessment and review of the literature. *J Alzheimers Dis*. 2014; 42: 369-77.

283. Beach PA, Huck JT, Zhu DC and Bozoki AC. Altered behavioral and autonomic pain responses in Alzheimer's disease are associated with dysfunctional affective, self-reflective and salience network resting-state connectivity. *Front Aging Neurosci*. 2017; 9: 297.

284. Meel-van den Abeelen AS, Lagro J, Gommer ED, Reulen JP and Claassen JA. Baroreflex function is reduced in Alzheimer's disease: a candidate biomarker? *Neurobiol Aging*. 2013; 34: 1170-6.

285. Allan LM, Ballard CG, Allen J, Murray A, Davidson AW, McKeith IG and Kenny RA. Autonomic dysfunction in dementia. *J Neurol Neurosurg Psychiatry*. 2007; 78: 671-7.

286. Idiaquez J and Roman GC. Autonomic dysfunction in neurodegenerative dementias. *Journal of the neurological sciences*. 2011; 305: 22-7.

287. Wang SJ, Liao KK, Fuh JL, Lin KN, Wu ZA, Liu CY and Liu HC. Cardiovascular autonomic functions in Alzheimer's disease. *Age Ageing*. 1994; 23: 400-4.

288. Issac TG, Chandra SR, Gupta N, Rukmani MR, Deepika S and Sathyaprabha TN. Autonomic dysfunction: A comparative study of patients with Alzheimer's and frontotemporal dementia - A pilot study. *J Neurosci Rural Pract*. 2017; 8: 84-88.

289. Algotsson A, Viitanen M, Winblad B and Solders G. Autonomic dysfunction in Alzheimer's disease. *Acta Neurol Scand*. 1995; 91: 14-8.

290. Simic G, Stanic G, Mladinov M, Jovanov-Milosevic N, Kostovic I and Hof PR. Does Alzheimer's disease begin in the brainstem? *Neuropathology and applied neurobiology*. 2009; 35: 532-54.

291. Braak H and Braak E. Staging of Alzheimer's disease-related neurofibrillary changes. *Neurobiol Aging*. 1995; 16: 271-278; discussion 278-284.

292. Chu CC, Tranel D, Damasio AR and Van Hoesen GW. The autonomic-related cortex: pathology in Alzheimer's disease. *Cereb Cortex*. 1997; 7: 86-95.

293. Idiaquez J, Sandoval E and Seguel A. Association between neuropsychiatric and autonomic dysfunction in Alzheimer's disease. *Clin Auton Res*. 2002; 12: 43-6.

294. van Beek AH and Claassen JA. The cerebrovascular role of the cholinergic neural system in Alzheimer's disease. *Behavioural brain research*. 2011; 221: 537-42.

295. Jefferson AL, Tate DF, Poppas A, Brickman AM, Paul RH, Gunstad J and Cohen RA. Lower cardiac output is associated with greater white matter hyperintensities in older adults with cardiovascular disease. *Journal of the American Geriatrics Society*. 2007; 55: 1044-1048.

296. Gianni D, Li A, Tesco G, McKay KM, Moore J, Raygor K, Rota M, Gwathmey JK, Dec GW, Aretz T, Leri A, Semigran MJ, Anversa P, Macgillivray TE, Tanzi RE and del Monte F. Protein aggregates and novel presenilin gene variants in idiopathic dilated cardiomyopathy. *Circulation*. 2010; 121: 1216-26.

297. Green KN, Demuro A, Akbari Y, Hitt BD, Smith IF, Parker I and LaFerla FM. SERCA pump activity is physiologically regulated by presenilin and regulates amyloid beta production. *The Journal of cell biology*. 2008; 181: 1107-16.

298. Sarasija S and Norman KR. Role of Presenilin in Mitochondrial Oxidative Stress and Neurodegeneration in Caenorhabditis elegans. *Antioxidants (Basel)*. 2018; 7.

299. Broce IJ, Tan CH, Fan CC, Jansen I, Savage JE, Witoelar A, Wen N, Hess CP, Dillon WP, Glastonbury CM, Glymour M, Yokoyama JS, Elahi FM, Rabinovici GD, Miller BL, Mormino EC, Sperling RA, Bennett DA, McEvoy LK, Brewer JB, Feldman HH, Hyman BT, Pericak-Vance M, Haines JL, Farrer LA, Mayeux R, Schellenberg GD, Yaffe K, Sugrue LP, Dale AM, Posthuma D, Andreassen OA, Karch CM and Desikan RS. Dissecting the genetic relationship between cardiovascular risk factors and Alzheimer's disease. 2018.

300. Xue-Shan Z, Juan P, Qi W, Zhong R, Li-Hong P, Zhi-Han T, Zhi-Sheng J, Gui-Xue W and Lu-Shan L. Imbalanced cholesterol metabolism in Alzheimer's disease. *Clin Chim Acta*. 2016; 456: 107-114.

301. Troncone L, Luciani M, Coggins M, Wilker EH, Ho CY, Codispoti KE, Frosch MP, Kayed R and Del Monte F. Abeta Amyloid Pathology Affects the Hearts of Patients With Alzheimer's Disease: Mind the Heart. *Journal of the American College of Cardiology*. 2016; 68: 2395-2407.

302. Cornwell GG, 3rd, Murdoch WL, Kyle RA, Westermark P and Pitkanen P. Frequency and distribution of senile cardiovascular amyloid. A clinicopathologic correlation. *Am J Med*. 1983; 75: 618-23.

303. Mohammed SF, Mirzoyev SA, Edwards WD, Dogan A, Grogan DR, Dunlay SM, Roger VL, Gertz MA, Dispenzieri A, Zeldenrust SR and Redfield MM. Left ventricular amyloid deposition in patients with heart failure and preserved ejection fraction. *JACC Heart failure*. 2014; 2: 113-22.

304. Gonzalez-Lopez E, Gallego-Delgado M, Guzzo-Merello G, de Haro-Del Moral FJ, Cobo-Marcos M, Robles C, Bornstein B, Salas C, Lara-Pezzi E, Alonso-Pulpon L and Garcia-Pavia P. Wild-type transthyretin amyloidosis as a cause of heart failure with preserved ejection fraction. *European heart journal*. 2015; 36: 2585-94.

305. DeLoach SS and Townsend RR. Vascular stiffness: its measurement and significance for epidemiologic and outcome studies. *Clinical journal of the American Society of Nephrology : CJASN*. 2008; 3: 184-92.

306. Siddiqui TA, Chamarti KS, Tou LC, Demirjian GA, Noorani S, Zink S and Umair M. The Merits, Limitations, and Future Directions of Cost-Effectiveness Analysis in Cardiac MRI with a Focus on Coronary Artery Disease: A Literature Review. *Journal of cardiovascular development and disease*. 2022; 9.